

# **ANALYSIS OF WALL PROPERTIES AND SLIP PARAMETER ON THE PHAN-THIEN-TANNER (PTT) FLUID**

By

**MARIYAM DUREZ**



**NATIONAL UNIVERSITY OF MODERN LANGUAGES**

**ISLAMABAD**

**March, 2024**

# **Analysis Of Wall Properties And Slip Parameter On The Phan-Thien-Tanner (PTT) Fluid**

**By**

**MARIYAM DUREZ**

MS MATH, National University of Modern Languages, Islamabad, 2023

A THESIS SUBMITTED IN PARTIAL FULFILMENT OF  
THE REQUIREMENTS FOR THE DEGREE OF

**MASTER OF SCIENCE**

**In Mathematics**

To

FACULTY OF ENGINEERING & COMPUTING



NATIONAL UNIVERSITY OF MODERN LANGUAGES ISLAMABAD

© Mariyam Durez, 2024



## THESIS AND DEFENSE APPROVAL FORM

The undersigned certify that they have read the following thesis, examined the defense, are satisfied with overall exam performance, and recommend the thesis to the Faculty of Engineering and Computing for acceptance.

**Thesis Title:** Analysis of Wall Properties and Slip Parameter on the Phan-Thien-Tanner (PTT) Fluid.

**Submitted By:** Mariyam Durez

**Registration #:** 59 MS/Math/S22

Master of Science in Mathematics (MS)

Title of the Degree

Mathematics

Name of Discipline

Dr. Hadia Tariq

Name of Research Supervisor

\_\_\_\_\_  
Signature of Research Supervisor

Dr. Sadia Riaz

Name of HOD (Math)

\_\_\_\_\_  
Signature of HOD (Math)

Dr. Noman Malik

Name of Dean (FEC)

\_\_\_\_\_  
Signature of Dean(FEC)

12-March, 2024

## AUTHOR'S DECLARATION

I Mariyam Durez

Daughter of Muhammad Durez

Registration # 59 MS/Math/S22

Discipline Mathematics

Candidate of **Master of Science in Mathematics (MS MATH)** at the National University of Modern Languages do hereby declare that the thesis **Analysis of Wall Properties and Slip Parameter on the Phan-Thien-Tanner (PTT) Fluid** submitted by me in partial fulfillment of MS degree, is my original work, and has not been submitted or published earlier. I also solemnly declare that it shall not, in future, be submitted by me for obtaining any other degree from this or any other university or institution. I also understand that if evidence of plagiarism is found in my thesis/dissertation at any stage, even after the award of a degree, the work may be cancelled and the degree revoked.

\_\_\_\_\_  
Signature of Candidate

Mariyam Durez  
Name of Candidate

12-March, 2024

Date

## ABSTRACT

**Title: Analysis of Wall Properties and Slip Parameter on the Phan-Thien-Tanner (PTT) Fluid**

This thesis delves into a comprehensive exploration of the peristaltic movement of a non-Newtonian Phan-Thien-Tanner (PTT) fluid within a symmetric flexible channel characterized by sinusoidal peristaltic waves. The study employs the long wavelength and low Reynolds number approximation, focusing on the flow within a wave frame of reference that travels at the velocity of the peristaltic waves. The investigation encompasses a detailed analysis of the influences of wall properties, porosity, and slip parameter on the behavior of the PTT fluid. The mathematical representation of the system relies on partial differential equations (PDEs), with subsequent utilization of similarity transformations to effectively reduce the number of dependent variables. The analytical solution is employed to resolve mathematical complexities and provide conclusive results for the problem. Through the presentation of graphs, the study meticulously examines the impact of various physical parameters on streamlines, pressure distribution, and velocity within the system.

# TABLE OF CONTENTS

CHAPTER	TITLE	PAGE
	<b>AUTHOR'S DECLARATION</b>	iii
	<b>ABSTRACT</b>	iv
	<b>TABLE OF CONTENTS</b>	v
	<b>LIST OF FIGURES</b>	viii
	<b>LIST OF ABBREVIATIONS</b>	x
	<b>LIST OF SYMBOLS</b>	xi
	<b>ACKNOWLEDGEMENT</b>	xiii
	<b>DEDICATION</b>	xiv
<b>1</b>	<b>Chapter 1</b>	<b>2</b>
	1.1 Overview	2
	1.1.1 Applications of Fluids	2
	1.2 Newtonian and non-Newtonian Fluids	3
	1.2.1 Applications of Newtonian Fluids	4
	1.2.2 Applications of non-Newtonian Fluids	5
	1.3 Peristalsis Flow	5
	1.4 Slip Flow	6
	1.5 Wall Properties	7
	1.6 Phan-Thien-Tanner (PTT) Fluid	8
	1.7 Porosity	9
	1.8 Thesis Organization	9

<b>2</b>	<b>Chapter 2</b>	<b>11</b>
2.1	Overview of Related Literature	11
<b>3</b>	<b>Chapter 3</b>	<b>25</b>
3.1	Fluid	25
3.1.1	Types of Fluids	25
3.1.2	Applications of Fluids	26
3.2	Hydrostatic Stress Condition	27
3.2.1	Types of Hydrostatic Stress Condition	27
3.2.2	Applications of Hydrostatic Stress Condition	27
3.3	Fluid Mechanics	28
3.3.1	Types of Fluid Mechanics	28
3.3.2	Applications of Fluid Mechanics	29
3.4	Newtonian Fluids	30
3.4.1	Types of Newtonian Fluids	30
3.4.2	Applications of Newtonian Fluids	30
3.5	Non-Newtonian Fluids	31
3.5.1	Types of non-Newtonian Fluids	32
3.6	Shear Stress	32
3.6.1	Types of Shear Stress	32
3.6.2	Applications of Shear Stress	33
3.7	Shear Strain Rate	33
3.7.1	Types of Shear Strain Rate	34
3.7.2	Applications of Shear Strain Rate	34
3.8	Viscosity	35
3.8.1	Types of Viscosity	35
3.8.2	Applications of Viscosity	35
3.9	Compressible Fluid	36
3.9.1	Applications of Compressible Fluid	36
3.10	Incompressible Fluid	37
3.10.1	Applications of Incompressible Fluid	37
3.11	Linear Momentum	38
3.11.1	Applications of Linear Momentum	38

3.12	Continuity Equation	39
3.12.1	Applications of Continuity Equation	39
3.13	Amplitude	40
3.14	Wavelength	40
3.15	Density	41
3.16	Pressure	41
3.17	Cauchy Stress Tensor	41
3.18	Permeability	42
3.19	Weissenberg Number	42
<b>4</b>	<b>Chapter 4</b>	<b>44</b>
4.1	Introduction	44
4.2	Mathematical Formulation	44
4.3	Exact Analytical Solution	47
4.4	Methodology	48
4.5	Results and Discussion	49
<b>5</b>	<b>Chapter 5</b>	<b>59</b>
5.1	Introduction	59
5.2	Mathematical Formulation	59
5.3	Perturbation Solution	62
5.3.1	System of Order $We^0$	62
5.3.2	System of Order $We^2$	63
5.4	Results and Discussion	64
<b>6</b>	<b>Chapter 6</b>	<b>75</b>
6.1	Conclusion	75
6.2	Future Work	76
	<b>REFERENCES</b>	<b>77</b>

## LIST OF FIGURES

FIGURE NO.	TITLE	PAGE
1.1	Behavior of the different types of Fluids.	3
1.3	Behavior of the peristalsis.	6
4.1	Streamlines for $\beta = 0, 0.1$ and $0.25$ .	48
4.2	Streamlines for $m = -0.35, 0$ and $0.35$ .	49
4.3	Streamlines for $K = 0.05, 0.2$ and $K \rightarrow \infty$ .	50
4.4	Streamlines for $M = 0, 2$ and $4$ .	51
4.5	Velocity distribution for $\beta = 0, 0.1$ and $0.2$ .	52
4.6	Velocity distribution for $m = -0.3, 0$ and $0.3$ .	52
4.7	Velocity distribution for $K = 0.5, 2$ and $K \rightarrow \infty$ .	53
4.8	Velocity distribution for $M = 2, 3$ and $4$ .	53
4.9	Temperature distribution for $K = 0.4, 2$ and $K \rightarrow \infty$ .	54
4.10	Temperature distribution for $\beta = 0, 0.1$ and $0.2$ .	54
4.11	Temperature distribution for $m = -0.2, 0$ and $0.2$ .	55
4.12	Temperature distribution for $M = 3, 4$ and $5$ .	55
5.1	Streamlines for $E_1 = 0.1, 0.5$ and $1.2$ .	63
5.2	Streamlines for $E_2 = 0.1, 0.5$ and $0.9$ .	64
5.3	Streamlines for $E_3 = 0.1, 0.5$ and $0.8$ .	65
5.4	Streamlines for $We^2 = 0.001, 0.01$ and $0.02$ .	66
5.5	Streamlines for $\sigma = 0.1, 1$ and $2$ .	67
5.6	Streamlines for $\beta = 0, 0.1$ and $0.2$ .	68
5.7	Velocity distribution for $\sigma = 0.01, 0.2$ and $0.3$ .	69
5.8	Velocity distribution for $\beta = 0, 0.01$ and $0.02$ .	69
5.9	Velocity distribution for $We^2 = 0, 0.001$ and $0.002$ .	70
5.10	Velocity distribution for $E_1 = 0.1, 0.2$ and $0.3$ , $E_2 = 0.1, 0.2$ and $0.3$ and $E_3 = 0.1, 0.2$ and $0.3$ .	70

5.11	Pressure distribution for $\sigma = 0.1, 0.5$ and 1.	71
5.12	Pressure distribution for $\beta = 0, 0.1$ and 0.2.	71

## LIST OF ABBREVIATIONS

PTT	-	Phan-Thien-Tanner
MHD	-	Magnetohydrodynamic
PDE	-	Partial Differential Equation
UCM	-	Upper Convected Maxwell Model

## LIST OF SYMBOLS

$u, v$	-	Velocity components in x and y directions
$\rho$	-	Fluid density
$\mu$	-	Coefficient of viscosity or dynamic viscosity
$p$	-	Pressure
$d$	-	Half width of the channel
$a$	-	Amplitude
$\lambda$	-	Wavelength
$c$	-	Phase speed of the wave
$m'$	-	Non-uniformity of the channel
$k$	-	Thermal conductivity or relaxation time
$L^*$	-	Motion of stretched membrane
$\tau$	-	Elastic tension
$m$	-	Mass per unit area or non-uniform parameter
$C$	-	Coefficient of viscous damping forces
$p_o$	-	Pressure on the outside of the wall
$H$	-	Slip parameter
$\varepsilon, \delta$	-	Geometric parameter
$Re$	-	Reynolds number
$E_1, E_2, E_3$	-	Elasticity parameters or Wall parameters
$\beta$	-	Knudsen number (slip parameter)
$T$	-	Fluid temperature or Cauchy stress tensor
$Pr$	-	Prandtl number
$Br$	-	Brinkman number
$Z$	-	Coefficient of heat transmission
$M$	-	Hartmann number
$t$	-	Time
$We$	-	Weissenberg number
$K$	-	Permeability parameter
$I$	-	Identity tensor

$V$	-	Velocity
$S$	-	Extra-stress tensor
$s^\nabla$	-	Oldroyd's upper-convected derivative
$tr$	-	Trace
$\sigma$	-	Porosity
$D$	-	Deformation-rate tensor
$E$	-	Eckert number

## ACKNOWLEDGMENT

All praise and appreciation to ALLAH (SWT), the most benevolent and merciful. I am grateful to the last Prophet Muhammad (P.B.U.H) for bringing the word of ALLAH (SWT) and permitting men to persue knowledge.

It is my pleasure to express deep sense of gratitude to my supervisor Dr. Hadia Tariq from the department of Mathematics, NUML Islamabad for her professional guidance, technical discussions, kind behavior and constructive criticism throughout my research work. Special gratitude to Maj. Gen. Shahid Kiayani, Rector NUML, who has keen interest to provide research-oriented atmosphere and facilities for the research scholars of MS.

I am greatly thankful to Dr. Sadia Riaz, Head of the department of Mathematics, for her outstanding support and encouragement. I wish to express my sincere thanks to my friends for providing constant help and building my courage throughout my research work.

Finally, I am grateful to my parents and family for their continuous support during the pursuance of my education and completion of thesis. Their encouragements have always been with me.

## DEDICATION

*This thesis work is dedicated to my parents, brothers and my teachers throughout my education career who have not only loved me unconditionally, but whose good examples have taught me to work hard for the things that I aspire to achieve.*

# CHAPTER 1

## INTRODUCTION

### 1.1 Overview

A state of matter known as fluid is distinguished by its capacity to flow and adapt to the shape of its surroundings. A fluid is any liquid, gas, or other substance that continuously deforms (flows) as a result of an external force or shear stress. They have zero shear modulus, or more simply put, they are substances that cannot withstand any applied shear force. Liquids like water, milk, juice, oil, blood etc. and gases like air, carbon dioxide, steam etc are included in fluids. Daily life examples of fluids are drinking a glass of water, boiling water, inhaling air etc. Newtonian fluids and Non-Newtonian fluids are the two main categories of fluids. Its properties are fluidity, viscosity, density, compressibility and pressure. Its applications include transportations, hydraulic systems, heating and cooling, manufacturing process, medical applications and environmental studies.

#### 1.1.1 Applications of Fluids

**i) Transportation:** Different transportation systems depend heavily on fluids. Examples include gasoline or diesel fuels are used as energy sources for vehicles, air is used in pneumatic systems.

**ii) Hydraulic Systems:** Hydraulic systems, which use the pressure that fluids exert to deliver power, frequently use fluids. It is found in machinery, such as cranes, hydraulic lifts and forklifts.

**iii) Cooling and Heating:** In cooling devices like air conditioners and freezers, fluids like water or refrigerants are utilized to absorb heat from the environment. Similarly, fluids like oil or steam are used in heating systems to transfer heat energy.

**iv) Manufacturing Processes:** The use of fluids in manufacturing processes is widespread. For instance, in metalworking, coolants and lubricants are used to reduce friction, dissipate heat and cutting of metals.

**v) Medical Applications:** Medical applications require fluids to function. Patients are given intravenous fluids to stay hydrated. Understanding blood flow in the circulatory and respiratory systems requires knowledge of fluid dynamics.

**vi) Environmental Studies:** Understanding weather patterns, ocean currents, and the flow of toxins in the environment all depend heavily on fluid dynamics. In order to model and anticipate the phenomenon, fluid simulations are utilized, which supports environmental research and conservation efforts.

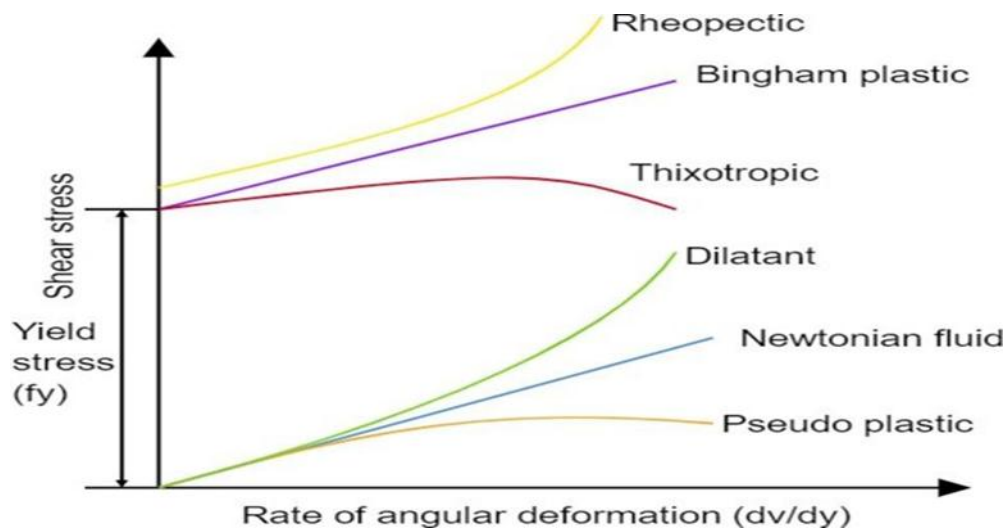


**Figure 1.1** Behavior of the different types of Fluids.

## 1.2 Newtonian and Non-Newtonian Fluids

The two basic types of fluids are Newtonian fluids and Non-Newtonian fluids.

**I) Newtonian Fluids:** The viscosity law of Newton is observed by Newtonian fluids, a particular category of fluid. This law indicates that the shear stress is directly related to the rate of shear strains or the velocity gradient between neighboring layers of a fluid. Newtonian fluids have a constant viscosity independent of the shear force that is being applied. For

examples, water, gasoline, milk, oil etc. Its properties are constant viscosity; shear tension and shear rate are linearly related, without regard to time and incompressible.

The constitutive equation relating the shear stress ( $\tau$ ) to the velocity gradient  $\left(\frac{du}{dy}\right)$  for Newtonian fluids is as follows:

$$\tau = \mu \left(\frac{du}{dy}\right),$$

where  $\tau$  is the fluid layer under shear stress,  $\mu$  is the fluid's dynamic viscosity and  $\frac{du}{dy}$  is the velocity gradient in the direction perpendicular to the flow.

### 1.2.1 Applications of Newtonian Fluids

Newtonian has the following applications:

- i) Water Distribution:** Water's consistent viscosity makes it ideal for use in plumbing, water supply networks, and other purposes.
- ii) Oil and Gas Industry:** In the oil and gas business, Newtonian fluids like crude oil and natural gas have consistent viscosity and flow characteristics and are used for processing and transportation.
- iii) Food and Beverage Industry:** Milk, fruit juices, and syrups are examples of Newtonian fluids that are frequently employed in the food and beverage sector.

**II) Non-Newtonian Fluids:** Fluids that do not follow Newton's viscosity law are referred to as "non-Newtonian fluids". The viscosity of non-Newtonian fluids can change with shear stress or strain rate. For examples, ketchup, toothpaste, cornstarch and water mixture, paint, honey, blood etc. Its properties include variable viscosity, connection between shear stress and shear rate that is nonlinear, time dependent behavior, compressibility and flow behavior classification.

Non-Newtonian fluids' constitutive equations are more intricate and link the shear stress ( $\tau$ ) to the velocity gradient  $\left(\frac{du}{dy}\right)$ . The constitutive formula is as follows:

$$\tau = K \left(\frac{du}{dy}\right)^n,$$

where  $\tau$  is the shear stress on the fluid layer,  $K$  is the consistency coefficient,  $\frac{du}{dy}$  is the velocity gradient in the direction perpendicular to the flow and  $n$  is the flow behavior index.

### 1.2.2 Applications of Non-Newtonian Fluids

Applications for non-Newtonian include:

- i) Personal Care Product:** Personal care items including toothpaste, shampoo, and lotions use non-Newtonian fluids.
- ii) Paints and Coatings:** Paints, coatings, controlled application, and the avoidance of drips and sagging all involve non-Newtonian fluids.
- iii) Biomedical Engineering:** Numerous biomedical applications, such as tissue engineering, blood flow, and drug delivery systems, are explored and make use of non-Newtonian fluids.
- iv) Geological and Environmental Studies:** Non-Newtonian fluids, such as drilling muds.
- v) Polymer processing:** In procedures like injection molding, extrusion, and 3D printing, many polymer solutions and melts display non-Newtonian behavior.

### 1.3 Peristalsis Flow

The movement of materials through tubular structures is known as peristalsis, which is the coordinated contraction and relaxation of muscles in a wave-like fashion. Circular and longitudinal muscles are sequentially contracted to produce a squeezing force that moves the fluid or substance ahead. Like the gastrointestinal system, the urinary system, and the blood arteries. Swallowing, digesting, urination, and blood circulation are examples from daily life.

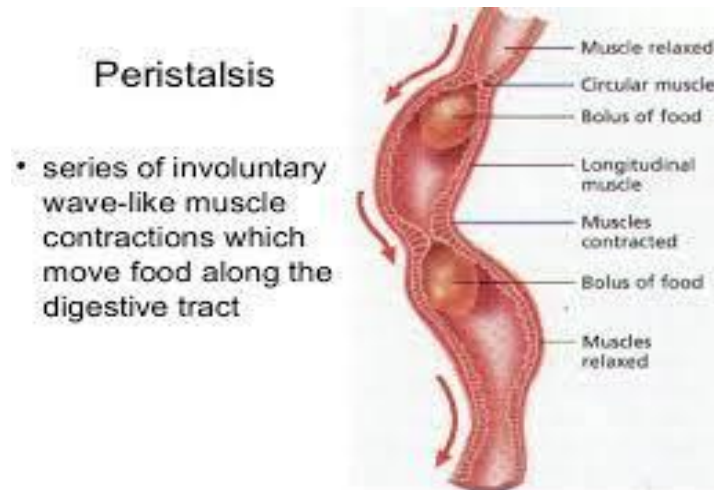


**Figure 1.3** Behavior of the peristalsis.

## 1.4 Slip Flow

Slip flow is a type of fluid flow in which a thin layer of fluid close to a solid barrier moves relative to the boundary or slips in that direction. Slip happens when the fluid near the boundary has a velocity gradient, as opposed to the no-slip situation, when fluid molecules stick to the boundary and travel at the same speed as the boundary. Examples include gas flow in micro channels, thin liquid films and lubrications. Daily life examples include water flow on hydrophobic surfaces, slippery surfaces and air flow surfaces.

Based on how the fluid behaves close to the solid boundary, there are two basic forms of slip flow: velocity slip and temperature slip. Different facets of the relative motion between the fluid and the boundary are described by these many forms of slip flow. These are the several forms of slip flow:

**i) Velocity slip:** It describes a scenario in which there is relative motion at the fluid-solid boundary, causing a gradient in velocity close to the border. In velocity slip, the fluid close to the solid surface moves more slowly than the barrier it does. It develops for a number of reasons, including the presence of a gas layer with low friction or molecular interactions between the fluid and solid surface. It is observed in gas flow at small length scales, such as in micro channels or at low pressures.

**ii) Temperature Slip:** It also goes by the name "thermal slip," and it happens when the boundary between the fluid and the solid has a temperature gradient. In this instance, when

compared to the boundary temperature, the fluid near the solid surface is warmer. It develops as a result of things like gas molecules fitting onto a solid surface or energy transfer at the fluid-solid interface. It is observed in rarefied gas flows or at low temperatures.

Velocity slip, velocity gradient, reduced friction, slip layer thickness, and temperature slip are all characteristics of slip flow. These slip flow applications include microfluidics, gas sensing, drag reduction, and more.

The slip length, which represents the distinctive length scale of the slip effect, can be used to express the slip flow equation. The symbol for the slip length is " $\lambda$ ". The slip flow equation can be found in:

$$u = \lambda * \frac{\partial u}{\partial n},$$

where  $u$  is the slip velocity at a point near the solid boundary,  $\lambda$  is the slip length and  $\frac{\partial u}{\partial n}$  is the velocity gradient going in the solid surface's normal direction.

## 1.5 Wall Properties

Wall properties are the features and qualities of a surface or boundary that influence how fluids or other materials behave when they come into touch with it. These characteristics are significant in a variety of scientific, engineering, and real-world situations. Roughness, porosity, permeability, smoothness, thermal conductivity, reflectivity, etc. are a few examples.

The behavior of fluids or other materials in contact with walls is influenced by a variety of wall features. Here are the main types of wall properties:

**i) Roughness:** It alludes to the texture or imperfections on a wall's surface. It alters the smooth flow patterns, encourages turbulence, and expands the surface area for contact, which all have an impact on fluid flow. Wall roughness is sometimes divided into two categories, microscopic roughness and macroscopic roughness, depending on the height and spacing of the surface flaws.

**ii) Porosity:** It alludes to the existence of voids or unfilled areas inside a wall's construction. It has an impact on a material's permeability and fluid flow. For examples, influencing filtration, absorption, or diffusion process.

**iii) Smoothness:** It alludes to a wall surface that is free of blemishes or roughness. It encourages laminar flow, lessens the effects of friction, etc.

**iv) Adhesion:** It speaks to a wall surface's capacity to adhere or bond to other materials. It is influenced by the wall's material's chemical composition, degree of roughness, and surface energy.

Here are some often occurring characteristics linked to wall characteristics: impact on fluid flow, surface interactions, transport phenomena, surface energy, etc. Wall properties have numerous applications across various fields. The applications are structural support, thermal insulation, acoustic insulation, fire resistance etc.

## 1.6 Phan-Thien-Tanner (PTT) Fluid

The Phan-Thien-Tanner (PTT) fluid rheological model is utilized to explain how viscoelastic fluids, which are non-Newtonian fluids, behave. It is frequently used to examine complicated fluids like suspensions and solutions of polymers. For examples shear thinning or shear thickening and elastic effects. Daily life examples include polymer solutions, biopolymers, suspensions etc.

To accurately represent the viscoelastic behavior of fluids, the PTT model combines viscous and elastic components. It's assumed that the fluid is made up of structures that resemble elastic dumbbells that communicate with one another and the surrounding fluid.

A set of equations that connect the PTT model is explained by the stress tensor ( $\sigma$ ) and the rate of deformation tensor (D). The formula for the equation is:

$$\sigma = \mu * D + \lambda * (tr(D)I - D) + G * H,$$

$$D = \frac{1}{2} * (grad(v) + grad(v)^T),$$

where  $\mu$  is the dynamic viscosity,  $\lambda$  is the relaxation time,  $tr(D)$  is the trace of D, I is the identity tensor, G is the elastic modulus and H is the representing the orientation of the dumbbell-like structures, grad (v) is the tensor of velocity gradient and T is the transpose operation.

## **1.7 Porosity**

The percentage of empty or void spaces within a material is referred to as porosity, and is often expressed as a fraction or percentage. It is a ratio of a substance's total volume to the amount of open space or pores contained in that substance. It is a crucial factor that impacts the way that materials behave physically, mechanically, and when they are transported. Porous substances feature connected or isolated spaces that can contain liquids like air or water. Examples include sponges, soil, bread etc. Daily life examples include porous membranes, insulation materials, sponge and cleaning products etc.

Porosity can be divided into numerous categories according to its source, arrangement, and shape. Porosity has a number of characteristics, including porosity fraction, void size and distribution, permeability, fluid retention and absorption, mechanical strength, and others. Due to its special characteristics, porosity has many uses in a variety of disciplines and businesses. These include filtration and separation, insulation, absorption and absorption, catalyst support, energy storage, and other frequent uses of porosity.

## **1.8 Thesis Organization**

The rest of thesis is organized in the following manner:

### **Chapter 2**

Chapter 2 presents the literature review. This chapter provides an insight of the research relevant to our proposed model.

### **Chapter 3**

Chapter 3 presents the fundamental concepts and basic laws. This chapter provides an insight to the principal definitions that have been utilized to pursue this research work.

### **Chapter 4**

Chapter 4 presents review work. We have reviewed the work done by Sirinivas [36] in detail. The mathematical results are achieved by solving the systems of PDEs and applying perturbation technique. The results are illustrated through graphs.

## **Chapter 5**

Chapter 5 presents the extension work. This chapter includes the extension of the work discussed in chapter 4. We have added porous medium and changed the fluid model. The mathematical results are achieved by applying similar techniques used in the review work. The results are illustrated through graphs.

## **Chapter 6**

Chapter 6 gives the summary of the extension work. This chapter sums up all the results obtained in chapter 5 and also comprises of the future recommendations.

## CHAPTER 2

### LITERATURE REVIEW

#### 2.1 Overview of Related Literature

The synchronized muscle contraction and movement known as peristalsis relaxation that propels materials through the hollow organs of the body. For example, esophagus, stomach, small intestine, large intestine etc. Peristalsis flow is a mechanism in which biological or psychological fluid is driven axially along a tube or duct by sinusoidal waves. Peristalsis is a sequence of coordinated rhythmic contractions of smooth muscles that propel contents through a tube-like design. It is somewhat muscular action that happens often in the ureters, esophagus, and numerous other bodily organs. In the context of fluid flow, peristalsis refers to the movement of a fluid through a tube or channel as a result of the rhythmic contractions of the surrounding muscles.

Mitra *et al.* [1] assumed that the muscle's driving force takes the form of a moderately amplitude sinusoidal wave applied to the channel's flexible walls. Formato *et al.* [2] determined that the best way to simulate peristaltic pump operating conditions additionally to developing a numerical model of the peristaltic pump under consideration would be to improve and optimize the peristaltic pump under consideration's operational features. Tripathi [3] investigated the outcome of the peristaltic flow model for a finite porous channel. The mathematical model from which a set of governing equations in one dimensionless space subject to suitable boundary conditions was generated.

Ansar *et al.* [4] studied an incompressible Williamson fluid is flowing peristaltically through a curved tube while being surrounded by a magnetic field. The issue is explained in terms of its frame of reference for waves. Mathematical model was developed by using induction, linear momentum, and continuity equations. Siddiqui *et al.* [5] explored the impact

of non-Newtonian material coefficients and inertial terms on fluid transport. Moreover, calculating the pressure rise per wavelength with respect to time and flow rate.

Tripathi *et al.* [6] discovered the analysis of viscoelastic fluid flow using the fractional Maxwell model. Takabatake *et al.* [7] elaborated the numerical results for pressure rise and the shearing stress while examining the impacts of the peristaltic wave's geometric shape on the flow field. With high Reynolds numbers, the reflux phenomena is found close to the center axis, whereas at low Reynolds numbers, it is found close to the wall. The distribution of Eulerian velocities determines how a fluid particle moves. Hayat *et al.* [8] explored the Hall Effect. For the free pumping of Hall parameter, analytical solutions have been derived using the regular perturbation method. As the Hall parameter is increased, the mean velocity decreased.

Hayat *et al.* [9] discussed the effects of the effects of Soret, Joule heating, and heat generation on the peristaltic activity of pseudoplastic fluid with Hall current applied in a slanted channel. In this study hall parameter  $m$  and the fluid parameter  $\xi$  both exhibit increasing behavior for a velocity field. Rising Reynolds number values ( $Re$ ), rise the temperature range. The bolus size increases for  $E_1$  and  $E_2$ , while it decreases for  $E_3$ . Rashid *et al.* [10] investigated the impact of peristaltic flow generated by magnetic field for Williamson fluids in the curved channel. In this research it has been found that as  $k$  grows in the pumping zone, pressure rise  $\Delta p$  rises as well, whereas pressure rise  $\Delta p$  decreases for increases in  $k$  in the copumping region. Williamson fluid experiences a greater pressure rise than viscous fluid. In the inner and outer halves of a channel, the velocity profile declines with increasing  $k$  values. The velocity profile increases as  $We$  increases in the inner half of a channel while decreasing in the outer half. Javed and Naz [11] studied the peripheral flow of a realistic fluid in an asymmetric channel affected by elastic walls explorations are investigated in the current investigation. In this the  $a$ ,  $h$ ,  $T$ , and  $\lambda_1$  variations on  $D_1$  are polar opposites of the  $\lambda_2$  variation. The flow reversal occurs close to the boundaries. In comparison to that close to the bottom wall, the flow reversal is substantially greater. When  $\lambda_1 = \lambda_2 = 0$ , the results for a viscous fluid can be determined.

Abd elmaboud *et al.* [12] under the long wavelength assumption, examined at the non-Newtonian pair stress fluid flowing peristaltically in a rotating frame of reference. In this

research under the influence of  $T$  and  $\gamma$ , the pressure gradient,  $\frac{dp}{dx}$ , has a periodic character. Contrary to  $T$ , which has a minor impact on it, the pair stress parameter greatly influences  $\frac{dp}{dx}$ , leading it to decline. Up until a certain point in the peristaltic pumping zone, the pressure rise,  $\Delta p$ , in the retrograde pumping diminishes. At that point, the pumping rate increases by raising  $T$  and  $\gamma$  in the peristaltic and co-pumping regions. Free pumping depends on large values of  $T$  and  $\gamma$  on, where the pressure does not increase against the peristaltic wave's direction and so helps the flow. Noreen *et al.* [13] looked at the peristaltic pump-induced Carreau fluid flow in an inclined, asymmetric conduit. In this concern about the Weissenberg number  $We$  are used to obtaining expressions of interest in their approximative form, such as the temperature distribution, pressure gradient, pressure rise, and velocity profile. It has been found that with rising magnetic field  $\beta$  inclination and Weissenberg number  $We$ , the pumping rate falls. The axial velocity's magnitude is greater in an asymmetrically inclined conduit. In comparison to Carreau fluids, viscous fluid has a higher axial velocity.

Imran *et al.* [14] examined non-Newtonian fluid flowing with peristaltic motion due to an uneven vertical tube using nanoparticle analysis. While in this the behavior for the thermophoresis parameters  $Nt$  is the contrary, the pressure rise reduces as the value of increases  $\alpha$ . As the values of the thermophoresis parameter  $Nt$  increase, the velocity and temperature profiles decrease. While increasing values of the thermophoresis parameter  $Nt$  raise the concentrated nanoparticle field, which lowers for larger values of the Brownian motion parameter  $Nb$ . When the velocity field, Brownian motion parameter  $Nb$ , and thermophoresis parameter  $Nt$  are all raised the thermophoresis parameter  $Nt$  is increased, it decreases. The pressure gradient increases as increases  $\phi$ . When we increase the parameter  $\alpha$ , the frictional forces rise, but for  $Nt$ , the impact is the opposite. Noreen *et al.* [15] performed a research on EOF powered by peristaltic pumping through wavy microchannels has proven possible. On the temperature, pressure gradient, shear stress, Nusselt number, velocity, and material parameters  $A$  and  $B$  have opposing effects. Expanding Eyring parameter, electroosmotic parameter, and averaged temporal flow rate cause axial velocity to increase in the core region of a wavy microchannel. For the pressure gradient, Helmholtz-Smoluchowski velocity, and Eyring fluid parameter is greater, while it decreases for the electroosmotic parameter and the average time flow rate. Nusselt number rises with increasing viscous heating (Brinkman number). Shear stress, electroosmotic parameter, and Helmholtz-Smoluchowski velocity are all closely correlated. Ramesh *et al.* [16] studied the dusty Jeffrey

fluid model's electro-osmotic flow influenced by the magnetic and electric fields in an asymmetric microchannel. Electro-osmotic and Helmholtz-Smoluchowski parameters both significantly hinder the flow. Although the flow is opposed by the zeta potential, slip conditions boost fluid velocity throughout the entire domain. The Helmholtz-Smoluchowski parameter and the electro-osmotic parameter have a tendency to minimize the wall shear stress. On a pressure gradient profile, Helmholtz-Smoluchowski and electro-osmotic parameters behave in opposite ways. The pressure gradient is increased in both the fluid phase and the particle phase by strong slip effects and the fluid parameter, respectively.

Slip flow is a type of fluid flow that occurs near a solid surface, where the fluid particles close to the surface experience a different velocity than those in the bulk of the fluid. This phenomenon arises due to the interaction of the surface and fluid, which can cause the fluid particles near the surface to slow down. Slip flow is often observed in microscale or nanoscale systems, where the fluid-solid interface becomes significant.

Farooq *et al.* [17] analyzed the slip effects at velocity, temperature, and concentration. The magnetic parameter drops as the velocity slip parameter slows centre velocity while the Hall parameter enhances the velocity and temperature. Temperature became increasingly affected by the thermal slip parameter. Non-Newtonian materials have the highest temperature, while Newtonian materials have the lowest. Concentration decreased as the concentration slip parameter enhanced. Shehzad *et al.* [18] examined how the magnetic field affects, which was considered variable, along with the slip parameter on the peristaltic movement of fluid in a curved conduit according to Carreau-Yasuda. In their study, Ali *et al.* [19] investigated a theoretical model that investigated the effects of various variables on peristaltic motion in a curved passage, including fluid rheology, the magnetic field, amplitude ratio, and wall slip. They discovered that when the applied magnetic field was strong enough, the velocity of the fluid in the curved channel adopted a boundary layer characteristic. By the increase in the slip parameter, an increase in velocity at both channel walls was observed. Farooq *et al.* [20] discussed the flow behavior within the channel created by the rapid sinusoidal wave propagation. They concluded that the axial velocity was enhanced because of hybrid nanoparticle insertion into base material also, hybrid nanoparticles upsurged the temperature of the fluid.

Hayat *et al.* [21] Jeffrey nanofluid's peristaltic flow in a conduit with wall characteristics was investigated. They also examined the results of combined convection and ion slip. In this research they observed enhancement in the velocity and decline in the temperature by the expansion of the ion slip and Hall parameters. Imran *et al.* [22] investigated the peristaltic mechanism for the Rabinowitsch nanofluid model in an asymmetric channel to see effects of basic density, Brownian parameter, thermophoresis parameter, and thermal Grashof number. In the study, bvp4c solver is used by Wahid *et al.* [23] to numerically investigate the heat-generating slip flow of a hybrid nanofluid over a permeable exponentially extending or contracting sheet. They discover that with an appropriate amount of suction, dual solutions are possible in the diminishing surface region, but only the first solution is stable. In the shrinking surface region, the local Nusselt number rises while the skin friction coefficient decreases as the velocity slip parameter is increased. In another study, Elmaboudy *et al.* [24] investigated the vertical passageway in which Carreau fluid flows peristaltically. They used the long wavelength approximation to reduce the governing equations to a set of nonlinear PDEs and obtain solutions for the temperature and velocity fields using the homotopy analysis method (HAM).

Akram *et al.* [25] studied a particle fluid suspension model in a non-uniform rectangular duct with slip borders, to examine the impact of lateral walls on peristaltic transport is investigated. While in this in the regions of peristaltic pumping ( $\Delta p > 0; Q > 0$ ) and retrograde pumping ( $\Delta p > 0; Q < 0$ ) the pumping rate increases with an increase in  $M$ ; however, the behavior is precisely the contrary in the copumping ( $\Delta p < 0; Q > 0$ ) zone. In the peristaltic pumping ( $\Delta p > 0; Q > 0$ ) and retrograde pumping ( $\Delta p > 0; Q < 0$ ) areas, the pressure rise decreases while remaining constant in the copumping zone ( $\Delta p < 0; Q > 0$ ). The pressure rise decreases as  $K$  rises throughout the board, while the pressure rises as increases in  $\phi$  to climb. Rani *et al.* [26] examined a MHD elastico-viscous fluid's peristalsis under slip conditions. The present research is predicated on the notion that peristaltic waves have lengthy wavelengths compared to channel width. Due to the symmetry of the flow, the highest flow occurs at the centre line of the parabolic axial velocity profile. All other parameters have the opposite effects on the central line and the walls, with the exception of the amplitude ratio parameter  $\varepsilon$ . Hayat *et al.* [27] looked at how thermal radiation and Joule heating affect the fourth-grade nanoliquid's MHD peristaltic motion. In this velocity increases when and  $\beta_1$  and  $\Gamma$  decreases when  $M$  is higher.  $Nb$  and  $Nt$  have comparable qualitative effects on temperature. The effects of  $\beta_2$  and  $\beta_3$  on temperature and concentration are very

different. Temperature and concentration increase with an increase in  $E_1$  and  $E_2$ , but decline with an increase in  $E_3$ .

Tanveer and Malik [28] investigated the flow of nanofluid in this case is examined in a curved channel with periodic wave transport in light of physiological and industrial peristalsis. The problem has been studied and examined for MHD Ree-Eyring fluid in terms of the effects of thermophoresis, Brownian diffusion, wall compliance, and slip circumstances. There is a drop in temperature and velocity for this Ree-Eyring fluid characteristic. Slip causes a decrease in the mass transfer of nanoparticles while increasing the nanofluid's speed and temperature. The viscosity parameter has an opposite effect on velocity and temperature. The curvature parameter exhibits similar behavior with respect to velocity and temperature, but has the opposite effect on mass transfer. Eldesoky *et al.* [29] studied the peristaltic motion of the fluid through the tube in it also examines fluid flow behavior while examining the effectiveness of various flow and wall features when heat transfer is present. In this that show the compressibility factor, which decreases  $\chi$  as  $Q$  increases, has a substantial effect on the net flux. Additionally, slip condition appears to have an impact on the maximum net flux is observed at  $K_n = 0.15$  (totally slip flow), and it grows as the slip factor,  $K_n$  increases the net flow rate. Wall characteristics, which have a big impact on flow rate behavior, are the important parameter. For example, however, increasing wall stiffness  $K$  and wall tension  $T$  increases net flux, whilst increasing wall damping factor  $D$  decreases net flux (resisting flow), creating the impression of backflow with  $T$  effect being more obvious than  $K$  effect profiles.  $Pr$ ,  $Re$ , and  $\alpha$  are being increased, which is expanding the temperature distribution.

Das *et al.* [30] in an endoscope explored the peristaltic wave motion of electromagnetic nano-blood pumping in the presence of Hall and ion slip currents. The effects of the heat source, the convective boundary condition, and the wall features are all included. The governing equations are made simpler by the long wavelength and low Reynolds number assumptions even if the effects of the Hall and ion slip parameters are in conflict, the blood velocity in axial direction is reduced close to the endoscope wall as a result of an increase in Hartmann number. The hybrid  $AgAl_2O_3$ /blood have the highest axial velocity value, while  $Ag$ -blood has the lowest value. When the clot height, Hall and ion slip parameters, and other factors are increased, the tension on the wall is lowered. However, the opposite behavior is seen as the volumetric concentration of hybrid nanofluid particles rises. Hall and ion slip

currents do not considerably alter the streamlines. Rafiq *et al.* [31] investigated the peristaltic motion of a viscous nanofluid during conduit with a compliant wall under strong magnetic field conditions that result in Hall and ion-slip phenomena. Temperature ( $\theta$ ) and velocity ( $u$ ) show a reduction for improving Hartman number  $M$ . When compared to Hartman number  $M$ , reverse behavior for velocity is observed with rising Hall and ion-slip parameters ( $\beta_e$  and  $\beta_i$ ). Temperatures are increased via stronger thermophoresis and Brownian motion parameters ( $Nb$ ) and ( $Nt$ ). On the concentration profile are diametrically opposed. Streamlines behave differently for  $\beta_e$  and  $\beta_i$ . Riaz *et al.* [32] examined second-order slip at the channel walls in a curved channel for low Reynolds number and long wavelength peristaltic nanofluid flow. Pressure rise profile with  $\beta_1$  increases in half of the domain and lowers in the other half, while  $Da$  and  $\beta_2$  exhibit the opposite behavior. The concentration of nanoparticles rises with  $Nb$  while falling with  $\gamma_1$  and  $Nt$ . The temperature profile  $\theta$  rises with and falls with but increases with  $\beta_1$  and  $\gamma$ . Although it can be shown that the velocity  $u$  increases with the parameters  $\beta_1$  and  $Gr$ , the parameters  $\beta_2$ ,  $Da$ , and  $Gr$  exhibit the opposite behavior. The readings for slip parameters  $\beta_1$  and  $\beta_2$  are completely different.

Vaidya *et al.* [33] investigated the peristaltic flow of Jeffrey nanofluid when subjected to various slip effects. In this research, the velocity and thermal slip parameters improve the velocity profiles, whereas the concentration slip parameter exhibits the opposite behavior. Temperature and velocity both have a decreasing effect on the magnetic parameter. The profiles of velocity and concentration demonstrate the Grashof number's decreasing behavior. Vaidya *et al.* [34] investigated are the various impacts of heat conductivity and viscosity on the peristaltic motion of the Jeffrey liquid. In a non-uniform tube, by virtue of the effects of slip and wall characteristics, the properties of heat/mass transit are examined. The velocity profile in the non-uniform tube increases as a result of the elastic factors  $E_1$  and  $E_2$  providing fewer barriers to fluid motion. Variable thermal conduction and viscosity improve the temperature distribution. When the Schmidt number is bigger, the fluid particles with low density accelerate and acquire higher molecular vibrations, which lower the liquid concentration.

Wall properties in fluid mechanics refer to the characteristics of a solid surface that is in contact with a fluid flow. These characteristics are crucial in influencing how the fluid behaves close to the wall, as well as the overall flow behavior. There are several different wall

properties that are important to consider in fluid mechanics, including: roughness, thermal properties, chemical properties, geometric properties. Understanding the properties of walls is important for a variety of applications in fluid mechanics, including in the design of engines, pipes, and heat exchangers. Engineers and researchers must carefully consider the various wall properties in order to optimize the performance of these systems.

The channel wall characteristics on nanofluid peristaltic transport are investigated by Mustafa *et al.* [35]. Srinivas *et al.* [36] presented their research in how wall characteristics affect the peristaltic flow of MHD fluid. Slip effects were also considered in this study. Abd Elnaby *et al.* [37] inspected the mean velocity at the channel's boundaries. Hayat *et al.* [38] studied third-grade fluid flows peristaltically in a curved arrangement to transfer heat and mass. Under small Deborah number approximations, a perturbation solution was calculated. It was concluded that additionally, fluid reaches its maximum speed at the centre of the curved channel, when compared to a curved channel, the straight path has a larger heat transfer coefficient. Hayat and Hina [39] discussed the wall properties' impact on the Maxwell fluid.

Kothandapani *et al.* [40] examined MHD peristaltic flow with the lubrication approach on the impact of wall characteristics and heat transfer. Radhakrishnamacharya *et al.* [41] clarified the movement of a sticky incompressible Newtonian fluid in a 2D regular channel with wall impacts, the interaction of peristalsis with heat transfer has been examined. Velocity, warmth and heat transmission solutions have been found in their perturbation forms. Hina *et al.* [42] investigated pseudoplastic fluid's heat and mass analysis. The perturbation method was used to study the stream function, temperature, and analytical concentration expressions.

Kayani *et al.* [43] using a novel method, studied the peristaltic flow of a non-Newtonian nanofluid obeying the Carreau-Yasuda (CY) model through a single wall channel is calculated. A four parameter Carreau-Yasuda (CY) model, which defines the fluid's shear thinning/thickening feature, is used to construct momentum analysis. In this the perceived viscosity grows as the flow behavior index  $n$  rises, causing fluid to encounter more resistance. It turns out that axial velocity  $u$ , is a decreasing function of  $n$ . The axial velocity profile is similarly influenced by the parameter  $\beta$ . As parameter  $n$  (which is proportional to perceived viscosity) increases, the temperature in the channel decreases. When partial-slip situation is present, axial flow is accelerated. Naturally, the axially directed flow is more favorable due to flexibility of the wall and wall mass per area. The temperature profile is improved via

thermophoresis and Brownian diffusion, respectively. Wall elastic properties often boost the temperature and rate of heat transfer from the walls. There is a little area close to the upper wall that consistently  $\phi$  turns negative. Bhatti *et al.* [44] studied the effects of heat transfer and Hall current on peristaltic "sinusoidal" motion of particle-fluid over a uniform channel have been investigated. For high Hartmann numbers, the fluid's velocity falls and the Hall effect produces the opposite behavior. The velocity proficiency is also improved by the larger particle volume fraction has an impact. Wall stiffness and the wall tension parameter enhance the velocity profile. Similar to how the temperature is prone to increasing when the Prandtl number is high.

Nisar *et al.* [45] investigated the MHD peristaltic flow of the Eyring-Powell nanofluid in a channel, we examine the effects of thermal radiation and Joule heating. By taking into account effects along a homogeneous channel of wall and convective qualities, heat and mass transport features are examined. In this velocity increases with bigger  $A$  and  $\varepsilon$  decreases with increasing  $M$ . Prandtl and Eckert numbers behave similarly to one another as the temperature changes. The temperature is raised for  $Nb$  and  $Nt$ .  $E_3$  behaves differently from  $E_1$  and  $E_2$  in terms of concentration and temperature. Iftikhar *et al.* [46] looked at the impacts of thermal and velocity slip on a  $Cu$  water nanofluid in a non-uniform inclined tube. The velocity profile decreases as the nanoparticle volume fraction values rise. Near tube's end, viscous forces are more prevalent, which causes the velocity profile to fall; in contrast, buoyant forces are more prevalent in the middle of the tube, where velocity profile contributes to an increase. The flow encounters reduced resistance as a result of the wall's characteristics, and as a result, velocity rises with rising values for viscous damping force, rigidity, and stiffness parameters. Abbas *et al.* [47] analyzed the peristaltic transport of Casson fluid with mass and energy transfer under the effect of slip conditions. Additionally considered are the impacts of thermal radiation and wall features. For improved the parameter values  $\gamma_1$ ,  $Pr$ ,  $Du$ , and  $B$ , fluid temperature rises; however, the impact on the parameter  $R$  is the opposite. It grew, nonetheless, for the parameter  $R$ . Enlarged values of  $\zeta$  result in an increase in the velocity profile. When  $E_1$ ,  $E_2$ , and  $E_3$  have larger values, the velocity rises. It declined, though, for the parameter  $R$ .

Eldesoky *et al.* [48] presented a study on the peristaltic blood flow that occurs within an individual's circulatory system. When blood flowed through a porous medium in a flexible tube while being subjected to an outside magnetic field, it was represented by Maxwell fluid.

In this the net flow rate is decreased as a result of the wall dampening. The net flux increases as the porosity parameter is raised. As a result of the declining flow rate profiles, the backflow is boosted by lengthening the relaxation period and introducing a slip condition. The wave number and the greatest flow-capable net flow rate, have a proportionate relationship. After that, the relationship changes to an inverse relationship, at which point the backward flow may start to occur. Vaidya *et al.* [49] explored how a Rabinowitsch liquid is transported peristaltically in an inclined channel while having a compliant wall and changeable liquid properties. As it expands, it becomes more accurate in its estimation of varying viscosity, angle of inclination, velocity, and temperature field of dilatant liquids decreases for liquids that are Newtonian and pseudoplastic. Variable viscosity enhances fluid's temperature and velocity. Compared to Newtonian and pseudoplastic fluids, the dilatant fluid has a poor estimation of temperature and velocity. Variable viscosity reduces the amount of pressure rise and frictional force for a liquid that is shear thinned. The influence of  $E_1$  and  $E_2$  enhances the velocity and temperature profiles for Newtonian and pseudoplastic liquids., whereas it lessens for  $E_3$ ,  $E_4$ , and  $E_5$ .

Khan and Tariq [50] examined how the features of the walls affected the peristaltic motion of the dusty Walter's B fluid. The wave length is supposed to be lengthy, and the outcomes are examined for various factors. As the viscoelastic parameter  $\kappa$  is raised for the solid particles, on the right side, the bolus' size increases. Both the confined bolus of liquid and solid particles expands as the wave number  $\delta$  rises. The fluid and solid particle velocities increase as the values of various parameters rise the size of the bolus grows on the right-hand side. The flow rate of both liquid and solid particles increases as the values of  $E_1$ ,  $E_2$ , and increase. The flow rate of dust particles is improved by rising  $\delta$ . Rafiq and Abbas [51] investigated the thermal radiation and viscous dissipation effect on the peristaltic transport of the Rabinowitsch fluid model via an inclined tube with a non-uniform slope. In each of the three scenarios  $\alpha$ , the velocity increases when the deviations are increased. For all three examples, the temperature profile enlarges by increasing  $Br$ ; however, for the parameter  $R$ , the behavior is the opposite. Higher values of  $E_1$  and  $E_2$  increased the number of streamlines in the shear thickening case due to the liquid circulation, but the trend for  $E_3$  was in the reverse direction. For higher deviations of  $E_1$ ,  $E_2$ , and  $E_3$  for viscous liquid, the number of streamlines remains unchanged, but their size significantly increases.

The model by Phan-Thien-Tanner (PTT) uses a mathematical model to explain how complex fluids, particularly polymer solutions and suspensions, behave. Long, flexible polymer chains suspended in a solvent are considered by this non-Newtonian fluid model. And assume that the fluid consists of a three-dimensional network of polymer chains, which interact with each other and with the solvent molecules. The PTT model has been used to study many phenomena, including shear thinning, viscoelasticity, and non-Newtonian flow. It has applications in polymer processing, biofluid dynamics, and chemical engineering.

Hayat *et al.* [52] demonstrated that the investigation of such flow scenarios is the primary goal of this investigation. For a Newtonian fluid, peristalsis must exert more force against greater pressure rise in the pumping zone than it does for linear PTT fluid. There is no distinction between linear PTT fluid and Newtonian fluid in the free pumping and co-pumping zone. In this the exponential PTT model's shear stress is larger than the linear PTT models. Akbar *et al.* [53] investigated the PTT nanofluid's peristaltic flow in a diverging tube. Temperature and concentration profile homotopy perturbation solutions were evaluated, while velocity profile exact solutions were computed.

The electro-osmotic peristaltic PTT flow is studied by Hussain *et al.* [54]. Using well-known long wavelength and low Reynolds number approximations, the governing equations are streamlined. Butt *et al.* [55] examined how the dynamics of a PTT fluid model in a uniform horizontal cylinder are affected by heat transfer. Formulas generated for the fluid model consider the velocity, temperature, and pressure slope. It has been found that the velocity is linear to the mean flow rate and inversely to the Weissenberg number, reaching its highest value near the tube's center. Hayat *et al.* [56] examined the peristaltic action in the intestines, and small blood artery is made easier using PTT fluid.

Sarkar *et al.* [57] investigated the pressure-driven electrohydrodynamic streaming potential including analytical and semi-analytical techniques for Phan-Thien-Tanner fluids in a microchannel. Using the full-scale solution to the Poisson-Boltzmann equation, we can create a closed-form numerical model for the dimensionless electrical potential distribution, velocity profile, and volumetric flow rates. In this case, by intensifying surface charge, the flow field is enlarged. Vajravelu *et al.* [58] examined the peristaltic movement of PTT fluid through a porous, elastic medium while describing the long wavelength and low Reynolds number assumptions. Ali *et al.* [59] discovered the long wavelength and low Reynolds

number assumptions for the peristaltic movement of PTT fluid in an elastic medium with porous material. The lubrication theory's postulates have led to a simplification of the basic equations that describe blood flow. Vaidya et al. [60] investigated how several significant constraints affect the velocity of the non-Newtonian MHD Phan-Thien-Tanner fluid, temperature, concentration, and phenomena of entrapment. This model can be used in a variety of clinical settings, including catheters, cancer therapy, drug delivery, etc.

Prakash and Tripathi [61] studied the EDL phenomena, rheological effects, and magnetic field effects affect the peristaltic pumping of Phan-Thien-Tanner (PTT) fluids in an asymmetric microchannel. The solutions for the stream function, axial velocity, pressure gradient, and shear stress perturbation were discussed. The effects of the Helmholtz-Smoluchowski velocity, Hartmann number, PTT fluid parameter, electroosmosis parameter, and rheological parameter have been highlighted. In this the Weissenberg number ( $We$ ), a rheological parameter, causes the axial pressure and velocity gradient to decrease over the whole asymmetric channel. The PTT fluid parameter ( $\varepsilon$ ) has a significant impact on the gradient of pressure and axial velocity. The electroosmosis parameter ( $\kappa$ ), controls the EDL phenomenon, which modifies the peristaltic pumping and alters the axial velocity and pressure gradient. While the bending stress increases with EDL thickness, it decreases with increased magnetic field effects.

Faraz *et al.* [62] looked for a travelling wave solution in order to study the magnetohydrodynamic (MHD) flow of the Phan-Thien Tanner fluid (PTT). Using well-known methods such as He's semi-inverse approach and  $G'/G$ -expansion, a precise solution for the viscoelastic model has been shown. Instead of taking into account the wave transformation in this study, the system has been transformed into an ordinary differential equation by the introduction of dimensionless variables. In order to solve problems involving non-Newtonian fluids, it is discovered that the  $G'/G$ -expansion method and the He's semi inverse method are reliable approaches. Siddiqui *et al.* [63] investigated the PTT fluids' concentric n-layer flow through a cylindrical tube. Simulated and solved multiple layer steady flow of immiscible PTT fluids flowing concentrically through a conduit. Volume flow rates and velocity profiles have reported exact solutions. In this the conclusions are universal in that they can be utilized with the linear PTT model to derive identical quantities. Additionally, the results are not restricted to two fluid layers. Fluid velocity theories are significantly

influenced by non-Newtonian factors. When optimizing flow rates is needed with constrained pumping pressure gradients, flow rates have a wide range of industrial applications.

Porous refer to a material or surface that has small holes and spaces that allow liquids, gases, or particles to pass through it. The degree of porosity can vary depending on the size and arrangement of the pores and it can have significant effects on the material's properties, such as its strength, durability, and ability to absorb or filter substances.

Ellahi *et al.* [64] investigated the peristaltically flowing Jeffrey fluid. The effects of slip, porosity, low Reynolds number, and long wavelength limitations were incorporated. With time, the strength of the pressure gradient gradually weakens in accordance with rising slip and porosity parameter values. The trend of the velocity profile for the porosity parameter and the slip parameter, however, is completely different; in each domain, the fluid's velocity decreases as the porosity parameter rises. It is crucial to remember that by setting the non-Newtonian Jeffrey fluid parameter to zero, one can achieve the Newtonian fluid result. Vaidya *et al.* [65] examined the non-Newtonian fluid's magneto-hydrodynamic peristaltic flow in an asymmetric tapered channel with porous material. It is believed that the Jeffrey model, which has changing viscosity, can explain non-Newtonian behavior. In the zone of enhanced pumping, the magnetic parameter increases pressure while also reducing fluid velocity. For all the parameters examined, the increase in pressure and the behavior of imaginary forces. It is found that the axial fluid velocity in the centre of the channel is increasingly affected by greater values of variable viscosity. It is demonstrated that as the medium gets hotter and less porous, the fluid velocity increases. Lower velocity and higher temperature are caused by larger non-uniformity parameter values in the centre of the tapered channel.

Hasona *et al.* [66] examined the effect of temperature-dependent viscosity on Jeffrey nanofluid peristaltic flow in an asymmetric channel is investigated. The discussion of mixed convective peristaltic transport of incompressible Jeffrey nanofluid temperature-dependent viscosity parameters takes into account the effects of Joule heating and porous media effects. Pressure gradient decreases with an increase in  $\beta$ . Higher temperatures give molecules more energy, which leads to a decrease in the variable viscosity parameter and more easily flowing liquid. To obtain more realistic results, all nondimensional characteristics that depend on viscosity should be taken into account as variables when the viscosity is responsive to temperature variation. Vaidya *et al.* [67] studied the effect of varying thermal conductivity is

studied on the MHD peristaltic flow. The characteristics of heat and mass transmission are investigated through a uniform porous channel in relation to the effects of convective and wall properties. In this temperature and velocity profiles are decreased by the magnetic parameter. The wall tension and mass characterization parameter enhance the velocity and temperature distribution. The Biot number has a decreasing relationship with the temperature profile. As the temperature profile rises as the variable thermal conductivity value does.

Riaz *et al.* [68] studied how a nanofluid flows peristaltically through a porous conduit. Low Reynolds number and a long wavelength Simplified modelled equations are re-approximated. The velocity field grows as  $Nt$ ,  $Q$ ,  $Gr$ , and  $k$  are increased. The temperature profile exhibits an increase with rising  $Nb$  and  $\phi$ . Increases in  $Gr$ ,  $\phi$  and  $Nt$  are associated with a rise in  $k$  and  $\lambda_1$  and a decrease in the pressure gradient, respectively. At  $x = 0.5$ , the flow encounters its greatest resistance; at  $x < 0.2$  and  $x > 0.8$ , the pressure gradient is minimal. Noreen *et al.* [69] investigated the topic is heat effects in non-Darcy porous media electro-osmotic flow that are exacerbated by peristaltic pumping. For higher values of the Forchheimer and Darcy numbers, the axial velocity falls in the conduit's middle region while increasing near the conduit wall. The energy loss brought on by the presence of the Joule heating influence is particularly impacted by the heat transfer rate. Determining how well electro-osmosis and peristalsis are established in bio-micro-fluidics systems.

Manjunatha *et al.* [70] examined the effects of fluctuating heat conductivity and viscosity on peristaltic flow are investigated in this paper. A non-uniform porous channel is used to study the transmission of mass and heat.  $\alpha_1$  and  $Da$  accelerate the fluid velocity close to the channel walls, where their effects on velocity are more pronounced. While higher values of the wall property parameters  $E_3$ ,  $E_4$ , and  $E_5$  cause a decrease in velocity and temperature, the wall property parameters  $E_1$  and  $E_2$  are crucial in the development of the temperature and velocity profiles. When the prices of  $\gamma$ ,  $\alpha_1$ ,  $Br$ , and  $\lambda_1$  increase, the temperature rises. Reduced temperature profiles are caused by the rising value of the Biot number. The concentration profiles behave in the opposite way from the temperature profiles. The concentration profiles decrease as a result of the Soret and Schmidt numbers.

## CHAPTER 3

### FUNDAMENTAL CONCEPTS AND BASIC LAWS

#### 3.1 Definitions

##### Fluid

The property of flowing and taking on the shape of its container distinguishes the state of substance known as fluid. Because their particles are loosely structured and have the potential to flow past one another, fluids can change their shape and volume in contrast to solids, which have a fixed shape and volume. Examples of fluids includes: water, oil, milk, gasoline, honey etc. Here are some common daily life examples of fluids: drinking water, showering, cooking, swimming, weather phenomena, blood circulation, flue etc.

##### 3.1.1 Types of Fluids

Liquids, gases, Newtonian fluids, non-Newtonian fluids, rheopectic fluids, and thixotropic fluids are a few examples of typical fluid types.

**i) Newtonian Fluids:** Newtonian fluids have a constant viscosity, which means that no matter how much shear stress is applied, their flow resistance remains constant. Water and most common liquids are examples of Newtonian fluids.

**ii) Non-Newtonian Fluids:** Non-Newtonian fluids have varying viscosities based on the shear stress that is being applied. Their flow behavior can vary depending on the circumstances. Examples include ketchup, toothpaste, paint, and blood.

**a) Shear-thinning or Pseudoplastic Fluids:** When these fluids are subjected to shear stress, their viscosity decreases. The more agitated you are, the easier they flow. Examples include certain food sauces and polymer solutions.

**b) Shear-thickening or Dilatant Fluids:** When these fluids are under shear stress, they become more viscous. Their viscosity increases with force or agitation. A common example is a mixture of cornstarch and water.

**c) Bingham Plastic Fluids:** When a specific stress threshold is reached, Bingham plastic fluids start to act like solids. When this point is reached, they start to flow like a thick liquid. Examples include certain types of drilling fluids and toothpaste.

**iii) Rheopectic Fluids:** When rheopectic fluids are continuously subjected to shear stress, they gradually grow more viscous. Over time, they show a rising resistance to flow. Some mixtures of clay and water exhibit rheopectic behavior.

**iv) Thixotropic Fluids:** When continuously subjected to shear stress, thixotropic fluids gradually become less viscous. Over time, they show less flow resistance. Certain types of paints and gels demonstrate thixotropic behavior.

**v) Liquids:** Fluids with a known volume but no set shape are considered to be liquids. They can flow and assume the form of the vessels they are in. Examples include water, oil, milk, and beverages.

**vi) Gases:** Fluids known as gases lack a set shape or precise volume. They enlarge to take up the entire area that is available. Examples include air, oxygen, nitrogen, and carbon dioxide.

### 3.1.2 Applications of Fluid

Due to their special qualities and ability to flow, fluids are used in a wide range of fields and industries. Here are some notable applications of fluids:

**i) Manufacturing and Industry:** A lot of manufacturing processes require fluids. They are used in metalworking processes like drilling, milling, and machining as coolants, lubricants, and cutting fluids. Additionally, industrial fluids support hydraulic systems, numerous mechanical operations, and heat transfer.

**ii) HVAC and Refrigeration:** Heating, ventilation, air conditioning (HVAC), and refrigeration systems use fluids like refrigerants. To transport heat and control temperatures in structures, residences, and commercial areas, these fluids go through phase shifts (from liquid to gas and vice versa).

**iii) Food and Beverage Industry:** In the food and beverage sector, fluids are employed extensively. They act as preservatives, solvents, and additives. Examples include water, oils,

sauces, beverages, and liquid food processing operations like mixing, cooking, and fermentation.

## 3.2 Hydrostatic Stress Condition

The term "hydrostatic stress condition" describes a fluid under conditions of uniform stress in all directions. In other words, the fluid's pressure is constant throughout. When a fluid is at rest and not being affected by shear forces, this situation occurs. Examples of hydrostatic stress conditions include: pressure in a fluid at rest, atmospheric pressure, hydraulic systems, and deep-sea hydrostatic pressure. The hydrostatic stress state, where pressure within a fluid is uniform in all directions, occurs frequently in everyday life. Here are some daily life examples: drinking from a straw, bathing or showering, water towers, diving, and watering plants with a hose.

### 3.2.1 Types of Hydrostatic Stress Condition

A state of stress in a fluid when the stress is uniform in all directions is referred to as the hydrostatic stress condition. Although there aren't any particular "types" of hydrostatic stress conditions, understanding its various facets or components might be useful. Here are some concepts related to hydrostatic stress: hydrostatic pressure, pascal's law, pressure gradient and buoyant force.

### 3.2.2 Applications of Hydrostatic Stress condition

Its applications include:

- i) Engineering and Civil Construction:** When designing and constructing structures that use fluid pressure, consideration of the hydrostatic stress state is essential. Examples include: dam, retaining walls, and underground structures.
- ii) Hydraulic Systems:** In hydraulic systems, hydrostatic pressure is used to deliver force and power. Applications include: hydraulic machinery and hydraulic lifts.
- iii) Medical Applications:** When administering intravenous fluids and measuring blood pressure, the hydrostatic stress state is crucial in medical settings.

**iv) Hydrogeology and Geotechnical Engineering:** In the domains of hydrogeology and geotechnical engineering, groundwater flow and slope stability, an understanding of the hydrostatic pressure of groundwater is essential.

### 3.3 Fluid Mechanics

The area of physics and engineering known as fluid mechanics is concerned with the behavior, characteristics, and motion of fluids, including gases and liquids. It focuses on understanding how fluids react to different forces and how they flow under diverse circumstances. A framework for comprehending and analyzing fluid behavior, such as fluid motion, fluid forces, and the rules regulating fluid flow, is provided by fluid mechanics. Fluid mechanics encompasses several key areas: fluid statics, fluid dynamics, fluid kinematics, and fluid conservation laws. Here are some examples of how fluid mechanics i.e. blood flow in a human body etc. Here are some everyday examples where fluid mechanics is at work: faucet flow, traffic flow, drinking with a straw etc.

#### 3.3.1 Types of Fluid Mechanics

Fluid mechanics can be broadly categorized into two main branches:

- i) Fluid Statics:** Fluids in equilibrium or at rest are the focus of fluid statics. It focuses on the investigation of the pressure distribution within a fluid at rest as well as the forces acting on fluids. Key concepts in fluid statics include pressure, buoyancy, hydrostatic equilibrium, and the determination of forces on submerged surfaces.
- ii) Fluid Dynamics:** Fluids in motion are the focus of fluid dynamics. It entails the investigation of fluid forces and motion, including examination of fluid flow patterns, pressure distributions, velocity profiles, and the guiding principles of fluid motion.

Fluid dynamics can be further divided into:

**a) Incompressible Flow:** The term "incompressible flow" describes the movement of fluids that do not significantly alter their density. It is suitable to low-speed gas flows and liquids with constant density. Examples include water flow in pipes, flow around submerged objects, and flow in hydraulic systems.

**b) Compressible Flow:** Fluids that undergo large pressure and temperature fluctuations, as well as changes in density are considered to be examples of compressible flow. It is relevant

in high-speed gas flows, such as supersonic and hypersonic flows. Examples include the flow around aircraft, rocket propulsion, and gas dynamics in turbo machinery.

**c) Viscous Flow:** Fluids with internal friction and flow resistance are the subject of viscous flow. Viscosity's impacts on fluid behavior and flow characteristics are taken into account. Examples include the flow of liquids with high viscosity, lubrication systems, and the study of boundary layers in fluid flow.

**d) Turbulent Flow:** Fluid flow that is chaotic and erratic is referred to as turbulent flow. It entails the investigation of intricate vortices, alterations, and energy loss inside the flow. Turbulent flow is encountered in many practical applications, such as air flow around vehicles, rivers, and atmospheric phenomena.

**e) Multiphase Flow:** Multiphase flow, such as gas-liquid flow or solid-liquid flow, deals with the simultaneous flow of multiple phases. It entails researching how interactions between various phases affect how fluids behave. Examples include two-phase flow in pipelines, bubble columns, and sediment transport in rivers.

### 3.3.2 Application of Fluid Mechanics

Numerous real-world applications of fluid mechanics exist in numerous disciplines. Here are some notable applications: civil engineering, environmental engineering, energy and power generation, HVAC system, weather prediction etc.

**i) Civil Engineering:** Water supply and distribution, sewage, and drainage system design all make use of fluid mechanics. It helps in analyzing the flow of water in rivers and channels, designing dams and reservoirs, and studying flood control measures.

**ii) Energy and Power Generation:** Power generation and energy production both depend on fluid dynamics. It is used in the design and analysis of turbines, pumps, and hydraulic systems. It also plays a role in understanding fluid flow in oil and gas pipelines, optimizing wind turbine efficiency, and studying tidal and wave energy conversion.

**iii) Weather Prediction:** Numerical weather prediction models simulate air circulation, examine weather patterns, and forecast weather conditions using the principles of fluid mechanics. It helps in understanding atmospheric dynamics, analyzing air mass movements, and predicting weather phenomena.

## 3.4 Newtonian Fluids

Newton's law of viscosity is followed by Newtonian fluids, which have linear connections between shear stress and shear rate. This law states that the shear stress within a fluid is directly proportional to the rate of deformation or shearing of the fluid. In other words, regardless of the applied shear stress or shear rate, Newtonian fluids' viscosity is constant. Examples of Newtonian fluids include: water, air, oil, glycerin, motor oil, honey, ethanol, etc. Newtonian fluids are quite common in our daily lives. Here are some everyday examples of Newtonian fluids: water, milk, cooking oil, paint, shampoo, etc.

### 3.4.1 Types of Newtonian Fluid

Based on their flow behavior and viscosity characteristics, Newtonian fluids can be divided into various categories. Here are some common types of Newtonian fluids: low-viscosity Newtonian fluid, high-viscosity Newtonian fluid, Newtonian gases, pure liquids, simple solutions etc.

Newton's law of viscosity, which states that the shear stress ( $\tau$ ) is inversely proportional to the shear rate ( $\frac{du}{dy}$ ) or velocity gradient, governs Newtonian fluids:

$$\tau = \mu * \left(\frac{du}{dy}\right),$$

where  $\tau$  represents the shear stress (force per unit area) acting on the fluid,  $\mu$  is the dynamic viscosity, which is a constant for Newtonian fluids and  $\left(\frac{du}{dy}\right)$  denotes the shear rate or velocity gradient (change in velocity with respect to distance or height).

Regardless of the applied stress or shear rate, the dynamic viscosity remains constant and the relationship between shear stress and shear rate continues to be linear.

### 3.4.2 Applications of Newtonian Fluid

Newtonian fluids are used in a variety of real-world situations. Some notable applications include:

**i) Paints and Coatings:** The formulation of many paints and varnishes is based on Newtonian fluids. The consistent viscosity allows for precise application using brushes, rollers, or sprayers. A consistent and smooth finish is ensured by Newtonian behavior.

**ii) Printing Industry:** Inks used in the printing sector are frequently Newtonian fluids. The steady viscosity makes it possible to transfer ink onto substrates with accuracy and consistency during printing procedures.

**iii) Biomedical Applications:** Applications in biology and medicine use Newtonian fluids. They are employed in drug delivery systems, medical imaging contrast agents, and as blood plasma substitutes. For controlled and targeted administration, Newtonian fluids' predictable flow behavior is essential.

**iv) Environmental Engineering:** Applications of environmental engineering use Newtonian fluids. They are used in wastewater treatment processes, sedimentation, and filtration systems.

### 3.5 Non-Newtonian Fluids

A fluid type whose viscosity or flow behavior is not characterized by Newton's law of viscosity is known as a non-Newtonian fluid. Non-Newtonian fluids display varying viscosity or flow characteristics under various conditions, in contrast to Newtonian fluids, which have a constant viscosity independent of the applied shear stress or rate of deformation.

Different viscosity behaviors, such as shear-thinning, shear-thickening, yield stress, or viscoelasticity, can be seen in non-Newtonian fluids. A non-Newtonian fluid's viscosity may alter with shear rate, shear stress, or time.

There are numerous types of non-Newtonian fluids that display various viscosities and flow characteristics depending on the environment. Here are some common examples: ketchup, cornstarch, water mixture, shampoo, toothpaste, paint etc. Numerous parts of daily life involve non-Newtonian fluids. Here are some everyday examples of non-Newtonian fluids: shaving cream, body lotions and creams, hair gel, silly putty, slime etc.

### 3.5.1 Types of Non-Newtonian Fluids

There are several types of non-Newtonian fluids, each exhibiting distinct flow behaviors. Here are some common types: shear-thinning fluids, shear-thickening fluids, Bingham plastics, thixotropic fluids, rheopectic fluids, viscoelastic fluids etc.

Non-Newtonian fluids feature more intricate correlations between shear stress and shear rate, and a variety of mathematical models can be used to analyze their flow behavior. Some common models include:

### 3.6 Shear Stress

The force per unit area acting perpendicular to the plane of deformation in a material or fluid is measured as shear stress. It symbolizes a material's resistance to internal friction or shear deformation. Mathematically, shear stress  $\tau$  is defined as the ratio of the applied force (F) to the area (A) over which the force is applied:

$$\tau = \frac{F}{A}.$$

Here are some examples to illustrate shear stress: cutting with scissors, flow of fluids in pipes, deformation of solids etc. Here are some daily life examples that involve shear stress: walking or running, brushing hair, cutting or chopping food, mixing ingredients etc.

#### 3.6.1 Types of Shear Stress

Different kinds of shear stress can be recognized in the context of both fluid mechanics and solid mechanics. Here are some common types of shear stress: simple shear stress, shear stress in fluids, maximum shear stress and shear stress distribution.

Shear stress is influenced by the fluid's viscosity and the rate of deformation. The formula for shear stress in fluids is given by:

$$\tau = \mu * \left(\frac{du}{dy}\right),$$

where  $\tau$  represents shear stress,  $\mu$  is the dynamic viscosity of the fluid, and  $\left(\frac{du}{dy}\right)$  is the velocity gradient or rate of deformation along the direction perpendicular to the flow (y-direction).

### 3.6.2 Applications of Shear Stress

Numerous uses of shear stress can be found in many different fields. Here are some common applications of shear stress:

- i) Material Testing:** In order to ascertain the mechanical characteristics and behavior of materials, shear stress is frequently utilized in material testing. Shear stress is applied during testing procedures like shear tests, torsion tests, and rheological tests to gauge properties like shear strength, shear modulus, and viscosity.
- ii) Geological Processes:** Numerous geological processes, including faulting, earthquakes, and tectonic plate movements, include shear stress. Seismic activity can come from the building and release of shear stress along fault lines, which can cause rock displacement and deformation.
- iii) Biomechanics and Human Movement:** Shear stress is investigated in biomechanics in relation to human mobility and the mechanical forces that the body encounters. In disciplines like sports science and rehabilitation, it is critical to comprehend joint mechanics, muscle function, and injury prevention.

### 3.7 Shear Strain rate

Shear strain rate is a measurement of how quickly a substance or fluid deforms under shear. It calculates the rate of shape or deformation change over time.

Shear strain rate ( $\dot{\gamma}$ ) is mathematically defined as the derivative of shear strain with respect to time ( $t$ ).

$$\dot{\gamma} = \frac{dr}{dt}$$

Here are some examples to help illustrate shear strain rate: fluid flow, metal cutting, polymer processing, earthquake etc. However, there are examples from daily life when shear strain rate indirectly contributes to or influences specific events. Pouring a viscous liquid, stirring a thick mixture, spreading a tooth paste, brushing teeth etc.

### 3.7.1 Types of Shear Strain Rate:

Depending on the particular environment and the kind of deformation, it can change. Here are some common types of shear strain rate: constant shear strain rate, shear strain rate gradient, apparent shear strain rate, local shear strain rate etc.

The shear strain rate can be determined using the following formula in the situation of simple shear deformation, when the material is deformed along a single plane:

$$\gamma = \frac{V}{h},$$

where  $\gamma$  is the shear strain rate,  $V$  is the shear velocity and  $h$  is the distance between parallel surfaces.

### 3.7.2 Application of Shear Strain Rate

Shear strain rate is useful in many different sectors, especially those that focus on the flow and deformation of materials. Here are some applications of shear strain rate:

- i) Metal Forming:** Shear strain rate impacts material flow and deformation in metal forming operations like rolling, forging, and extrusion. For the produced metal components to have the correct shape and qualities, it is crucial to comprehend and manage the shear strain rate.
- ii) Geotechnical Engineering:** Geotechnical engineering, in particular the study of soil and rock mechanics, makes use of shear strain rate. It is useful for analyzing slope stability, subsurface excavations, and the stability and deformation of soil layers. The behavior of these materials under applied loads is influenced by the rate of shear strain, which can aid in predicting eventual failure or deformation.
- iii) Materials Testing:** When evaluating materials to determine their mechanical characteristics and behavior, shear strain rate is a factor. Shear strength, yield stress, and

viscoelastic qualities can all be measured using testing techniques like shear tests, torsion tests, and rheological tests.

## 3.8 Viscosity

A fundamental characteristic of fluids called viscosity describes how they resist flowing or deforming when shear stress is applied. It measures the internal friction inside the fluid and establishes how easily a fluid may flow. The resistance to flow of a fluid increases with increasing viscosity.

Examples of viscosity include: honey, water, motor oil, paint etc. Here are a few examples from everyday life to help you understand the notion of viscosity: pouring syrup, spreading jam, painting with different types of paints, toothpaste squeezing, shampoo hairing etc.

### 3.8.1 Types of Viscosity

Viscosity can be classified into different types based on its behavior and characteristics. Here are some common types of viscosity: dynamic or absolute viscosity, kinematic viscosity, and apparent viscosity, shear-thinning and shear thickening viscosity etc.

### 3.8.2 Application of Viscosity

As a fundamental characteristic of fluids, viscosity has many practical uses in a variety of industries. Here are some common applications of viscosity:

**i) Petroleum and Petrochemical Industry:** The oil and gas sector depends on viscosity. It aids in defining and categorizing various varieties of crude oil and petroleum products. Viscosity is critical for designing pipelines, optimizing fuel combustion, and formulating lubricants.

**ii) Pharmaceutical and Cosmetics:** When it comes to the creation and formulation of medications and cosmetics, viscosity is crucial. Topical creams, ointments, lotions, and gels

experience changes in consistency, spreadability, and stability as a result. Viscosity measurements aid in ensuring the performance and quality of a product.

**iii) Material Testing:** Viscosity measurements are used in material testing to evaluate a substance's mechanical characteristics, such as how concrete, asphalt, and polymers flow. Testing for viscosity is a useful tool for describing how materials behave under various loading scenarios.

### 3.9 Compressible Fluid

Compressible fluids are those that can be compressed and whose density can be changed by changes in pressure. Compressible fluids, as opposed to incompressible fluids like liquids, can contract or expand in response to outside forces. Key characteristics of compressible fluids include: change in volume, variation in density, speed of sound and gas behavior. Examples include gas dynamics, gas compressor, turbojet engines, air, helium and nitrogen. Air inside a balloon. Here are a few examples: air, aerosol cans, bicycle and tyres, HVAC systems etc.

#### 3.9.1 Application of Compressible Fluid

Because of their special characteristics, compressible fluids are used in many different industries. Here are some notable applications of compressible fluids:

**i) Aerospace Engineering:** The study of compressible fluid dynamics is essential to aerospace engineering. Applications include: jet engines and supersonic.

**ii) Energy Conversion and Power Generation:** Systems for energy conversion and power generation use compressible fluids. Examples include: gas turbines and steam power plants.

**iii) HVAC and Refrigeration Systems:** Heating, ventilation, and air conditioning (HVAC) and refrigeration systems require compressible fluids, usually refrigerants. Applications include: air conditioning and refrigeration.

**iv) Gas Pipelines and Storage:** Pipelines and storage facilities are used to transport and store compressible fluids, such as natural gas. Applications include: natural gas transmission and gas storage.

### 3.10 Incompressible Fluid

Incompressible fluids are those that cannot be compressed and maintain a constant density regardless of pressure changes. In other words, regardless of the pressure that is applied to it, an incompressible fluid maintains a fixed volume. Key characteristics of incompressible fluids include: constant volume, low compressibility, constant density and high bulk modulus. Examples of commonly encountered incompressible fluids include: water, oil and liquid metals. Here are some examples of incompressible fluids and their everyday applications: water, hydraulic systems, cooking and food preparation and blood and circulatory system.

#### 3.10.1 Applications of Incompressible Fluid

Due to their special characteristics, incompressible fluids have a wide range of uses in many different industries. Here are some notable applications of incompressible fluids:

- i) Hydraulic Systems:** In hydraulic systems, incompressible fluids typically hydraulic oil is extensively employed for power transmission and control. Applications include: heavy machinery, automotive industry and aircraft.
- ii) Plumbing and Pipelines:** Water and other incompressible fluids are frequently employed in plumbing and pipeline systems for a variety of applications. Applications include: domestic plumbing, municipal water supply and irrigation systems.
- iii) Cooling and Heat Transfer:** In applications involving cooling and heat transfer, incompressible fluids are essential. Examples include: HVAC systems, heat exchangers and radiators.
- iv) Marine and Naval Applications:** Systems for maritime and naval propulsion, control, and safety use incompressible fluids. Applications include: ship propulsion, steering systems and ballast system.

## 3.11 Linear Momentum

A fundamental idea in physics that describes how an item moves is called linear momentum, which is frequently just referred to as momentum. It is described as the result of the mass and the velocity of an object.

Mathematically, linear momentum ( $p$ ) is given by:

$$p = m * v,$$

where  $p$  is the linear momentum,  $m$  is the mass of the object and  $v$  is the velocity of the object.

Here are a few examples to illustrate the concept of linear momentum: a moving car, a baseball pitch, a person running and a moving train. Certainly! Here are some daily life examples of linear momentum: throwing a ball, riding a bicycle, swinging a hammer, jumping off a diving board etc.

### 3.11.1 Applications of Linear Momentum

Numerous applications of linear momentum can be found in many different fields. Here are some notable examples:

**i) Transportation and Vehicles:** Designing effective transportation systems requires an understanding of the linear momentum of moving objects. It aids in calculating the necessary power, force, and stopping distance for vehicles. Additionally, momentum is necessary for spaceship propulsion, in which the momentum created by gas expulsion drives the spacecraft forward.

**ii) Sports and Athletics:** A lot of sports rely on linear momentum's basic concepts. For example, in athletics, events like the javelin throw, shot put, and long jump involve maximizing linear momentum to achieve greater distances or heights. In sports like football, basketball, and hockey, momentum plays a key role in collisions, tackles, and the transfer of energy during player interactions.

**iii) Robotics and Automation:** Robots and automated systems are designed with linear momentum in mind. To ensure precise motions and interactions with objects, the momentum of robotic arms and manipulators must be carefully regulated.

### 3.12 Continuity Equation

The conservation of mass is connected to the flow of a fluid or the movement of a substance via the continuity equation, which is a fundamental tenet of physics. It states that, provided there are no sources or sinks of mass inside the system, the mass of a fluid moving through a certain region per unit time remains constant. The concept of mass conservation as it moves through a defined area is expressed by the equation.

Mathematically, the continuity equation is expressed as:

$$\rho \frac{d\vec{V}}{dt} = \vec{\nabla} \cdot \mathbf{S} + \rho \vec{f},$$

where  $\rho \frac{d\vec{V}}{dt}$  is convective part,  $\vec{\nabla} \cdot \mathbf{S}$  is inertial force/surface force,  $\rho \vec{f}$  is body force,  $\frac{d}{dt}$  is material time derivative,  $\rho$  is density of the fluid,  $\mathbf{S}$  is tensor (Cauchy stress tensor),  $\vec{f}$  is body force,  $\vec{V}$  is velocity.

The continuity equation can be used in a variety of circumstances involving the flow of fluids or the movement of substances and is related to the concept of mass conservation. Here are some examples, including everyday scenarios, where the continuity equation is applicable: fluid flow in a pipe, blood circulation, traffic flow, gas flow in a duct and river flow.

#### 3.12.1 Applications of Continuity Equation

Numerous applications of the continuity equation can be found in numerous fields. Here are some notable examples:

**i) Conservation Laws:** One of the fundamental parts of physics' conservation rules is the continuity equation. It is essential to the conservation of energy (in thermodynamics) as well

as the conservation of charge (in electromagnetic), in addition to the conservation of mass. These conservation principles can be utilized to analyze and comprehend the behavior of systems and quantities in many physical processes by applying the continuity equation.

**ii) Acoustics:** The continuity equation in acoustics is used to examine how sound waves go across various mediums. It helps in comprehending the conservation of acoustic energy and how sound behaves in a variety of settings, including rooms, auditoriums, and outdoor areas.

**iii) Heat and Mass Transfer:** The study of mass and heat transmission is another field in which the continuity equation is useful. It is used to examine how energy and matter flow and is conserved in systems that involve conduction, convection, and diffusion. Understanding the transmission of mass or heat in materials and systems including fluid-solid interactions, diffusion processes, and heat exchangers is made easier with the help of the continuity equation.

### 3.13 Amplitude

In physics, amplitude describes the largest deviation a wave makes from its equilibrium position. It stands for the wave's power or intensity. The amplitude is calculated from the equilibrium position to the wave's crest or trough, depending on which point is higher on the wave. Here are some examples of amplitude in different contexts: sound waves, light waves, water waves etc.

### 3.14 Wavelength

In physics, a wavelength is the separation between two successive wave points that are in phase or at the same place in their oscillation cycle. Depending on the wave's size, it is often represented by the symbol  $\lambda$  (lambda) and is measured in units like metres (m), centimetres (cm), or nanometers (nm). Here are some examples of wavelength in different contexts: radio waves, seismic waves, light waves etc.

### 3.15 Density

A substance's density is determined by how much mass it has in relation to its volume. It is determined by dividing the mass of an object or substance by its volume, and is frequently symbolized by the symbol  $\rho$  (rho).

Mathematically, density can be expressed as:

Density ( $\rho$ ) = Mass (m) / Volume (V)

$$\rho = \frac{m}{V}.$$

Here are some examples of density in different contexts: solids, liquids, gases, engineering and constructions, earth sciences etc.

### 3.16 Pressure

The force applied to a surface per unit area is referred to as pressure. It measures how much force is applied over a specific area and is expressed in quantities like Pascal's, pounds per square inch, and atmospheres. Here are some examples of pressure in different contexts: fluids, atmospheric pressure, hydraulic system, blood pressure etc.

### 3.17 Cauchy Stress tensor

In continuum mechanics, the distribution of forces inside a deformable material is described by a mathematical notion called the Cauchy stress tensor. It gives details about the forces acting on tiny planes within a material and describes the internal stresses at each place in the substance.

A second-order tensor, the Cauchy stress tensor is represented by the symbol. It links the stress vector to an incredibly small surface component. A 3x3 matrix can be used to describe the Cauchy stress tensor in three-dimensional Cartesian coordinates:

$$\sigma = [\sigma_{xx}, \sigma_{xy}, \sigma_{xz}][\sigma_{yx}, \sigma_{yy}, \sigma_{yz}][\sigma_{zx}, \sigma_{zy}, \sigma_{zz}].$$

The individual components ( $\sigma_{ij}$ ) of the Cauchy stress tensor represent the stress components acting on planes with normal vectors in the x, y, and z directions.

Here are a few examples to illustrate the concept of the Cauchy stress tensor: tensile stress, shear stress, hydraulic pressure etc.

### 3.18 Permeability

The ability of a material or substance to permit the flow or passage of another substance is referred to as permeability. It gauges how easily gases or liquids can pass through a substance.

Depending on the type of material and the makeup of the substances present, permeability can vary greatly. Here are a few examples to illustrate permeability: permeability in soil, permeability in membranes, permeability in rocks etc.

### 3.19 Weissenberg number

A dimensionless metric called the Weissenberg number  $We$  is employed in the study of rheology to measure how important elastic effects are in comparison to viscous effects in a viscoelastic fluid or material.

The typical deformation time scale multiplied by the shear rate yields the Weissenberg number. Mathematically, it can be expressed as:

$$We = \lambda \dot{\gamma},$$

where  $We$  is the Weissenberg number,  $\lambda$  is the characteristic relaxation time of the material, and  $\dot{\gamma}$  is the shear rate.

The dominant viscous or elastic behavior in a viscoelastic material is indicated by the Weissenberg number. A high Weissenberg number implies that the material has a strong elastic response because elastic effects are more important than viscous effects. A low

Weissenberg number, on the other hand, denotes a material that exhibits negligible elastic response and acts more like a viscous fluid.

Here are a couple of examples to illustrate the application of the Weissenberg number: polymer processing and biological fluids.

## CHAPTER 4

# THE INFLUENCE OF SLIP CONDITIONS, WALL PROPERTIES AND HEAT TRANSFER ON MHD PERISTALTIC TRANSPORT

### 4.1 Introduction

A uniform porous channel with elastic wall features has been used to study the effects of heat transfer and wall slip conditions on the peristaltic flow of MHD non-Newtonian fluid. Momentum and energy equations have been solved analytically. The graphs for the velocity, temperature distribution, coefficient of heat transfer, and streamlines have been studied. The analysis's findings for temperature, velocity, stream function, and heat transfer coefficient have been quantitatively assessed and briefly described. The result demonstrates that as the Knudsen number increases, more trapped bolus emerges.

### 4.2 Mathematical Formulation

Consider the movement of a non-Newtonian viscous fluid in a uniformly sized, two-dimensional conduit. The walls of the channel are treated as a stretched membrane and presumed to be flexible. Travelling sinusoidal waves with moderate amplitude are then forced on this membrane.

The channel wall's geometry is provided by

$$y = \eta(x, t) = d(x) + a \sin \frac{2\pi}{\lambda} (x - ct), \quad (4.1)$$

where

$$d(x) = d + m'x, \quad m' \ll 1. \quad (4.2)$$

For the current issue, the governing equations for the motion are

$$\frac{\partial u}{\partial x} + \frac{\partial v}{\partial y} = 0, \quad (4.3)$$

$$\rho \left[ \frac{\partial u}{\partial t} + u \frac{\partial u}{\partial x} + v \frac{\partial u}{\partial y} \right] = - \frac{\partial p}{\partial x} + \mu \left[ \frac{\partial^2 u}{\partial x^2} + \frac{\partial^2 u}{\partial y^2} \right] - \sigma B_o^2 u - \frac{\mu}{k} u, \quad (4.4)$$

$$\rho \left[ \frac{\partial v}{\partial t} + u \frac{\partial v}{\partial x} + v \frac{\partial v}{\partial y} \right] = - \frac{\partial p}{\partial y} + \mu \left[ \frac{\partial^2 v}{\partial x^2} + \frac{\partial^2 v}{\partial y^2} \right] - \frac{\mu}{k} v, \quad (4.5)$$

$$\zeta \left[ \frac{\partial T}{\partial t} + u \frac{\partial T}{\partial x} + v \frac{\partial T}{\partial y} \right] = \frac{\kappa}{\rho} \left[ \frac{\partial^2 T}{\partial x^2} + \frac{\partial^2 T}{\partial y^2} \right] + v \left[ 2 \left[ \left( \frac{\partial u}{\partial x} \right)^2 + \left( \frac{\partial v}{\partial y} \right)^2 \right] + \left( \frac{\partial u}{\partial y} + \frac{\partial v}{\partial x} \right)^2 \right], \quad (4.6)$$

where  $u$ ,  $v$  are the components of velocity along  $x$ - and  $y$ -directions respectively,  $\rho$  is the density,  $\mu$  is the coefficient of viscosity of the fluid,  $p$  is the pressure,  $d$  is the mean half width of the channel,  $a$  is the amplitude,  $\lambda$  is the wavelength,  $c$  is the phase speed of the wave,  $m'$  is the dimensional non-uniformity of the channel and  $k$  is the thermal conductivity of the fluid.

The flexible wall's governing equation of motion can be written as follows:

$$(L^*(\eta)) = p - p_o, \quad (4.7)$$

where the motion of a stretched membrane with viscous damping forces is represented by the operator  $L^*$ , such that

$$L^* = -\tau \frac{\partial^2}{\partial x^2} + m_1 \frac{\partial^2}{\partial t^2} + C \frac{\partial}{\partial t}. \quad (4.8)$$

Using the  $x$ -momentum equation and the stress continuity at  $y = \pm\eta$ , we obtain

$$\begin{aligned} \frac{\partial}{\partial x} L^*(\eta) &= \frac{\partial p}{\partial x} \\ &= \mu \left[ \frac{\partial^2 u}{\partial x^2} + \frac{\partial^2 u}{\partial y^2} \right] - \rho \left[ \frac{\partial u}{\partial t} + u \frac{\partial u}{\partial x} + v \frac{\partial u}{\partial y} \right] - \sigma B_o^2 u - \frac{\mu}{k} u, \end{aligned} \quad (4.9)$$

$$u = \mp h \frac{\partial u}{\partial y} \text{ at } y = \pm\eta = \pm [d + m'x + a \sin \frac{2\pi}{\lambda} (x - ct)], \quad (4.10)$$

$$T = T_o \text{ on } y = -\eta, \quad T = T_1 \text{ on } y = \eta, \quad (4.11)$$

where  $L^* = -\tau \frac{\partial^2}{\partial x^2} + m_1 \frac{\partial^2}{\partial t^2} + C \frac{\partial}{\partial t}$ . Here  $\tau$  is the elastic tension in the membrane,  $m$  is the mass per unit area;  $C$  is the coefficient of viscous damping forces,  $p_o$  is the pressure on the

outside surface of the wall due to tension in the muscles and  $h$  is the dimensional slip parameter. We presumed  $p_o = 0$ .

Introducing  $\psi$  such that  $u = \frac{\partial\psi}{\partial y}$  and  $v = -\frac{\partial\psi}{\partial x}$  and the subsequent non-dimensional amounts

$$\begin{aligned} x' &= \frac{x}{\lambda}, & y' &= \frac{y}{d}, & \psi' &= \frac{\psi}{cd}, & t' &= \frac{ct}{\lambda}, & \theta &= \frac{T - T_o}{T_1 - T_o}, & \eta' &= \frac{\eta}{d}, \\ p' &= \frac{d^2}{c\lambda\mu} p, & k &= \frac{k}{d^2}. \end{aligned} \quad (4.12)$$

After dropping primes, we ultimately obtain in equations (4.1) through (4.11), as:

$$\begin{aligned} Re\delta \left[ \frac{\partial\psi}{\partial y} \frac{\partial^2\psi}{\partial x\partial y} - \frac{\partial\psi}{\partial x} \frac{\partial^2\psi}{\partial y^2} \right] \\ = -\frac{\partial p}{\partial x} + \delta^2 \frac{\partial^3\psi}{\partial x^2\partial y} + \frac{\partial^3\psi}{\partial y^3} - M^2 \frac{\partial\psi}{\partial y} - \frac{1}{K} \frac{\partial\psi}{\partial y}, \end{aligned} \quad (4.13)$$

$$\begin{aligned} Re\delta^3 \left[ \frac{\partial^2\psi}{\partial t\partial x} + \frac{\partial\psi}{\partial y} \frac{\partial^2\psi}{\partial x^2} - \frac{\partial\psi}{\partial x} \frac{\partial^2\psi}{\partial x\partial y} \right] \\ = -\frac{\partial p}{\partial y} + \delta^2 \left[ \delta^2 \frac{\partial^3\psi}{\partial x^3} + \frac{\partial^3\psi}{\partial x\partial y^2} \right] - \frac{\delta^2}{K} \frac{\partial\psi}{\partial y}, \end{aligned} \quad (4.14)$$

$$\begin{aligned} Re\delta \left[ \frac{\partial\theta}{\partial t} + \frac{\partial\psi}{\partial y} \frac{\partial\theta}{\partial x} - \frac{\partial\psi}{\partial x} \frac{\partial\theta}{\partial y} \right] \\ = \frac{1}{Pr} (\delta^2 \frac{\partial^2}{\partial x^2} + \frac{\partial^2}{\partial y^2}) \theta \\ + E \left[ 4 \delta^2 \left( \frac{\partial^2\psi}{\partial x\partial y} \right)^2 + \left( \frac{\partial^2\psi}{\partial y^2} - \delta^2 \frac{\partial^2\psi}{\partial x^2} \right)^2 \right], \end{aligned} \quad (4.15)$$

$$\frac{\partial\psi}{\partial y} = \mp\beta \frac{\partial^2\psi}{\partial y^2} \text{ at } y = \pm\eta = \pm[1 + mx + \varepsilon \sin 2\pi(x-t)], \quad (4.16)$$

$$\begin{aligned} \delta^2 \frac{\partial^3\psi}{\partial x^2\partial y} + \frac{\partial^3\psi}{\partial y^3} - Re\delta \left[ \frac{\partial\psi}{\partial y} \frac{\partial^2\psi}{\partial x\partial y} - \frac{\partial\psi}{\partial x} \frac{\partial^2\psi}{\partial y^2} \right] - M^2 \frac{\partial\psi}{\partial y} - \frac{1}{K} \frac{\partial\psi}{\partial y} = \left[ E_1 \frac{\partial^3}{\partial x^3} + E_2 \frac{\partial^3}{\partial x\partial t^2} + \right. \\ \left. E_3 \frac{\partial^2}{\partial x\partial t} \right] (\eta), \end{aligned} \quad (4.17)$$

Additionally, it is believed that the streamline's zero value at the line  $y = 0$ , i.e.

$$\Psi(0) = 0, \quad (4.18)$$

$$\theta = 0 \text{ on } y = -\eta,$$

$$\theta = 1 \text{ on } y = \eta, \quad (4.19)$$

where  $\varepsilon = \frac{a}{d}$ ,  $\delta = \frac{d}{\lambda}$  are geometric parameter,  $Re = \frac{cd\rho}{\mu}$  is the Reynolds number,  $E_1 = -\frac{\tau d^3}{\lambda^3 \mu c}$ ,  $E_2 = \frac{m_1 c d^3}{\lambda^3 \mu}$ ,  $E_3 = \frac{c d^3}{\lambda^2 \mu}$  are the non-dimensional elasticity parameters,  $m = \frac{\lambda m'}{d}$  is non-uniform parameter, and  $\beta$  is the Knudsen number (Slip parameter).

### 4.3 Exact Analytical Solution

From equations (4.13) to (4.17), by applying the long wavelength approximation and disregarding the wave number and low Reynolds number, one may ascertain:

$$0 = -\frac{\partial p}{\partial x} + \frac{\partial^3 \psi}{\partial y^3} - M^2 \frac{\partial \psi}{\partial y} - \frac{1}{K} \frac{\partial \psi}{\partial y}, \quad (4.20)$$

$$0 = -\frac{\partial p}{\partial y}. \quad (4.21)$$

$$0 = \frac{1}{Pr} \frac{\partial^2 \theta}{\partial y^2} + E \left( \frac{\partial^2 \psi}{\partial y^2} \right)^2. \quad (4.22)$$

When equation (4.20) is differentiated with respect to  $y$ , the compatibility equation appears as follows:

$$\frac{\partial^4 \psi}{\partial y^4} - N^2 \frac{\partial^2 \psi}{\partial y^2} = 0, \quad (4.23)$$

where

$$N = \sqrt{M^2 + \frac{1}{K}}.$$

Equation (4.17) results in:

$$\frac{\partial^3 \psi}{\partial y^3} - N^2 \frac{\partial \psi}{\partial y} = \left[ E_1 \frac{\partial^3}{\partial x^3} + E_2 \frac{\partial^3}{\partial x \partial t^2} + E_3 \frac{\partial^2}{\partial x \partial t} \right] (\eta). \quad (4.24)$$

Equation (4.23) with boundary conditions (4.16), (4.18), and (4.24) has the following closed form solution:

$$\psi = \frac{8\varepsilon\pi^3 [(E_1 + E_2) \cos 2\pi(x-t) - \frac{E_3}{2\pi} \sin 2\pi(x-t)]}{N^2} * \left[ \frac{\sinh Ny}{N(\cosh N\eta + N\beta \sinh N\eta)} - y \right]. \quad (4.25)$$

If equation (4.25) is substituted for equation (4.22) and the temperature is subject to condition (4.19), then

$$\theta = \frac{1}{8\eta(\cosh N\eta + N\beta\sinh N\eta)^2} * [\eta Br L_{333}(2N^2y^2 - \cosh 2Ny) + 4(y + \eta)(\cosh N\eta + N\beta\sinh N\eta)^2 + \eta Br L_{333}[\cosh 2N\eta - 2\eta^2 N^2]], \quad (4.26)$$

where

$$L_{333} = \frac{8\epsilon\pi^3 \left[ \frac{E_3}{2\pi} \sin 2\pi(x - t) - (E_1 + E_2) \cos 2\pi(x - t) \right]}{N^2},$$

where the Brinkman number is given as,  $Br = EPr$ .

The coefficient of heat transmission at the wall is:

$$Z = \eta_x \theta_y. \quad (4.27)$$

#### 4.4 Methodology

Using the mathematical software ‘‘Mathematica’’ we have plotted the graphs to investigate the behavior of parameters on the velocity, temperature and streamline patterns of the fluid. Graphical demonstration of the parameters like the slip parameter ( $\beta$ ), non-uniform parameter ( $m$ ), permeability parameter ( $K$ ), and Hartmann number ( $M$ ) in order to understand the behavior of the distributions of the axial velocity ( $u$ ).

## 4.5 Results and Discussion

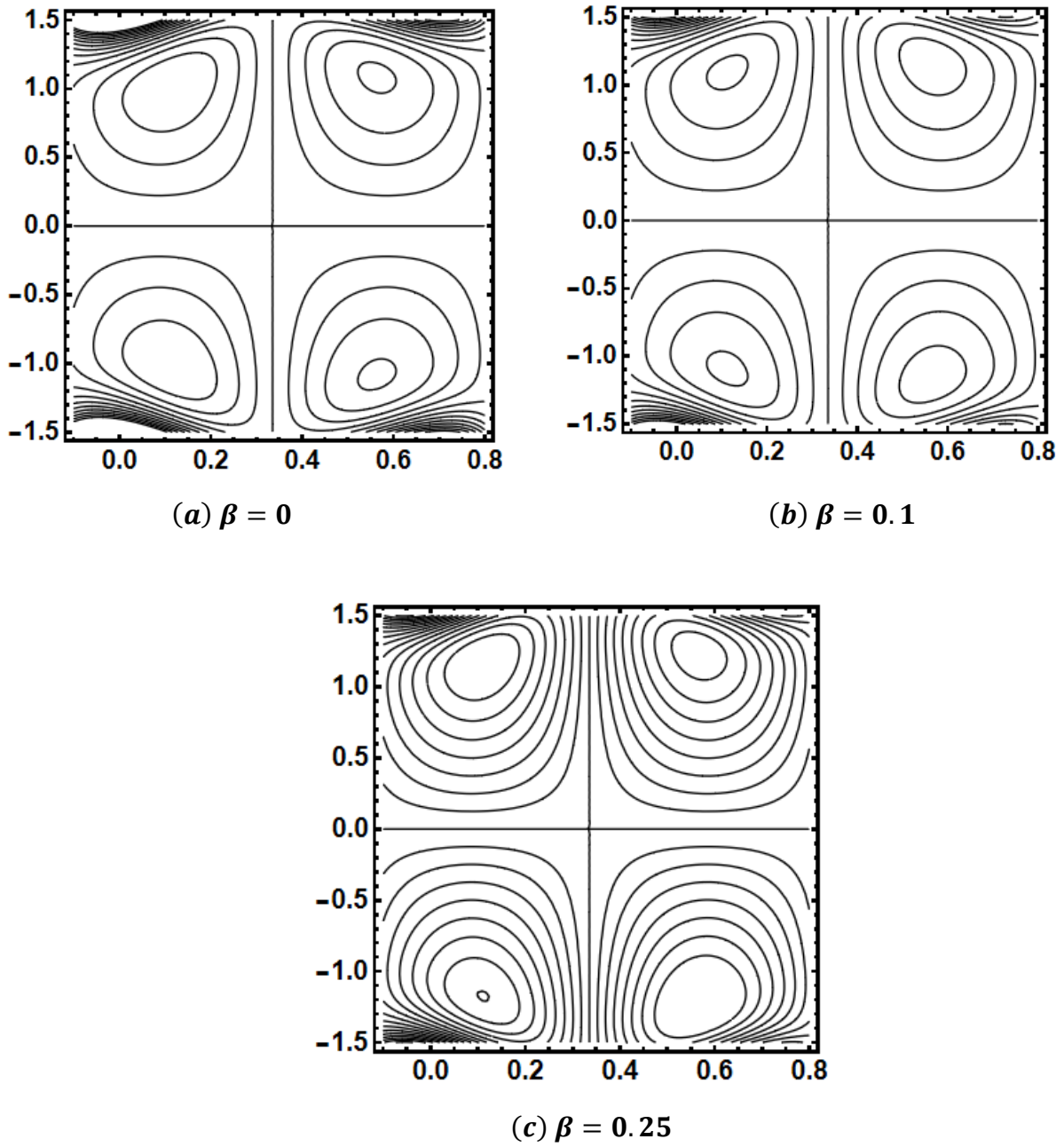


**Fig 4.1** Streamlines for (a)  $\beta = 0$ , (b)  $\beta = 0.1$ , (c)  $\beta = 0.25$  with  $E_1 = 0.6, E_2 = 0.4, E_3 = 0.1, \varepsilon = 0.2, M = 4, K = 0.05, m = 0.1, t = 0.1$ .

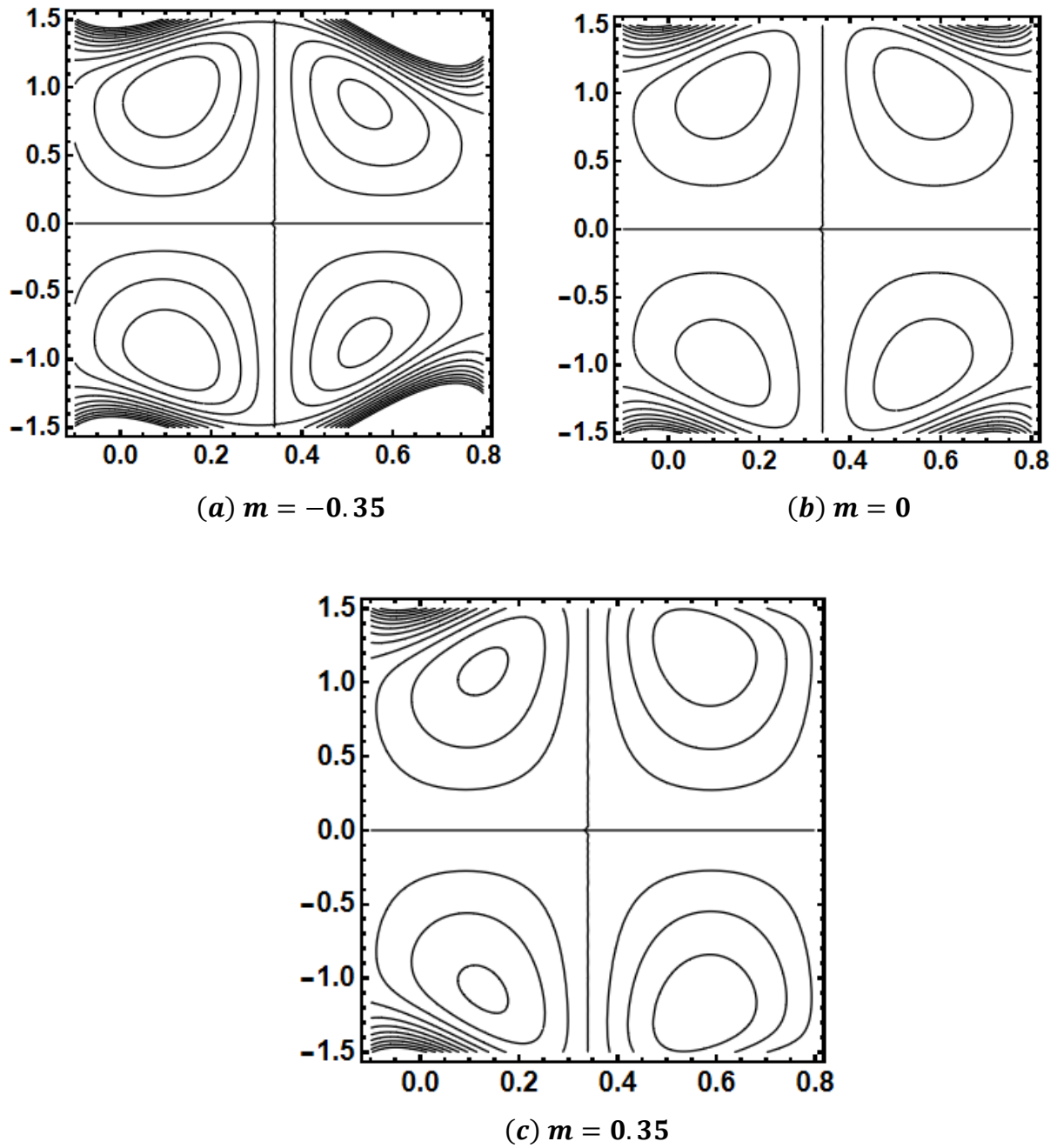


**Fig 4. 2** Streamlines for (a)  $m = -0.35$ , (b)  $m = 0$ , (c)  $m = 0.35$  with  $E_1 = 0.4$ ,  $E_2 = 0.1$ ,  $E_3 = 0.2$ ,  $\varepsilon = 0.2$ ,  $M = 4$ ,  $K = 0.1$ ,  $\beta = 0$ ,  $t = 0.1$ .

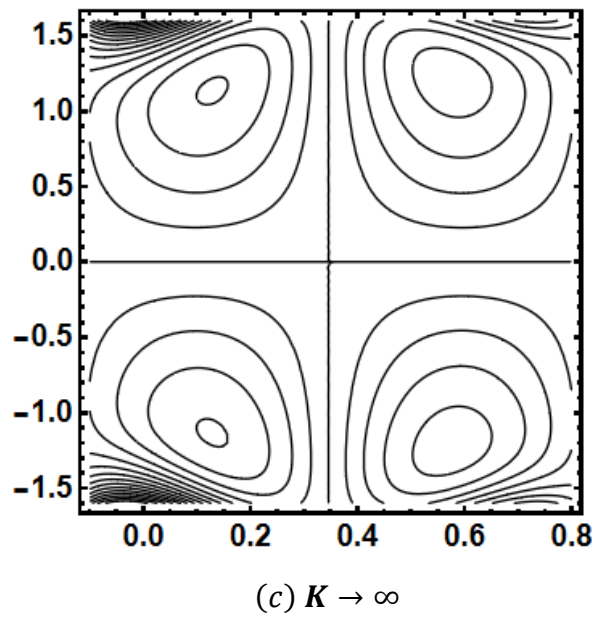
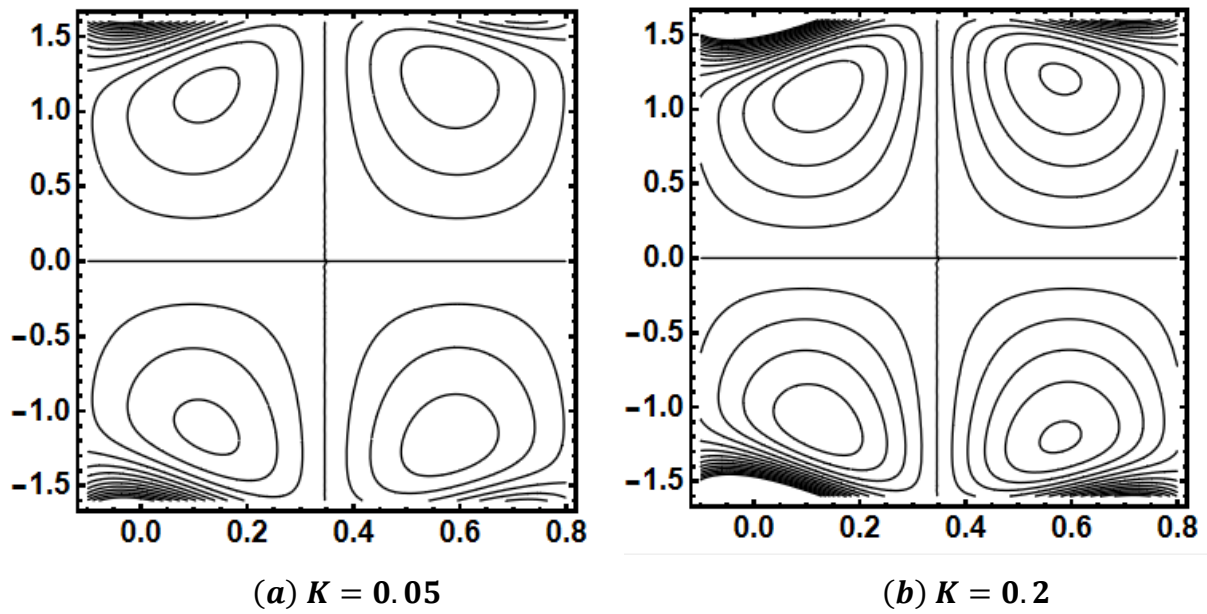


**Fig 4. 3** Streamlines for (a)  $K = 0.05$ , (b)  $K = 0.2$ , (c)  $K \rightarrow \infty$  with  $E_1 = 1.2, E_2 = 0.5, E_3 = 0.1, \varepsilon = 0.15, M = 5, m = 0.2, \beta = 0.1, t = 0.1$ .

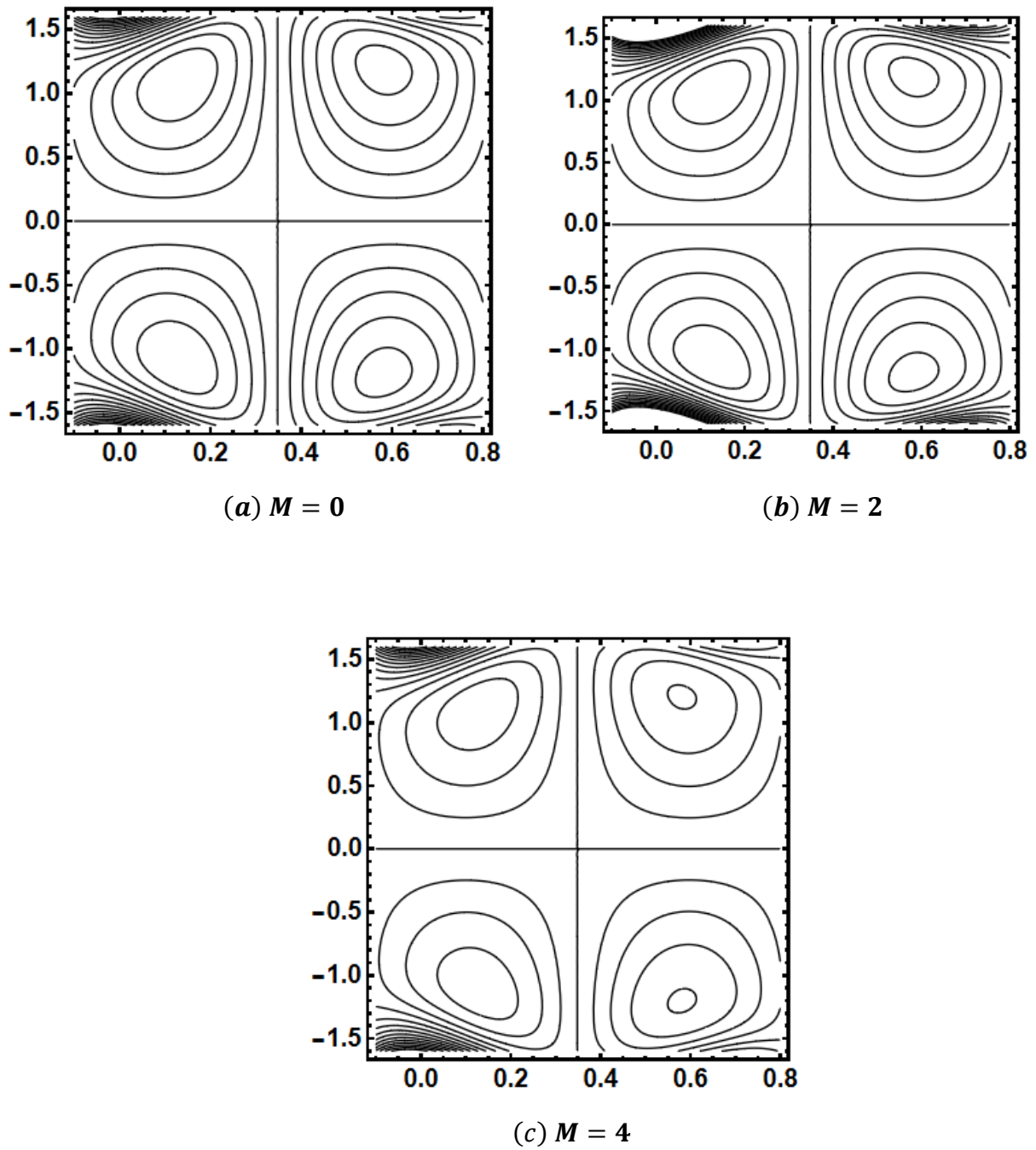


**Fig 4. 4** Streamlines for (a)  $M = 0$ , (b)  $M = 2$ , (c)  $M = 4$  with  $E_1 = 0.7, E_2 = 0.7, E_3 = 0.1, \varepsilon = 0.15, K = 0.05, m = 0.25, \beta = 0.05, t = 0.1$ .

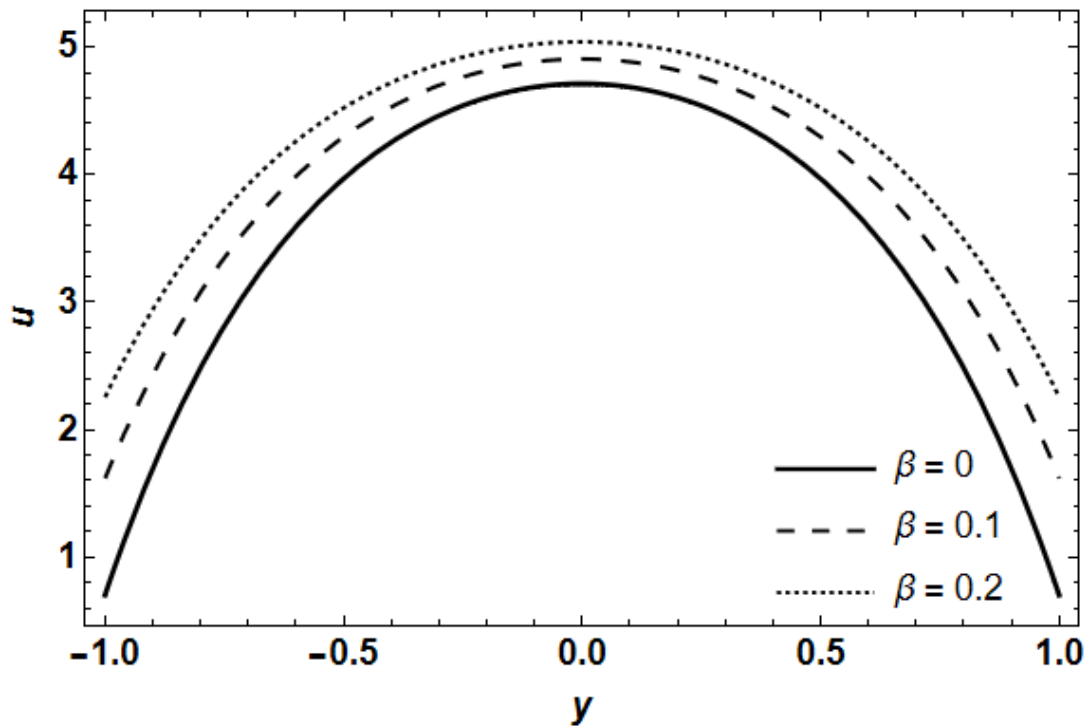


**Fig 4.5** Velocity distribution for (a) $\beta = 0$ , (b) $\beta = 0.1$ , (c) $\beta = 0.2$  with ( $x = 0.2, t = 0.1$ ),  $E_1 = 1, E_2 = 0.5, E_3 = 0.5, \varepsilon = 0.1, M = 2, K = 1, m = 0$ .

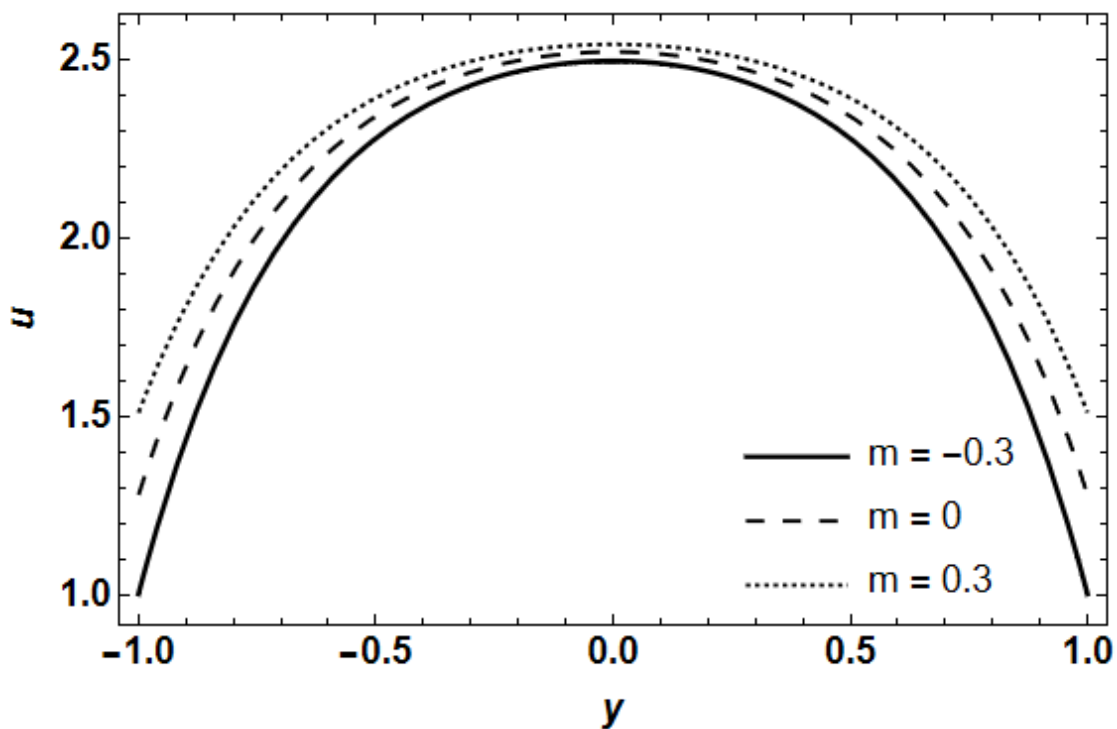


**Fig 4.6** Velocity distribution for (a) $m = -0.3$ , (b) $m = 0$ , (c) $m = 0.3$  with ( $x = 0.2, t = 0.1$ ),  $E_1 = 0.8, E_2 = 0.5, E_3 = 0.4, \varepsilon = 0.1, K = 2, M = 3, \beta = 0.2$ .

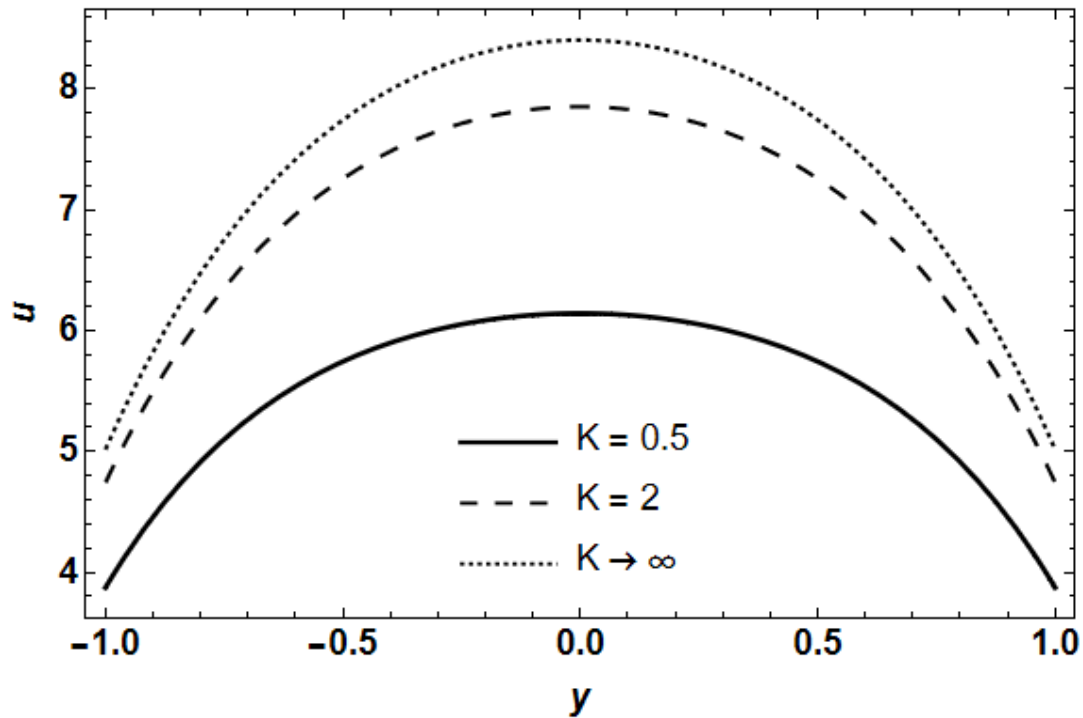


**Fig 4. 7** Velocity distribution for (a) $K = 0.5$ , (b) $K = 2$ , (c) $K \rightarrow \infty$  with ( $x = 0.2, t = 0.1$ ),  $E_1 = 0.5, E_2 = 0.5, E_3 = 0.1, \varepsilon = 0.2, M = 2, m = 0.1, \beta = 0.3$ .

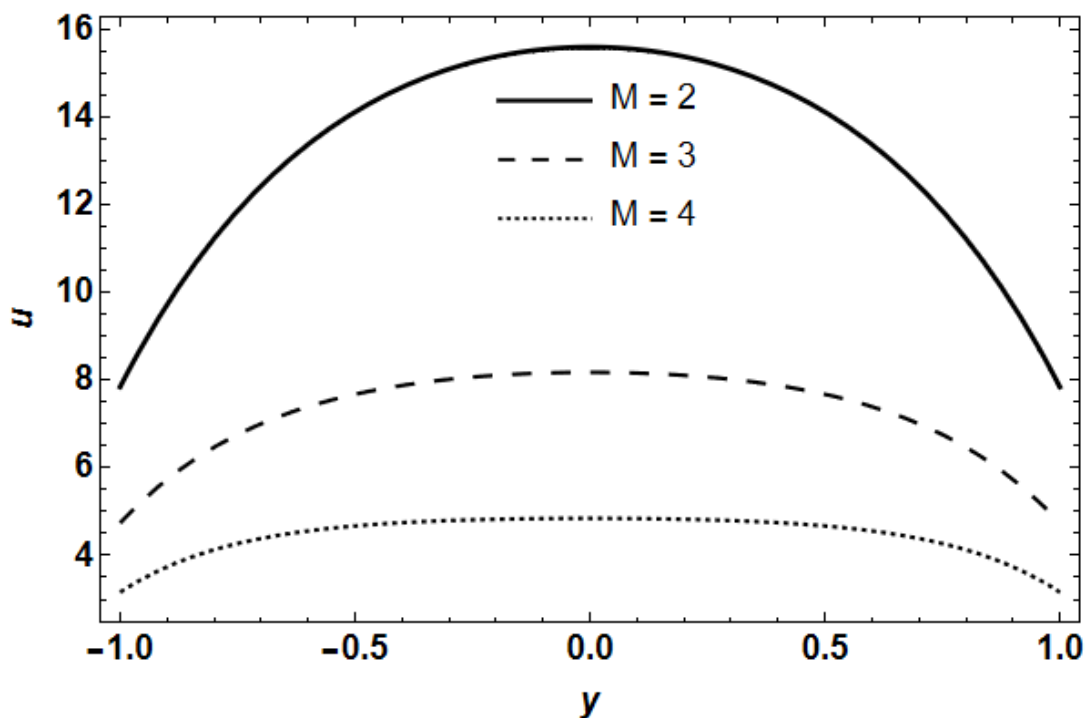


**Fig 4. 8** Velocity distribution for (a) $M = 2$ , (b) $M = 3$ , (c) $M = 4$  with ( $x = 0.2, t = 0.1$ ),  $E_1 = 2, E_2 = 0.7, E_3 = 0.1, \varepsilon = 0.15, K = 2, m = 0.1, \beta = 0.2$ .

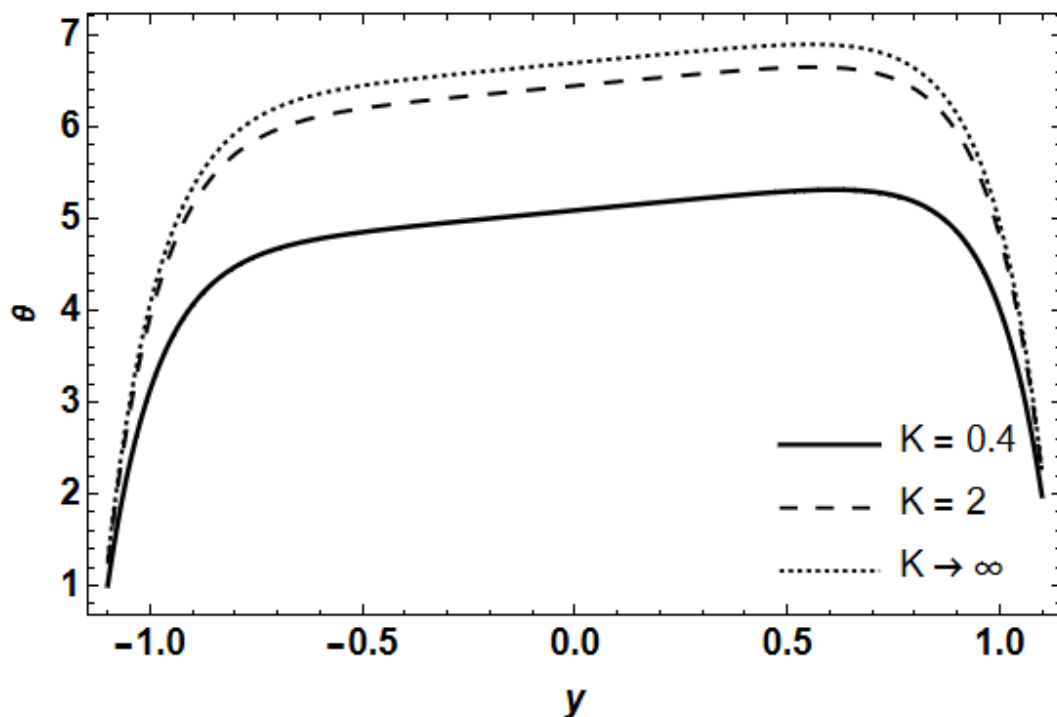


**Fig 4. 9** Temperature distribution for (a) $K = 0.4$ , (b) $K = 2$ , (c) $K \rightarrow \infty$  with ( $x = 0.2, t = 0.1$ ),  $E_1 = 0.7, E_2 = 0.5, E_3 = 0.2, Br = 3, \varepsilon = 0.2, M = 3, K = 2, m = 0.1$ .

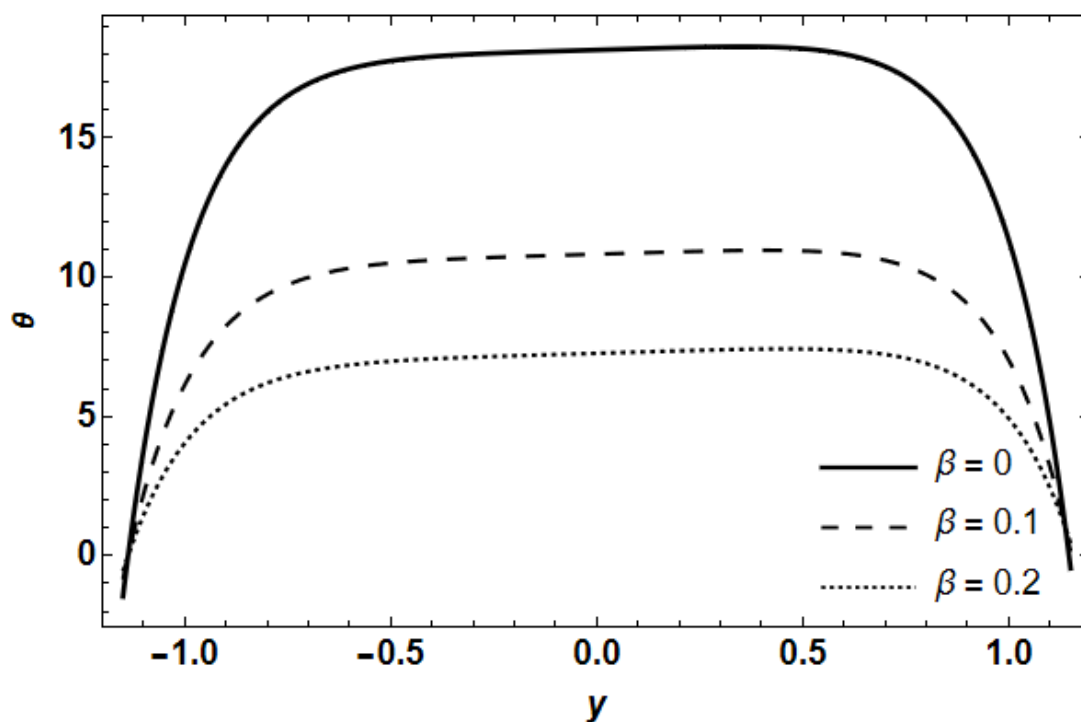


**Fig 4. 10** Temperature distribution for (a) $\beta = 0$ , (b) $\beta = 0.1$ , (c) $\beta = 0.2$  with ( $x = 0.2, t = 0.1$ ),  $E_1 = 1, E_2 = 0.2, E_3 = 0.1, Br = 4, \varepsilon = 0.15, K = 0.2, M = 2, \beta = 0.1$ .

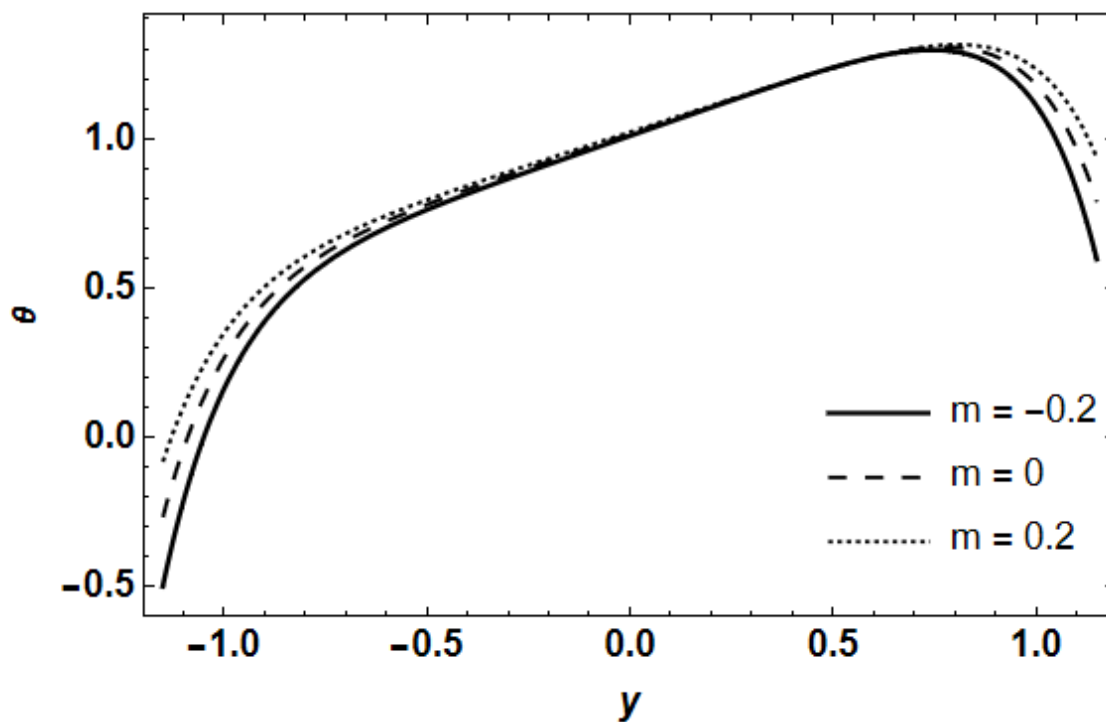


**Fig 4. 11** Temperature distribution for (a) $m = -0.2$ , (b) $m = 0$ , (c) $m = 0.2$  with ( $x = 0.2, t = 0.1$ ),  $E_1 = 1.2, E_2 = 0.5, E_3 = 0.1, Br = 5, \varepsilon = 0.15, M = 4, \beta = 0.1$ .

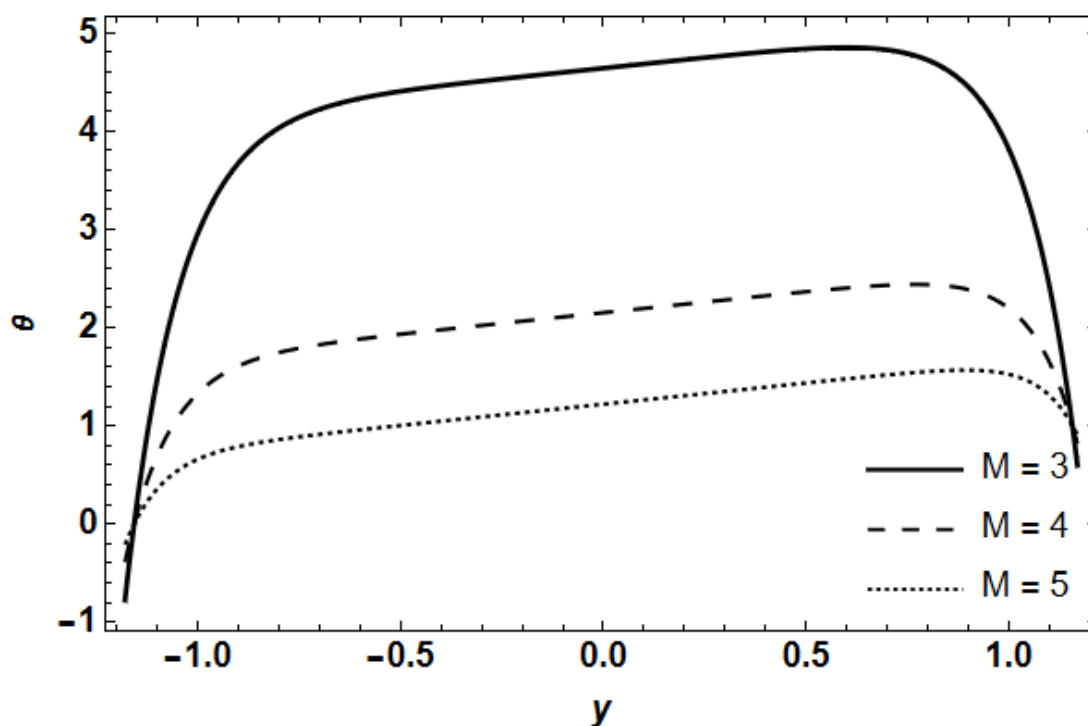


**Fig 4. 12** Temperature distribution for (a) $M = 3$ , (b) $M = 4$ , (c) $M = 5$  with ( $x = 0.2, t = 0.1$ ),  $E_1 = 0.8, E_2 = 0.6, E_3 = 0.1, Br = 2, \varepsilon = 0.2, K = 0.2, m = 0.2, \beta = 0.2$ .

## Streamlines

Figures are created to show streamlines nature for different values considered in this work. Trapping is a fascinating peristaltic transport event. Fig: 4.1 (a), (b), and (c) shows how the slip parameter affects the trapping. In fluid dynamics, the relative velocity between a fluid and a solid surface is represented by the slip parameter. It measures the degree of slippage or absence of slippage at the fluid-solid interface. We see that as the slip parameter is increased, more trapped bolus appears and streamlines close loops produce a cellular flow pattern in the channel. The ability of a material to permit the passage of fluids, such as liquids or gases, through it is measured by the permeability parameter. It measures how easily chemicals can flow across a membrane or porous material. Fig 4.2: (a), (b), and (c) depict the streamlines for uniform and non-uniform channels. The conclusion is that for convergent channels, the size of the trapped bolus is large on the left side of the channel, whereas for divergent channels, it behaves differently. Furthermore, for uniform channels, the size of the bolus is symmetric. Fig: 4.3 (a), (b), and (c) analyze how  $K$  affects trapping. It demonstrates that as  $K$  increases, more trapped bolus appears and the volume of the trapped bolus grows. In magnetohydrodynamics, the Hartmann number is a dimensionless quantity that expresses how important magnetic forces are in relation to viscous forces in a conducting fluid flow. The portions of Fig: 4.4 (a), (b), and (c) show how  $M$  affects trapping. We notice that as  $M$  increases, the bolus size decreases.

## Velocity distribution

Figs: 4.5 - 4.8 are created to show velocity profile of the fluid for different values considered in this work. In fluid dynamics or particle physics, the pattern or arrangement of fluid or particle velocities inside a certain location is referred to as the "velocity distribution." The velocity distribution increases as  $\beta$  increases, as shown in Fig: 4.5. According to Fig: 4.6, a divergent channel's ( $m > 0$ ) velocity is higher than a uniform channel's velocity ( $m = 0$ ), whereas a convergent channel's velocity ( $m < 0$ ) is lower. Fig: 4.7 shows the impact of  $K$  on the velocity distribution. It demonstrates that the axial velocity rises as  $K$  rises. Additionally, the permeability parameter makes the wall-based sliding slip stronger. The impact  $M$  has on the velocity field for constant values of the other parameters is shown in Fig: 4.8. It is evident that as  $M$  increases, velocity decreases.

## Temperature distribution

Figures 4.9 – 4.12 are created to show temperature distribution of the fluid for different values considered in this work. Temperature variance describes how temperature varies from one place to another within a specified range or inside a particular area. Figures 4.9 – 4.12 provides an illustration of the impact of heat transfer on the fluid flow. The temperature distribution is plotted in Fig: 4.9 to show how the permeability parameter affect it. Increasing the permeability parameter, can be seen to have an opposite effect on the temperature profile. The temperature variation ( $\theta$ ) for various values of  $\beta$  is made visible in Fig: 4.10. The relative motion between a fluid and a solid surface is represented by the slip parameter in the context of fluid dynamics. It measures how much slide or no slip is there at the fluid-solid interface. The temperature profiles are seen to be almost parabolic, and as the slip parameter  $\beta$  increases, the temperature field decreases. The impact of  $m$  on the temperature distribution is shown in Fig: 4.11. When compared to other straight and convergent channels, the temperature amplitude for divergent channels is larger, as can be seen. The temperature distribution is plotted in Fig: 4.12 to show how the Hartmann number  $M$  affect it. Increasing the Hartmann number, can be seen to have an opposite effect on the temperature profile.

## CHAPTER 5

### ANALYSIS OF WALL PROPERTIES AND SLIP PARAMETER ON THE PHAN-THIEN-TANNER (PTT) FLUID

#### 5.1 Introduction

This chapter concerns the characteristics of Phan-Thien-Tanner (PTT) fluid with wall properties and slip parameter. Appropriate similarities transformations are used to reduce the number of dependent variables. Motivated by the review article [36], in the present work, analysis of wall properties and slip parameter on Phan-Thien-tanner (PTT) fluid is investigated. The governing equations of Phan-Thien-Tanner fluid model are solved by a perturbation technique. The results have been obtained using the perturbation approach. Diverse parameters impact have been depicted graphically and are analyzed in depth.

#### 5.2 Mathematical Formulation

Consider the movement of non-Newtonian PTT fluid flowing past a symmetric channel. The walls of the channel are assumed to be stretchable and flexible and are induced with peristaltic waves creating sinusoidal mechanism.

The geometry of the channel wall is given by

$$y = \eta(x, t) = d + a \sin \frac{2\pi}{\lambda} (x - ct), \quad (5.1)$$

where  $d$  is the mean half width of the channel,  $a$  is the amplitude,  $\lambda$  is the wavelength,  $c$  is the phase speed of the wave.

The PTT model's constitutive equations are

$$\mathbf{T} = -p\mathbf{I} + \mathbf{S}, \quad (5.2)$$

$$f(\text{tr}(\mathbf{s}))\mathbf{s} + k\mathbf{s}^\nabla = 2\mu\mathbf{D}, \quad (5.3)$$

$$\mathbf{s}^\nabla = \frac{d\mathbf{s}}{dt} - \mathbf{s} \cdot \mathbf{L}^* - \mathbf{L} \cdot \mathbf{s}, \quad (5.4)$$

$$\mathbf{L} = \text{grad}V, \quad (5.5)$$

where  $p$  is the pressure,  $I$  is the identity tensor,  $V$  is the velocity,  $T$  is the Cauchy stress tensor,  $\mu$  is the dynamic viscosity,  $S$  is an extra-stress tensor,  $D$  is the deformation-rate tensor,  $k$  is the relaxation time,  $\mathbf{s}^\nabla$  denotes Oldroyd's upper-convected derivative,  $\frac{d}{dt}$  the material time derivative,  $\text{tr}$  is the trace and asterisk(\*) denotes the transpose.

The linearized PTT model's function  $f$ , which satisfies

$$f(\text{tr}(\mathbf{s})) = 1 + \frac{\varepsilon k}{\mu} \text{tr}(\mathbf{s}), \quad (5.6)$$

Note that when the extensional parameter  $\varepsilon$  is zero, the PTT model reduces to an upper convected Maxwell model (UCM).

For the current issue, the equations governing the motion are

$$\frac{\partial u}{\partial x} + \frac{\partial v}{\partial y} = 0, \quad (5.7)$$

$$\rho \left[ \frac{\partial u}{\partial t} + u \frac{\partial u}{\partial x} + v \frac{\partial u}{\partial y} \right] = -\frac{\partial p}{\partial x} + \frac{\partial}{\partial x} S_{xx} + \frac{\partial}{\partial y} S_{xy} - \frac{\mu}{k} u, \quad (5.8)$$

$$\rho \left[ \frac{\partial v}{\partial t} + u \frac{\partial v}{\partial x} + v \frac{\partial v}{\partial y} \right] = -\frac{\partial p}{\partial y} + \frac{\partial}{\partial x} S_{xy} + \frac{\partial}{\partial y} S_{yy} - \frac{\mu}{k} v, \quad (5.9)$$

where  $u$ ,  $v$  are the components of velocity along  $x$ - and  $y$ -directions respectively,  $\rho$  is the density,  $\mu$  is the coefficient of viscosity of the fluid,  $p$  is the pressure, and  $k$  is the thermal conductivity of the fluid.

The extra stress tensor components are given as:

$$fS_{xx} + k \left[ u \frac{\partial S_{xx}}{\partial x} + v \frac{\partial S_{xx}}{\partial y} - 2 \frac{\partial u}{\partial x} S_{xx} - 2 \frac{\partial u}{\partial y} S_{xy} \right] v = 2\mu \frac{\partial u}{\partial x}, \quad (5.10)$$

$$\begin{aligned} fS_{xy} + k \left[ u \frac{\partial S_{xy}}{\partial x} + v \frac{\partial S_{xy}}{\partial y} - \frac{\partial v}{\partial x} S_{xx} - \frac{\partial v}{\partial y} S_{xy} - \frac{\partial u}{\partial x} S_{xy} - \frac{\partial u}{\partial y} S_{yy} \right] \\ = \mu \left( \frac{\partial u}{\partial y} + \frac{\partial v}{\partial x} \right), \end{aligned} \quad (5.11)$$

$$fS_{yy} + k \left[ u \frac{\partial S_{yy}}{\partial x} + v \frac{\partial S_{yy}}{\partial y} - 2 \frac{\partial v}{\partial x} S_{xy} - 2 \frac{\partial v}{\partial y} S_{yy} \right] = 2\mu \frac{\partial v}{\partial y}, \quad (5.12)$$

$$f = 1 + \frac{\varepsilon k}{\mu} (S_{xx} + S_{yy}). \quad (5.13)$$

Here we use equation from previous chapter i.e. equation (4.7 - 4.11).

Introducing  $\psi$  such that  $u = \frac{\partial\psi}{\partial y}$  and  $v = -\frac{\partial\psi}{\partial x}$  and the non-dimensional quantities defined below:

$$\begin{aligned} x' &= \frac{x}{\lambda}, & y' &= \frac{y}{d}, & \psi' &= \frac{\psi}{cd}, & t' &= \frac{ct}{\lambda}, & \eta' &= \frac{\eta}{d}, & p' &= \frac{d^2}{c\lambda\mu} p, \\ k &= \frac{k}{d^2}, & u' &= \frac{u}{c}, & v' &= \frac{v}{\delta c}, & \delta &= \frac{d}{\lambda}, & Re &= \frac{\rho cd}{\mu}, \\ d &= \frac{d_2}{d_1}, & a' &= \frac{a}{d}, & b' &= \frac{b}{d}, & S_{ij}' &= \frac{S_{ij}}{\mu c} d, & We &= \frac{kc}{d}, \\ \sigma &= \frac{d}{\sqrt{k_0}}, \text{ and } u = \frac{\partial\psi}{\partial y} \text{ and } v = -\frac{\partial\psi}{\partial x}. \end{aligned} \quad (5.14)$$

After eliminating primes, we ultimately obtain in equations:

$$Re\delta \left[ \frac{\partial\psi}{\partial y} \frac{\partial^2\psi}{\partial x\partial y} - \frac{\partial\psi}{\partial x} \frac{\partial^2\psi}{\partial y^2} \right] = -\frac{\partial p}{\partial x} + \delta \frac{\partial S_{xx}}{\partial x} + \frac{\partial S_{xy}}{\partial y} - \sigma^2 \frac{\partial\psi}{\partial y}, \quad (5.15)$$

$$Re\delta^3 \left[ -\frac{\partial\psi}{\partial y} \frac{\partial^2\psi}{\partial x^2} + \frac{\partial\psi}{\partial x} \frac{\partial^2\psi}{\partial y\partial x} \right] = -\frac{\partial p}{\partial y} + \delta^2 \frac{\partial S_{xy}}{\partial x} + \delta \frac{\partial S_{yy}}{\partial y} + \sigma^2 \delta \frac{\partial\psi}{\partial x}, \quad (5.16)$$

$$\frac{\partial\psi}{\partial y} = \mp\beta \frac{\partial^2\psi}{\partial y^2} \text{ at } y = \pm\eta = \pm d + a \sin \frac{2\pi}{\lambda} (x - ct), \quad (5.17)$$

$$\begin{aligned} E_1 \frac{\partial^3}{\partial x^3} + E_2 \frac{\partial^3}{\partial x\partial t^2} + E_3 \frac{\partial^2}{\partial x\partial t} = \delta \frac{\partial}{\partial x} S_{xx} + \frac{\partial}{\partial y} S_{xy} - \frac{1}{k} \frac{\partial\psi}{\partial y} - Re\delta \left[ \frac{\partial\psi}{\partial y} \frac{\partial^2\psi}{\partial x\partial y} - \right. \\ \left. \frac{\partial\psi}{\partial x} \frac{\partial^2\psi}{\partial y^2} \right], \end{aligned} \quad (5.18)$$

where  $\varepsilon = \frac{a}{d}$ ,  $\delta = \frac{d}{\lambda}$  are geometric parameter,  $Re = \frac{cd\rho}{\mu}$  is the Reynolds number,  $E_1 = -\frac{\tau d^3}{\lambda^3 \mu c}$ ,  $E_2 = \frac{m_1 c d^3}{\lambda^3 \mu}$ ,  $E_3 = \frac{c d^3}{\lambda^2 \mu}$  are the non-dimensional elasticity parameters, and  $\beta$  is the Knudsen number (Slip parameter).

The fundamental equations were reduced by using the long wavelength approximations.

$$\frac{dp}{dx} = \frac{\partial S_{xy}}{\partial y} - \sigma^2 \frac{\partial\psi}{\partial y}, \quad (5.19)$$

$$\frac{\partial p}{\partial y} = 0, \quad (5.20)$$

$$fS_{xx} = 2We \frac{\partial^2\psi}{\partial y^2} S_{xy}, \quad (5.21)$$

$$fS_{yy} = 0, \quad (5.22)$$

$$fS_{xy} = -We \frac{\partial^2\psi}{\partial y^2} S_{yy} + \frac{\partial^2\psi}{\partial y^2}. \quad (5.23)$$

$S_{yy} = 0$  is the result of equation (5.22) and equation (5.19) respectively.

$$S_{xy} = y \frac{dp}{dx} + \sigma^2 \psi. \quad (5.24)$$

The use of (5.22) and (5.23) allows us to write

$$S_{xx} = 2We S_{xy}^2. \quad (5.25)$$

Equations (5.13), (5.22) and (5.25) provide the following results:

$$\frac{\partial^2 \psi}{\partial y^2} = S_{xy} + 2\varepsilon We^2 S_{xy}^3. \quad (5.26)$$

When we change (5.24) to (5.26) we obtain

$$\frac{\partial^2 \psi}{\partial y^2} = y \frac{dp}{dx} + \sigma^2(\psi) + 2\varepsilon We^2 \left( y \frac{dp}{dx} + \sigma^2(\psi) \right)^3. \quad (5.27)$$

As for the boundary conditions,

$$\frac{\partial \psi}{\partial y} = \pm \beta \frac{\partial^2 \psi}{\partial y^2}, \text{ at } y = \pm \eta. \quad (5.28)$$

### 5.3 Perturbation Solution

Because of the non-linear nature of equation (5.27) and the impossibility of finding an exact solution, we use the perturbation approach to locate the answer. We expand the flow quantities in a power series of the tiny parameter  $We^2$  as follows for the perturbation solution:

$$\Psi = \psi_0 + We^2 \psi_1 + O(We^4),$$

$$\frac{dp}{dx} = \frac{dp_0}{dx} + We^2 \frac{dp_1}{dx} + O(We^4), \quad (5.29)$$

$$S_{xy} = S_{0xy} + We^2 S_{1xy} + O(We^4). \quad (5.30)$$

We get a system of equations of various orders by using the aforementioned formulas in equation (5.27). These systems of equations have been extracted by using DSolver command in Mathematica. Motivated by the article by Vaidya *et al.* adopted the techniques [60].

#### 5.3.1 System of Order $We^0$

The zeroth-order problem's governing equations and boundary conditions are

$$\frac{\partial^2}{\partial y^2} S_{0xy} - \sigma^2 \frac{\partial^2 \psi_0}{\partial y^2} = 0, \quad (5.31)$$

$$\frac{dp_0}{dx} = \frac{1}{y} \frac{\partial^2 \psi_0}{\partial y^2} - \frac{1}{y} \sigma^2 \psi_0, \quad (5.32)$$

with boundary conditions:

$$\frac{\partial \psi}{\partial y} = \pm \beta \frac{\partial^2 \psi}{\partial y^2} \text{ at } y = \pm \eta, \quad (5.33)$$

$$\frac{\partial S_{0xy}}{\partial y} = \frac{\partial^2 \psi_0}{\partial y^2} = \left( E_1 \frac{\partial^3}{\partial x^3} + E_2 \frac{\partial^3}{\partial x \partial t^2} + E_3 \frac{\partial^2}{\partial x \partial t} \right) \eta, \text{ at } y = \pm \eta. \quad (5.34)$$

### 5.3.2 System of Order $We^2$

The first-order problem's governing equations and boundary conditions are

$$\frac{\partial^2}{\partial y^2} S_{1xy} - \sigma^2 \frac{\partial^2 \psi_1}{\partial y^2} = 0, \quad (5.35)$$

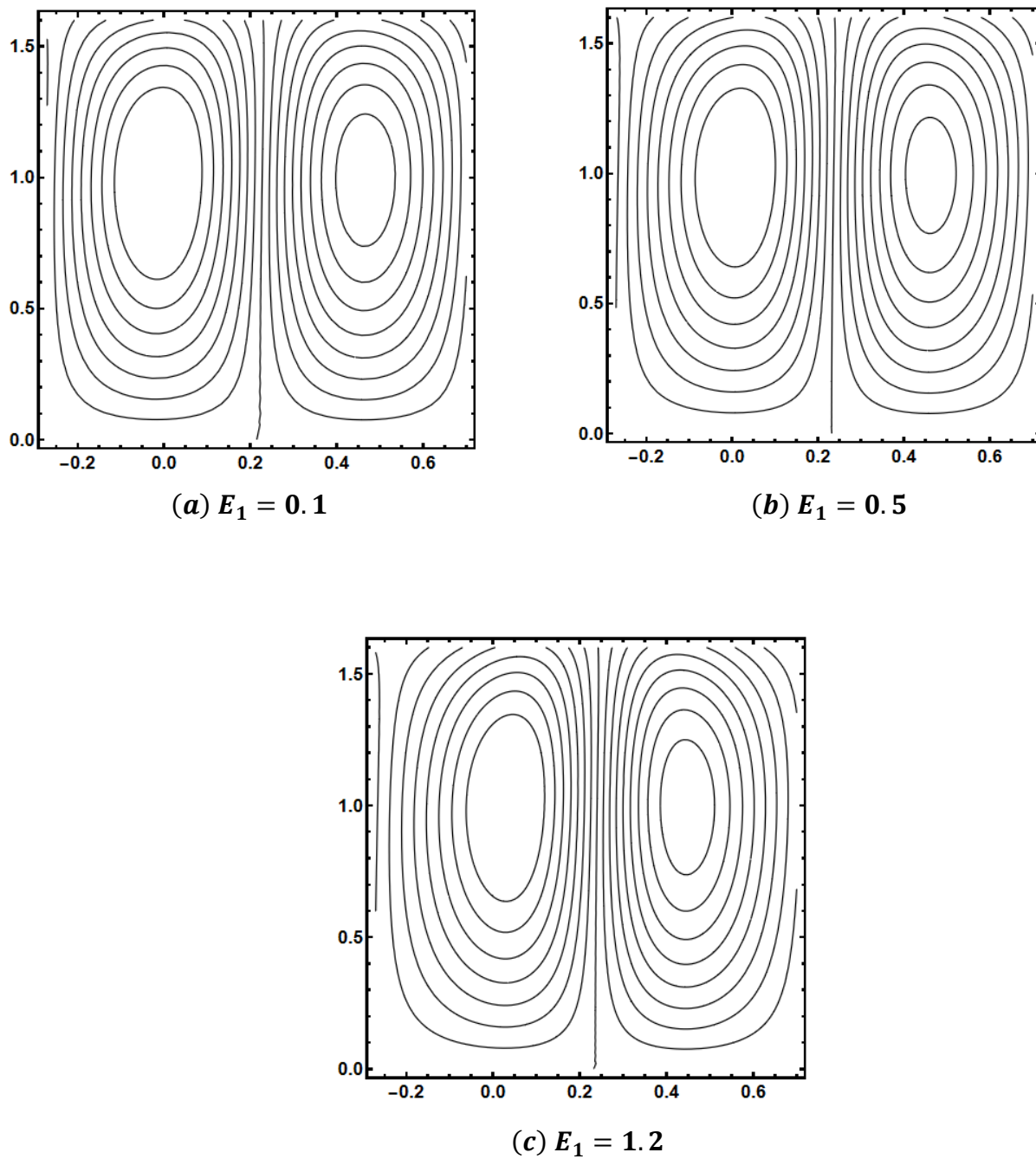
$$\frac{dp_1}{dx} = \frac{1}{y} \frac{\partial^2 \psi_1}{\partial y^2} - \frac{1}{y} \sigma^2 \psi_1 - \frac{1}{y} 2\varepsilon \left( y \frac{dp_0}{dx} + \sigma^2 \psi_0 \right)^3, \quad (5.36)$$

with boundary conditions:

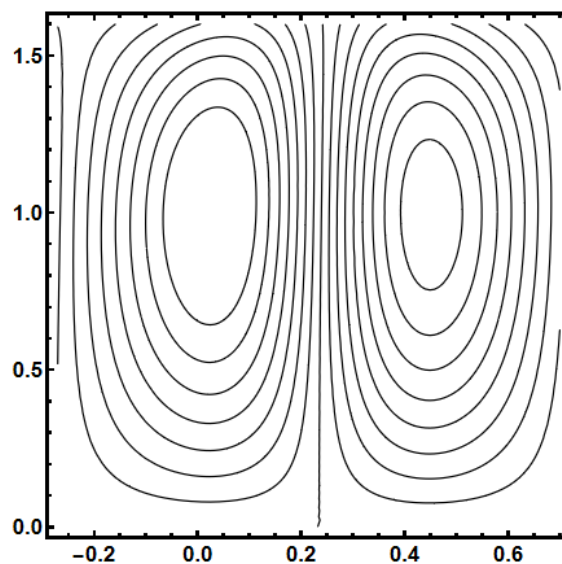
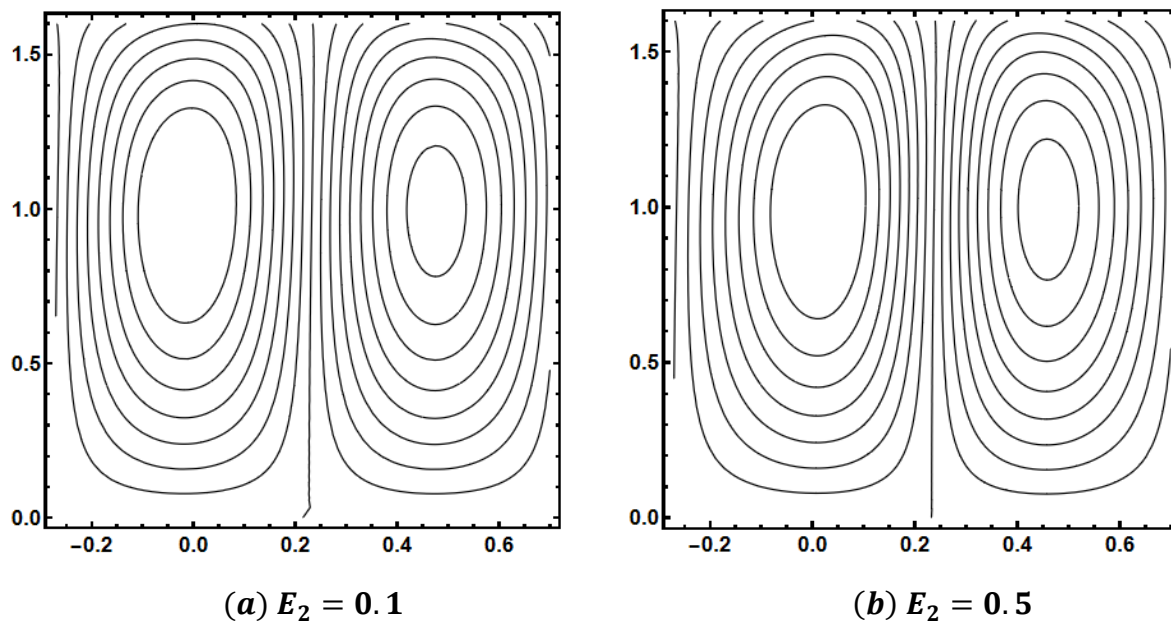
$$\frac{\partial \psi_1}{\partial y} = \pm \beta \frac{\partial^2 \psi_1}{\partial y^2}, \text{ at } y = \pm \eta, \quad (5.37)$$

$$\frac{\partial}{\partial y} S_{1xy} = 0, \text{ at } y = \pm \eta.$$

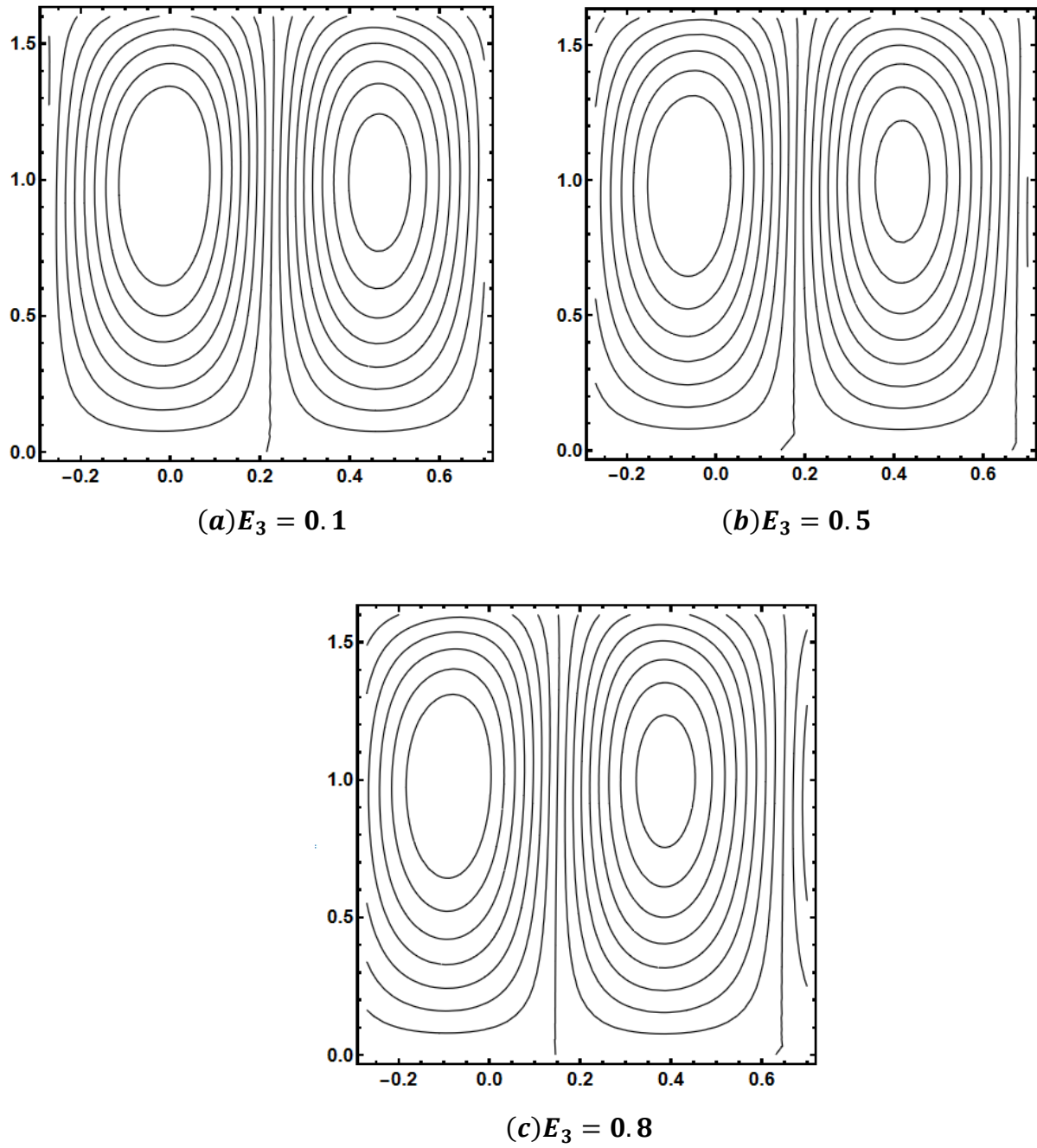
## 5.4 Results and Discussion



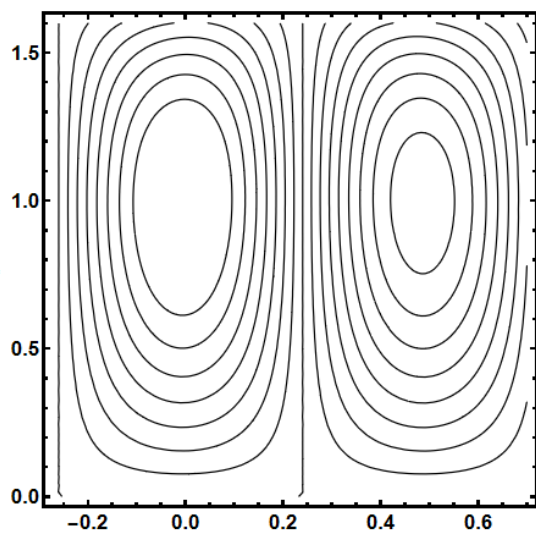
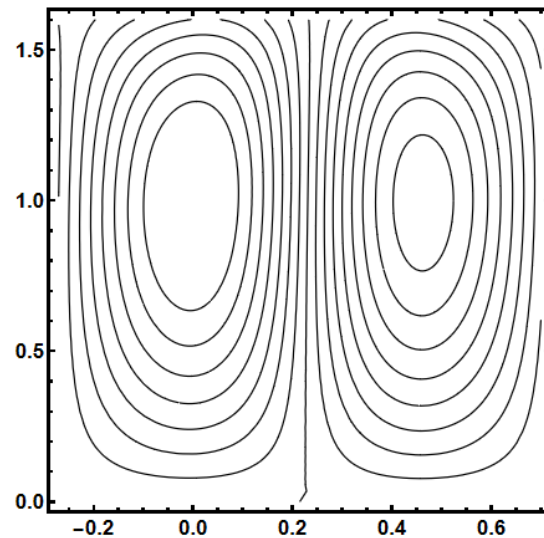
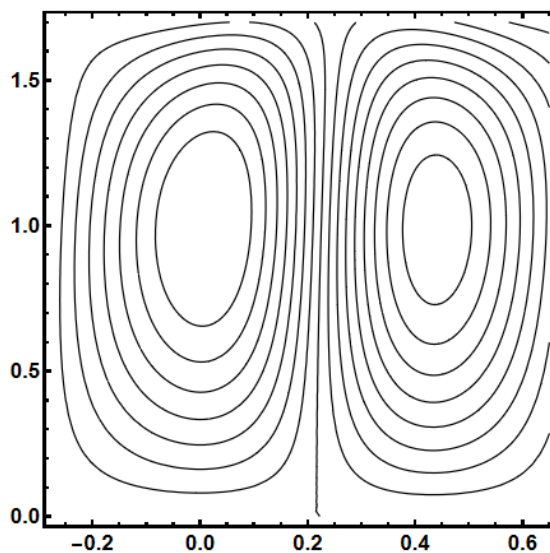
**Fig 5. 1** Streamlines for (a) $E_1 = 0.1$ , (b) $E_1 = 0.5$ , (c) $E_1 = 1.2$  with  $E_3 = 0.1$ ,  $E_2 = 0.1$ ,  $We^2 = 0.01$ ,  $\epsilon = 0.1$ ,  $\beta = 0.3$ ;  $\sigma = 0.1$ ,  $t = 1$ .



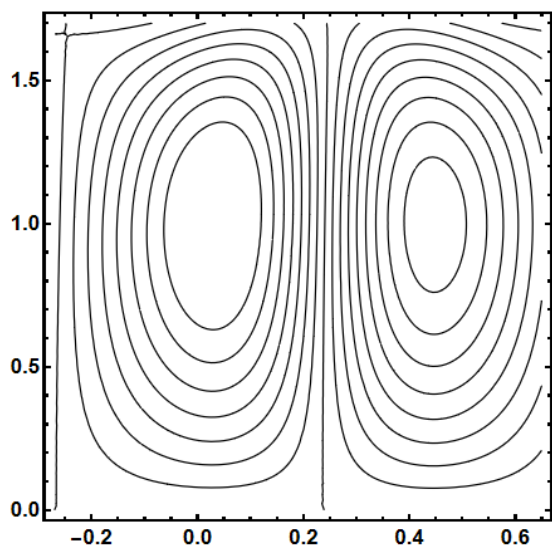
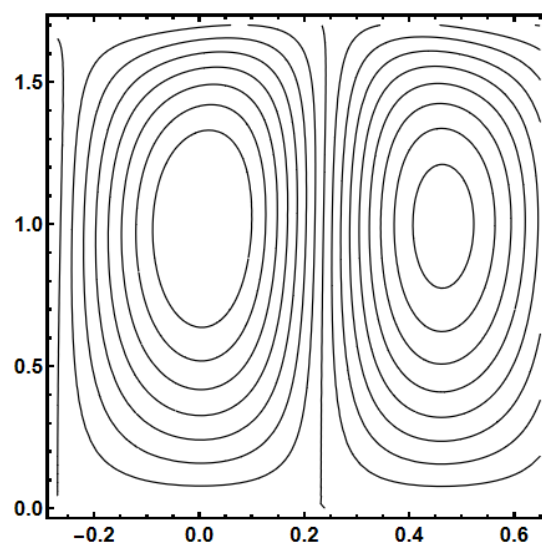
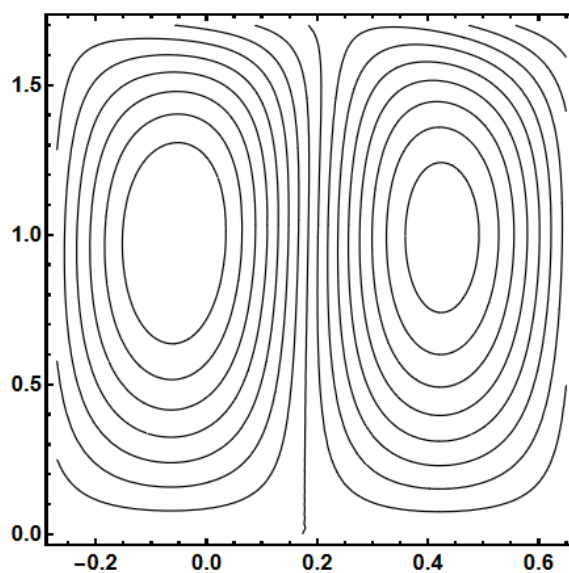
**Fig 5.2** Streamlines for (a) $E_2 = 0.1$ , (b) $E_2 = 0.5$ , (c) $E_2 = 0.9$  with  $E_1 = 0.2$ ,  $E_3 = 0.1$ ,  $We^2 = 0.01$ ,  $\epsilon = 0.1$ ,  $\beta = 0.3$ ;  $\sigma = 0.1$ ,  $t = 1$ .



**Fig 5.3** Streamlines for (a)  $E_3 = 0.1$ , (b)  $E_3 = 0.5$ , (c)  $E_3 = 0.8$  with  $E_1 = 0.1$ ,  $E_2 = 0.1$ ,  $We^2 = 0.01$ ,  $\epsilon = 0.1$ ,  $\beta = 0.3$ ;  $\sigma = 0.1$ ,  $t = 1$ .

(a)  $We^2 = 0.001$ (b)  $We^2 = 0.01$ (c)  $We^2 = 0.02$ 

**Fig 5.4** Streamlines for (a)  $We^2 = 0.001$ , (b)  $We^2 = 0.01$ , (c)  $We^2 = 0.02$  with  $E_3 = 0.15$ ,  $E_2 = 0.15$ ,  $E_1 = 0.15$ ,  $\epsilon = 0.1$ ,  $\beta = 0.3$ ;  $\sigma = 0.1$ ,  $t = 1$ .

(a)  $\sigma = 0.1$ (b)  $\sigma = 1$ (c)  $\sigma = 2$ 

**Fig 5. 5** Streamlines for (a)  $\sigma = 0.1$ , (b)  $\sigma = 1$ , (c)  $\sigma = 2$  with  $E_3 = 0.15, E_2 = 0.15, E_1 = 0.25, \epsilon = 0.1, \beta = 0.3; We^2 = 0.001, t = 1$ .

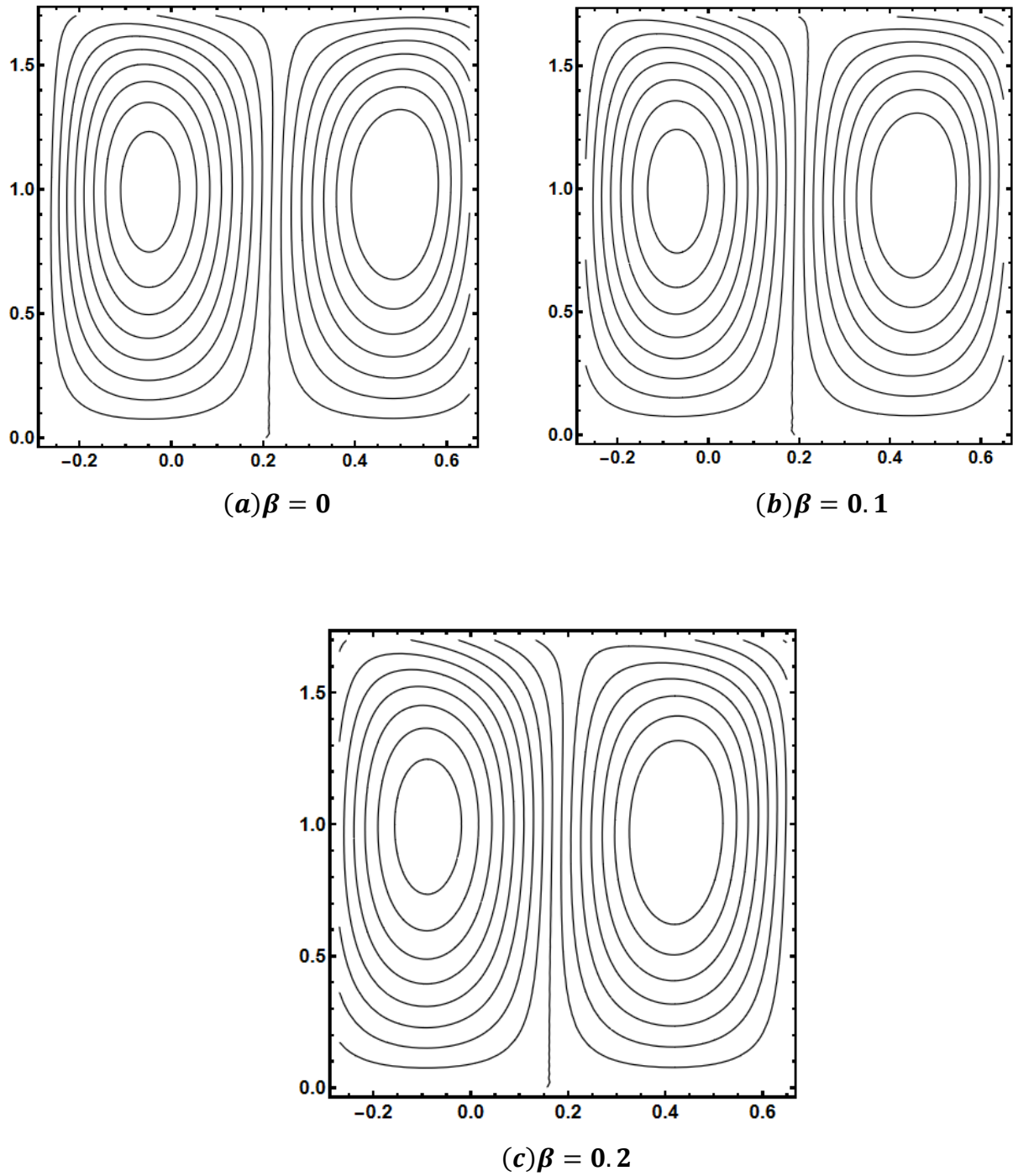


**Fig 5. 6** Streamlines for (a)  $\beta = 0$ , (b)  $\beta = 0.1$ , (c)  $\beta = 0.2$  with  $E_3 = 0.15$ ,  $E_2 = 0.15$ ,  $E_1 = 0.25$ ,  $\epsilon = 0.1$ ,  $\sigma = 0.3$ ;  $We^2 = 0.001$ ,  $t = 1$ .

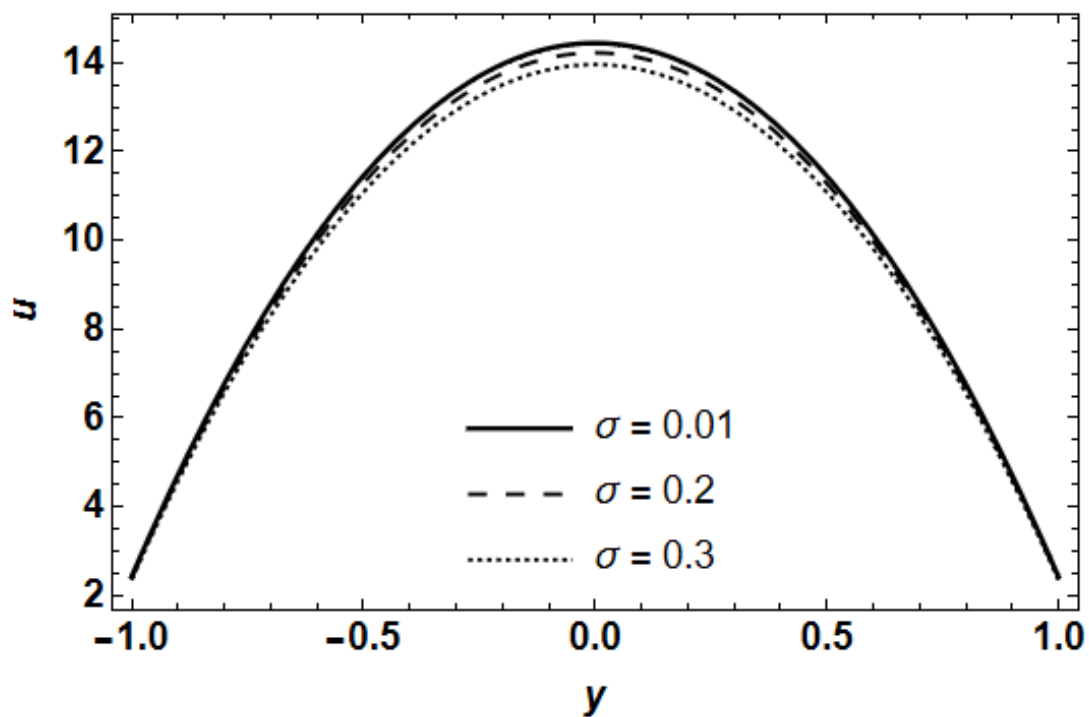


**Fig 5.7** Velocity distribution for  $\sigma = 0.01, \sigma = 0.2, \sigma = 0.3$  with  $E_3 = 0.15, E_2 = 0.15, E_1 = 0.25, \epsilon = 0.1, \beta = 0.1; We^2 = 0.001$ .

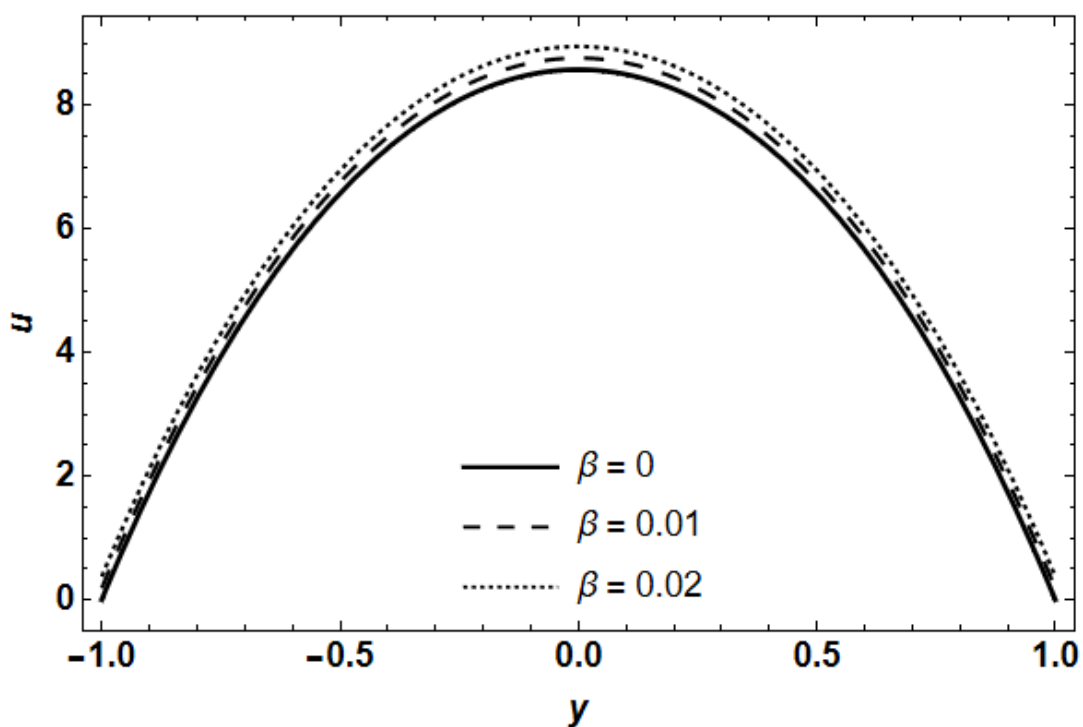


**Fig 5.8** Velocity distribution for  $\beta = 0, \beta = 0.01, \beta = 0.02$  with  $E_3 = 0.15, E_2 = 0.15, E_1 = 0.25, \epsilon = 0.1, \sigma = 0.1; We^2 = 0.01$ .

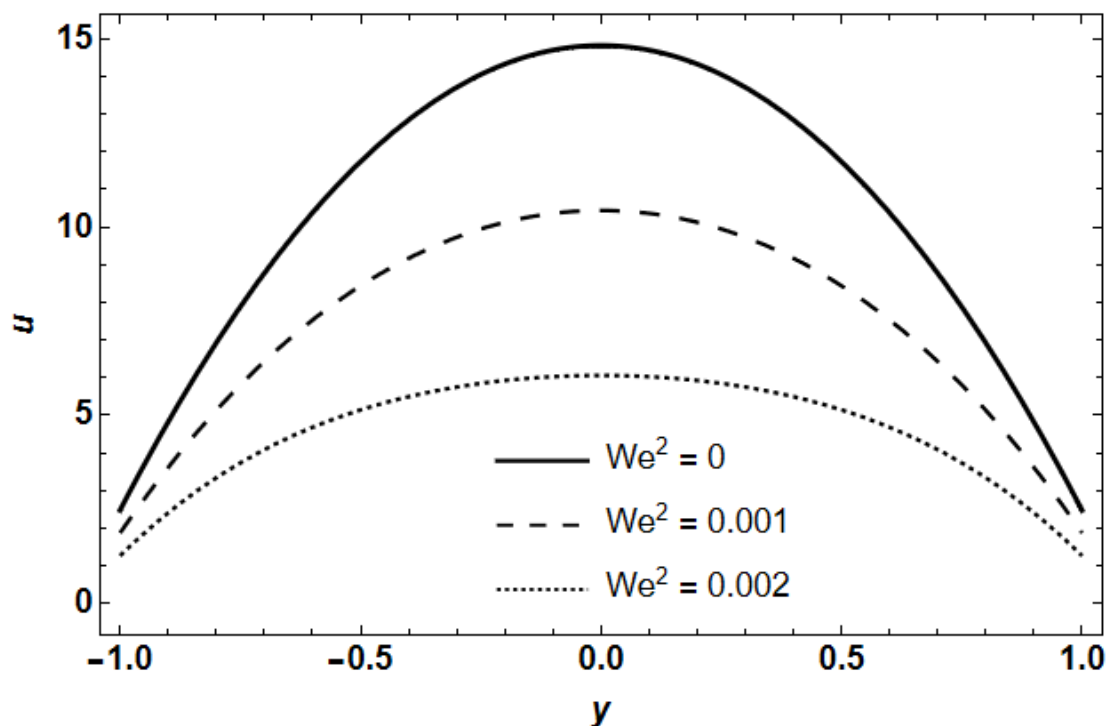


**Fig 5. 9** Velocity distribution for  $We^2 = 0, We^2 = 0.001, We^2 = 0.002$  with  $E_1 = 0.5, E_2 = 0.5, E_3 = 0.5, \beta = 0.1, \sigma = 0.1, \varepsilon = 0.1$ .

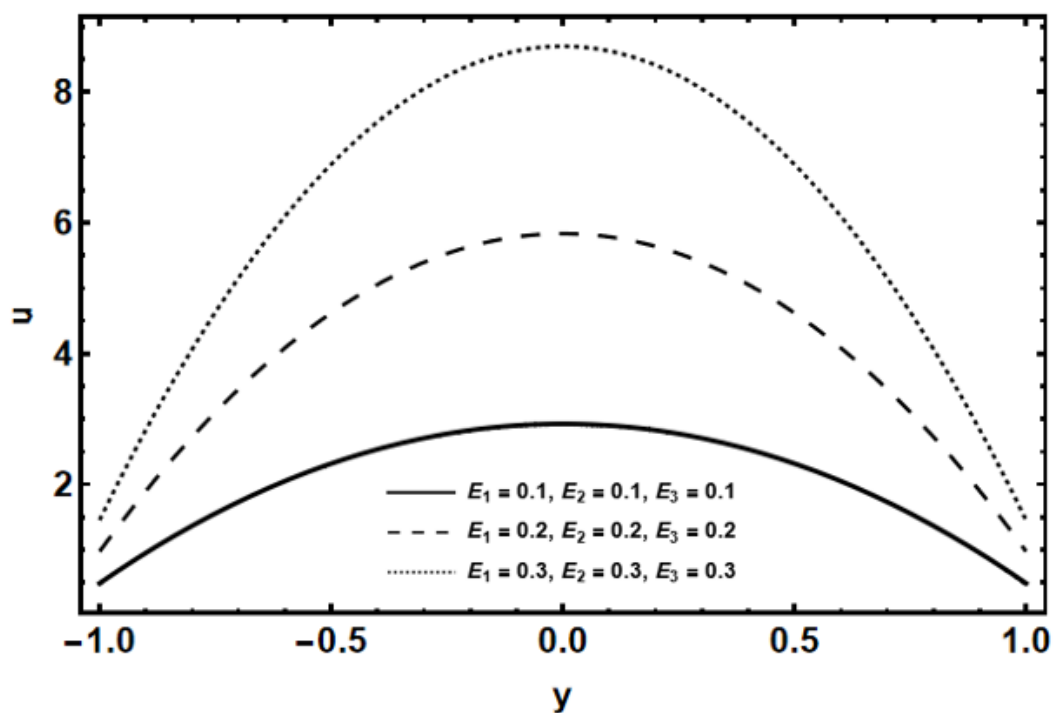


**Fig 5. 10** Velocity distribution for  $E_1 = 0.1, 0.2, 0.3, E_2 = 0.1, 0.2, 0.3, E_3 = 0.1, 0.2, 0.3$  with  $\beta = 0.1, \sigma = 0.1, We^2 = 0.001, \varepsilon = 0.1$ .

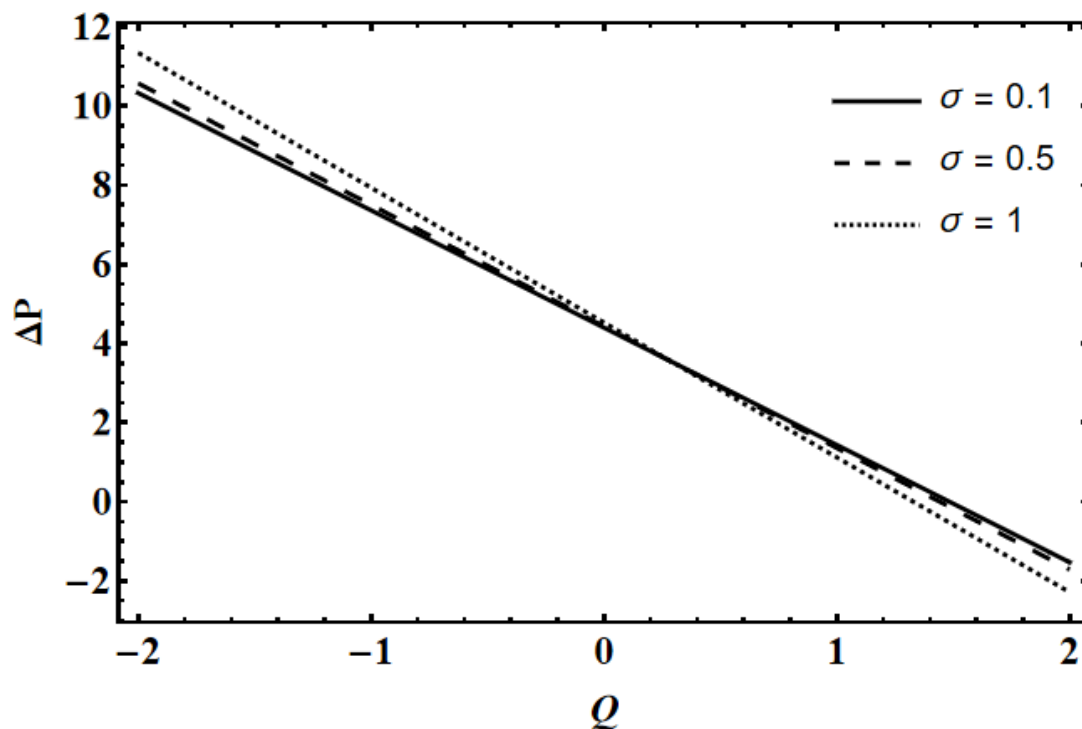


**Fig 5.11** Pressure distribution for  $\sigma = 0.1, \sigma = 0.5, \sigma = 1$  with  $E_1 = 0.2, E_2 = 0.3, E_3 = 0.2, \beta = 0.1, We^2 = 0.001$ .

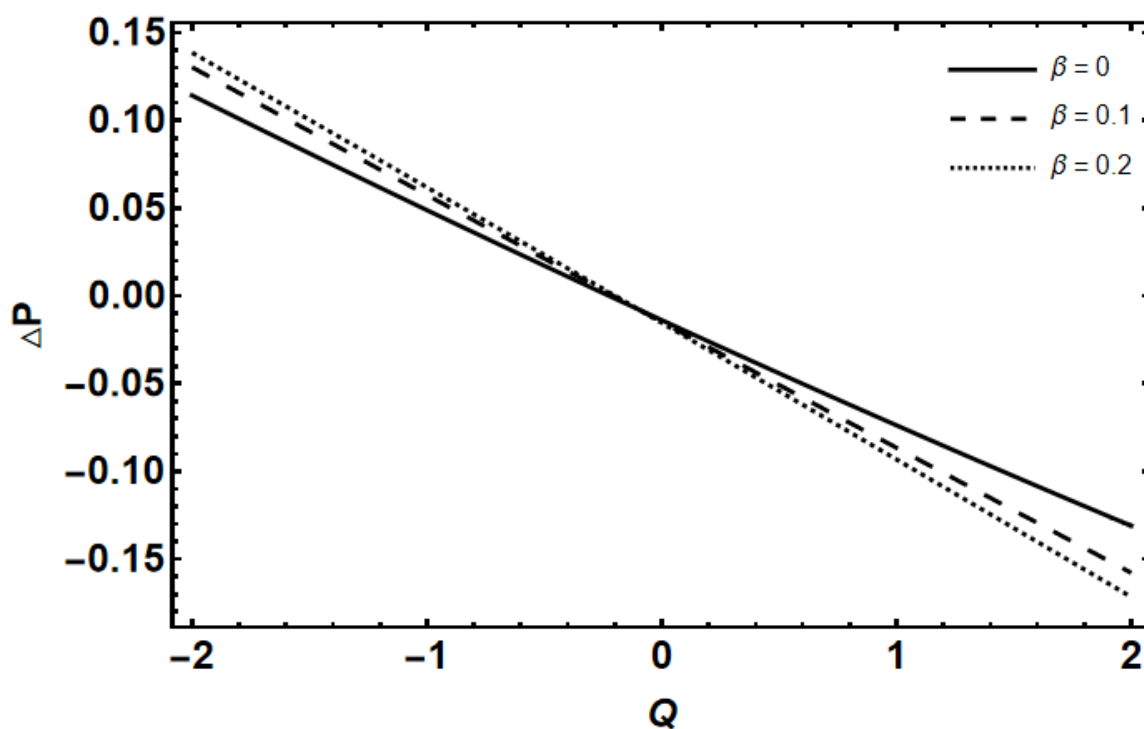


**Fig 5.12** Pressure distribution for  $\beta = 0, \beta = 0.1, \beta = 0.2$  with  $E_1 = 0.2, E_2 = 0.3, E_3 = 0.2, \beta = 0.1, We^2 = 0.001, \sigma = 0.1$ .

## Streamlines

For each value taken into consideration in this study, figures illustrating the nature of the streamlines are generated. Fluid flow patterns can be seen visually with the help of streamlines, which are hypothetical lines that depict the instantaneous trajectories taken by fluid particles in a flowing fluid. One intriguing peristaltic transport event is trapping. When we raise  $E_1$  in Fig. 5.1 demonstrate that the bolus size is the same on the left and right sides and that the lines are producing and getting closer to one another on the left side. The number of trapped boluses is the same on the left side of all three figures when we raise  $E_2$  in Fig. 5.2. However, their size expands on the right side. When we raise  $E_3$  in Fig. 5.3 demonstrate that the bolus's size is the same on the left side but is decreasing on the right; also, the first figure shows fewer lines formed, but the second and third figures show more lines produced gradually. When we raise Weissenberg number  $We^2$  the bolus in Fig 5.4 has the same size on the left and right sides, and the line created on the left side of the first image is gradually getting smaller. The right side is where the lines are starting to develop, and it is completely finished. When we raise porosity  $\sigma$  in Fig. 5.5 demonstrate that the bolus size is the same on the left and right sides, that the lines are gradually fading from both sides and that the bolus size is growing as a result of the line removal. When we raise  $\beta$  in Fig. 5.6 demonstrate that the bolus size is the same on the left and right sides and that the lines are created slowly on each side.

## Velocity Profiles

As  $\sigma$  increases, the velocity distribution decreases, as Fig. 5.7 illustrates. Fig. 5.8 illustrates how the velocity distribution rises with an increase in  $\beta$ . In rheology, the elastic response and viscous reaction of a material under deformation are related by a dimensionless quantity called the Weissenberg number. The effect of  $We^2$  on the velocity distribution can be seen in Fig. 5.9. This illustrates that when  $We^2$  enhance, the axial velocity decreases. Wall characteristics in a fluid flow simulation, the parameters  $E_1$ ,  $E_2$ , and  $E_3$  in computational fluid dynamics (CFD) are used to specify the parameters and properties of various surface types, such as wall roughness and temperature conditions. The effect that  $E_1$ ,  $E_2$ , and  $E_3$  have on the velocity field at constant values of the other parameters is displayed in Fig. 5.10. It is clear that velocity rises with increase in  $E_1$ ,  $E_2$ , and  $E_3$ .

## Pressure

For each value taken into consideration in this study, figures illustrating the nature of the pressure are generated. The force that a material, like a gas or liquid, exerts on its surroundings per unit area is known as pressure, and it is commonly measured in pascals (Pa). The effects of constant porosity ( $\sigma$ ) in the material on pressure rise are shown in Fig. 5.8 section (a). This graphic allows for the identification of three separate regions. The peristaltic pumping region is defined as the area where  $Q > 0, \Delta P > 0$ . To move the fluid forward in this area, peristalsis must struggle against the pressure rise. A free pumping zone is defined as the region where  $Q = 0, \Delta P = 0$ . Free pumping flux is the value of  $Q$  that corresponds to  $\Delta P = 0$ . The free pumping flux may only be attributed to peristaltic waves, as  $\Delta P = 0$ . An enhanced pumping zone is the final area when  $Q > 0, \Delta P < 0$ . Because of peristalsis, the pressure helps the flow in this area. It is observed that when the specified flow rate is constant, an increase in  $\sigma$  increases the rise in pressure within the peristaltic pumping area. It is almost established that the free pumping flow is independent of  $\sigma$ . However, with a fixed value of mean flow rate  $Q$ , the help given by the pressure diminishes with rising  $\sigma$  in the augmented pumping zone. Fig. 5.8 section (b) shows how pressure rise is affected by the material constant slip parameter  $\beta$ . The results indicate that  $\sigma$  and  $\beta$  have comparable impacts on  $\Delta P$ . This graphic allows for the identification of three separate regions. The peristaltic pumping region is defined as the area where  $Q > 0, \Delta P > 0$ . To move the fluid forward in this area, peristalsis must struggle against the pressure rise. A free pumping zone is defined as the region where  $Q = 0, \Delta P = 0$ . Free pumping flux is the value of  $Q$  that corresponds to  $\Delta P = 0$ . The free pumping flux may only be attributed to peristaltic waves, as  $\Delta P = 0$ . An enhanced pumping zone is the final area when  $Q > 0, \Delta P < 0$ . Because of peristalsis, the pressure helps the flow in this area. It is observed that when the specified flow rate is constant, an increase in  $\beta$  increases the rise in pressure within the peristaltic pumping area. In free pumping where pressure is constant. However, with a fixed value of mean flow rate  $Q$ , the help given by the pressure diminishes with rising  $\beta$  in the augmented pumping zone.

## CHAPTER 6

### CONCLUSION AND FUTURE WORK

#### 6.1 Conclusion

This thesis delves into a comprehensive exploration of the peristaltic movement of a non-Newtonian Phan-Thien-Tanner (PTT) fluid within a symmetric flexible channel characterized by sinusoidal peristaltic waves. Employing the long wavelength and low Reynolds number approximations, the flow is scrutinized within a wave frame of reference that travels at the velocity of the peristaltic waves. The mathematical representation of the system utilizes partial differential equations (PDEs) to model the equation systems. To thoroughly analyze the impact of various physical parameters on streamlines, pressure, and velocity, graphical representations are employed.

The findings of the present study are succinctly encapsulated in the following overarching conclusion.

In the course of this investigation, it was observed that the size of the trapped bolus remains constant, while the spacing between lines diminishes with an increase in the value of wall characteristics  $E_1$ . Conversely, the size of the trapped bolus expanded proportionally with rising values of wall characteristics  $E_2$ . Additionally, the volume of the confined bolus exhibited a decrease as the wall characteristics  $E_3$  values increased.

The volume of the trapped bolus remains constant, and concurrently, the number of lines decreases with an increase in the Weissenberg number (We). Following a phase where the bolus size remains constant, its volume experiences an increase, accompanied by the thinning of the lines, as the porosity parameter ( $\sigma$ ) increases. Furthermore, the trapped bolus volume maintains constancy, while the emergence of lines unfolds gradually with an increase in the slip parameter ( $\beta$ ).

Under the influence of porosity ( $\sigma$ ), slip parameter ( $\beta$ ), Weissenberg number ( $We^2$ ), and wall characteristics ( $E_1$ ,  $E_2$ , and  $E_3$ ), the velocity profile ( $u$ ) exhibits an upward trend in certain scenarios. An increase in porosity ( $\sigma$ ) corresponds to a decrease in the velocity distribution. Both the slip parameter ( $\beta$ ) and velocity ( $u$ ) show growth with higher values. Simultaneously, the Weissenberg number ( $We^2$ ) increases, leading to a decrease in velocity ( $u$ ). Furthermore, the wall characteristics ( $E_1$ ,  $E_2$ , and  $E_3$ ) exhibit a parallel increase with the velocity ( $u$ ) value.

When considering porosity and slip parameter, an increasing trend is observed in the pressure. Specifically, pressure rise with increasing porosity ( $\sigma$ ) in the peristaltic zone, maintains a value of zero in the free pumping region, and experiences an increase with further increments in porosity ( $\sigma$ ) in the enhanced pumping region. Similarly, pressure demonstrates an ascending pattern with increasing slip parameter ( $\beta$ ) in the peristaltic zone, remains zero in the free pumping region, and diminished with higher values of slip parameter ( $\beta$ ) in the enhanced pumping region.

## 6.2 Future work

The proposed model can be expanded by adding diverse parameters like magnetic field, chemical reactions and viscous dissipations. This model can also be studied by considering the fluid models like Williamson, Burger, Maxwell and Jeffery, under the same boundary conditions. We can also extend this proposed work by taking different geometries like wedge, inclined channel or cylinder etc.

## REFERENCES

1. Mitra, T. K., & Prasad, S. N. (1973). On the influence of wall properties and Poiseuille flow in peristalsis. *Journal of biomechanics*, 6(6), 681-693.
2. Formato, G., Romano, R., Formato, A., Sorvari, J., Koiranen, T., Pellegrino, A., & Villecco, F. (2019). Fluid–structure interaction modeling applied to peristaltic pump flow simulations. *Machines*, 7(3), 50.
3. Tripathi, D. (2013). Study of transient peristaltic heat flow through a finite porous channel. *Mathematical and Computer Modelling*, 57(5-6), 1270-1283.
4. Rashid, M., Ansar, K., & Nadeem, S. (2020). Effects of induced magnetic field for peristaltic flow of Williamson fluid in a curved channel. *Physica A: Statistical Mechanics and its Applications*, 553, 123979.
5. Siddiqui, A. M., & Schwarz, W. H. (1994). Peristaltic flow of a second-order fluid in tubes. *Journal of Non-Newtonian Fluid Mechanics*, 53, 257-284.
6. Tripathi, D., Pandey, S. K., & Das, S. (2010). Peristaltic flow of viscoelastic fluid with fractional Maxwell model through a channel. *Applied Mathematics and Computation*, 215(10), 3645-3654.
7. Takabatake, S., & Ayukawa, K. (1982). Numerical study of two-dimensional peristaltic flows. *Journal of Fluid Mechanics*, 122, 439-465.
8. Hayat, T., Ali, N., & Asghar, S. (2007). Hall effects on peristaltic flow of a Maxwell fluid in a porous medium. *Physics Letters A*, 363(5-6), 397-403.
9. Hayat, T., Aslam, N., Khan, M. I., Khan, M. I., & Alsaedi, A. (2019). Physical significance of heat generation/absorption and Soret effects on peristalsis flow of pseudoplastic fluid in an inclined channel. *Journal of Molecular Liquids*, 275, 599-615.
10. Rashid, M., Ansar, K., & Nadeem, S. (2020). Effects of induced magnetic field for peristaltic flow of Williamson fluid in a curved channel. *Physica A: Statistical Mechanics and its Applications*, 553, 123979.
11. Javed, M., & Naz, R. (2020). Peristaltic flow of a realistic fluid in a compliant channel. *Physica A: Statistical Mechanics and its Applications*, 551, 123895.
12. Abd Elmaboud, Y., Abdelsalam, S. I., & Mekheimer, K. S. (2018). Couple stress

- fluid flow in a rotating channel with peristalsis. *Journal of Hydrodynamics*, 30, 307-316.
13. Noreen, S., Kausar, T., Tripathi, D., Ain, Q. U., & Lu, D. C. (2020). Heat transfer analysis on creeping flow Carreau fluid driven by peristaltic pumping in an inclined asymmetric channel. *Thermal Science and Engineering Progress*, 17, 100486.
  14. Imran, M. A., Shaheen, A., Sherif, E. S. M., Rahimi-Gorji, M., & Seikh, A. H. (2020). Analysis of peristaltic flow of Jeffrey six constant nano fluid in a vertical non-uniform tube. *Chinese Journal of Physics*, 66, 60-73.
  15. Noreen, S., Waheed, S., Lu, D. C., & Tripathi, D. (2021). Heat stream in electroosmotic bio-fluid flow in straight microchannel via peristalsis. *International Communications in Heat and Mass Transfer*, 123, 105180.
  16. Ramesh, K., Tripathi, D., Bhatti, M. M., & Khalique, C. M. (2020). Electro-osmotic flow of hydromagnetic dusty viscoelastic fluids in a microchannel propagated by peristalsis. *Journal of Molecular Liquids*, 314, 113568.
  17. Farooq, S., Khan, M. I., Hayat, T., Waqas, M., & Alsaedi, A. (2019). Theoretical investigation of peristalsis transport in flow of hyperbolic tangent fluid with slip effects and chemical reaction. *Journal of Molecular Liquids*, 285, 314-322.
  18. Shehzad, S. A., Abbasi, F. M., Hayat, T., Alsaadi, F., & Mousa, G. (2015). Peristalsis in a curved channel with slip condition and radial magnetic field. *International Journal of Heat and Mass Transfer*, 91, 562-569.
  19. Ali, N., Javid, K., & Sajid, M. (2016). Simulations of peristaltic slip-flow of hydromagnetic bio-fluid in a curved channel. *AIP Advances*, 6(2).
  20. Farooq, S., Khan, M. I., Waqas, M., Hayat, T., & Alsaedi, A. (2020). Transport of hybrid type nanomaterials in peristaltic activity of viscous fluid considering nonlinear radiation, entropy optimization and slip effects. *Computer Methods and Programs in Biomedicine*, 184, 105086.
  21. Hayat, T., Shafique, M., Tanveer, A., & Alsaedi, A. (2016). Hall and ion slip effects on peristaltic flow of Jeffrey nanofluid with Joule heating. *Journal of Magnetism and Magnetic Materials*, 407, 51-59.
  22. Imran, N., Javed, M., Sohail, M., Farooq, S., & Qayyum, M. (2020). Outcome of slip features on the peristaltic flow of a Rabinowitsch nanofluid in an asymmetric flexible channel. *Multidiscipline Modeling in Materials and Structures*, 17(1), 181-197.
  23. Wahid, N. S., Arifin, N. M., Khashi'ie, N. S., & Pop, I. (2020). Hybrid nanofluid slip flow over an exponentially stretching/shrinking permeable sheet with heat

- generation. *Mathematics*, 9(1), 30.
24. Abd Elmaboud, Y., Mekheimer, K. S., & Mohamed, M. S. (2015). Series solution of a natural convection flow for a Carreau fluid in a vertical channel with peristalsis. *Journal of Hydrodynamics, Ser. B*, 27(6), 969-979.
  25. Akram, S., Mekheimer, K. S., & Abd Elmaboud, Y. (2018). Particulate suspension slip flow induced by peristaltic waves in a rectangular duct: effect of lateral walls. *Alexandria engineering journal*, 57(1), 407-414.
  26. Rani, J., Hina, S., & Mustafa, M. (2020). A novel formulation for MHD slip flow of elastico-viscous fluid induced by peristaltic waves with heat/mass transfer effects. *Arabian Journal for Science and Engineering*, 45(11), 9213-9225.
  27. Hayat, T., Nisar, Z., & Alsaedi, A. (2020). Impacts of slip in radiative MHD peristaltic flow of fourth grade nanomaterial with chemical reaction. *International Communications in Heat and Mass Transfer*, 119, 104976.
  28. Tanveer, A., & Malik, M. Y. (2021). Slip and porosity effects on peristalsis of MHD Ree-Eyring nanofluid in curved geometry. *Ain Shams Engineering Journal*, 12(1), 955-968.
  29. Eldesoky, I. M., Abumandour, R. M., Kamel, M. H., & Abdelwahab, E. T. (2019). The combined influences of heat transfer, compliant wall properties and slip conditions on the peristaltic flow through tube. *SN Applied Sciences*, 1, 1-16.
  30. Das, S., Pal, T. K., & Jana, R. N. (2021). Electromagnetic hybrid nano-blood pumping via peristalsis through an endoscope having blood clotting in presence of hall and ion slip currents. *BioNanoScience*, 11(3), 848-870.
  31. Rafiq, M., Yasmin, H., Hayat, T., & Alsaadi, F. (2019). Effect of Hall and ion-slip on the peristaltic transport of nanofluid: A biomedical application. *Chinese Journal of Physics*, 60, 208-227.
  32. Riaz, A., Khan, S. U. D., Zeeshan, A., Khan, S. U., Hassan, M., & Muhammad, T. (2021). Thermal analysis of peristaltic flow of nanosized particles within a curved channel with second-order partial slip and porous medium. *Journal of Thermal Analysis and Calorimetry*, 143, 1997-2009.
  33. Vaidya, H., Rajashekhar, C., Prasad, K. V., Khan, S. U., Riaz, A., & Viharika, J. U. (2021). MHD peristaltic flow of nanofluid in a vertical channel with multiple slip features: an application to chyme movement. *Biomechanics and Modeling in Mechanobiology*, 20, 1047-1067.
  34. Vaidya, H., Makinde, O. D., Choudhari, R., Prasad, K. V., Khan, S. U., & Vajravelu,

- K. (2020). Peristaltic flow of non-Newtonian fluid through an inclined compliant nonlinear tube: application to chyme transport in the gastrointestinal tract. *The European Physical Journal Plus*, 135(11), 1-15.
35. Mustafa, M., Hina, S., Hayat, T., & Alsaedi, A. (2012). Influence of wall properties on the peristaltic flow of a nanofluid: analytic and numerical solutions. *International Journal of Heat and Mass Transfer*, 55(17-18), 4871-4877.
  36. Srinivas, S., Gayathri, R., & Kothandapani, M. (2009). The influence of slip conditions, wall properties and heat transfer on MHD peristaltic transport. *Computer Physics Communications*, 180(11), 2115-2122.
  37. Abd Elnaby, M. A., & Haroun, M. H. (2008). A new model for study the effect of wall properties on peristaltic transport of a viscous fluid. *Communications in Nonlinear Science and Numerical Simulation*, 13(4), 752-762.
  38. Hayat, T., Hina, S., Hendi, A. A., & Asghar, S. (2011). Effect of wall properties on the peristaltic flow of a third grade fluid in a curved channel with heat and mass transfer. *International journal of heat and mass transfer*, 54(23-24), 5126-5136.
  39. Hayat, T., & Hina, S. (2010). The influence of wall properties on the MHD peristaltic flow of a Maxwell fluid with heat and mass transfer. *Nonlinear analysis: Real world applications*, 11(4), 3155-3169.
  40. Kothandapani, M., & Srinivas, S. (2008). On the influence of wall properties in the MHD peristaltic transport with heat transfer and porous medium. *Physics letters A*, 372(25), 4586-4591.
  41. Radhakrishnamacharya, G., & Srinivasulu, C. (2007). Influence of wall properties on peristaltic transport with heat transfer. *Comptes Rendus Mecanique*, 335(7), 369-373.
  42. Hina, S., Mustafa, M., Hayat, T., & Alotaibi, N. D. (2015). On peristaltic motion of pseudoplastic fluid in a curved channel with heat/mass transfer and wall properties. *Applied Mathematics and Computation*, 263, 378-391.
  43. Kayani, S. M., Hina, S., & Mustafa, M. (2020). A new model and analysis for peristalsis of Carreau–Yasuda (CY) nanofluid subject to wall properties. *Arabian Journal for Science and Engineering*, 45, 5179-5190.
  44. Bhatti, M. M., Ellahi, R., Zeeshan, A., Marin, M., & Ijaz, N. (2019). Numerical study of heat transfer and Hall current impact on peristaltic propulsion of particle-fluid suspension with compliant wall properties. *Modern Physics Letters B*, 33(35), 1950439.
  45. Nisar, Z., Hayat, T., Alsaedi, A., & Ahmad, B. (2021). Wall properties and

- convective conditions in MHD radiative peristalsis flow of Eyring–Powell nanofluid. *Journal of Thermal Analysis and Calorimetry*, 144, 1199-1208.
46. Iftikhar, N., Rehman, A., Sadaf, H., & Khan, M. N. (2018). Impact of wall properties on the peristaltic flow of Cu-water nano fluid in a non-uniform inclined tube. *International Journal of Heat and Mass Transfer*, 125, 772-779.
  47. Abbas, Z., Rafiq, M. Y., Hasnain, J., & Javed, T. (2021). Peristaltic transport of a Casson fluid in a non-uniform inclined tube with Rosseland approximation and wall properties. *Arabian Journal for Science and Engineering*, 46, 1997-2007.
  48. Eldesoky, I. M., Nayel, M. S., Galal, A. A., & Raslan, H. M. (2020). Combined effects of space porosity and wall properties on a compressible Maxwell fluid with MHD peristalsis. *SN Applied Sciences*, 2(12), 2118.
  49. Vaidya, H., Rajashekhar, C., Manjunatha, G., & Prasad, K. V. (2019). Peristaltic mechanism of a Rabinowitsch fluid in an inclined channel with compliant wall and variable liquid properties. *Journal of the Brazilian Society of Mechanical Sciences and Engineering*, 41, 1-14.
  50. Khan, A. A., & Tariq, H. (2018). Influence of wall properties on the peristaltic flow of a dusty Walter's B fluid. *Journal of the Brazilian Society of Mechanical Sciences and Engineering*, 40(8), 368.
  51. Rafiq, M. Y., & Abbas, Z. (2021). Impacts of viscous dissipation and thermal radiation on Rabinowitsch fluid model obeying peristaltic mechanism with wall properties. *Arabian Journal for Science and Engineering*, 46, 12155-12163.
  52. Hayat, T., Noreen, S., Ali, N., & Abbasbanday, S. (2012). Peristaltic motion of Phan-Thien-Tanner fluid in a planar channel. *Numerical Methods for Partial Differential Equations*, 28(3), 737-748.
  53. Akbar, N. S., & Nadeem, S. (2012). Peristaltic flow of a Phan-Thien-Tanner nanofluid in a diverging tube. *Heat Transfer—Asian Research*, 41(1), 10-22.
  54. Hussain, S., Ali, N., & Ullah, K. (2019). Peristaltic flow of Phan-Thien-Tanner fluid: effects of peripheral layer and electro-osmotic force. *Rheologica Acta*, 58, 603-618.
  55. Butt, A. W., Akbar, N. S., & Mir, N. A. (2020). Heat transfer analysis of peristaltic flow of a Phan-Thien–Tanner fluid model due to metachronal wave of cilia. *Biomechanics and modeling in mechanobiology*, 19, 1925-1933.
  56. Hayat, T., Noreen, S., & Hendi, A. A. (2011). Peristaltic motion of Phan–Thien–Tanner fluid in the presence of slip condition. *Journal of biorheology*, 25, 8-17.
  57. Sarkar, S. (2020). Streaming-potential-mediated pressure-driven transport of Phan-

- Thien–Tanner fluids in a microchannel. *Physical Review E*, 101(5), 053104.
58. Vajravelu, K., Sreenadh, S., Lakshminarayana, P., Sucharitha, G., & Rashidi, M. M. (2016). Peristaltic flow of Phan-Thien-Tanner fluid in an asymmetric channel with porous medium. *Journal of Applied Fluid Mechanics*, 9(4), 1615-1625.
  59. Ali, A., Jana, R. N., & Das, S. (2021). Significance of entropy generation and heat source: the case of peristaltic blood flow through a ciliated tube conveying Cu-Ag nanoparticles using Phan-Thien-Tanner model. *Biomechanics and Modeling in Mechanobiology*, 20(6), 2393-2412.
  60. Vaidya, H., Prasad, K. V., Khan, M. I., Mebarek-Oudina, F., Tlili, I., Rajashekhar, C., ... & Al-Gamdi, S. G. (2022). Combined effects of chemical reaction and variable thermal conductivity on MHD peristaltic flow of Phan-Thien-Tanner liquid through inclined channel. *Case Studies in Thermal Engineering*, 36, 102214.
  61. Prakash, J., & Tripathi, D. (2020). Study of EDL phenomenon in Peristaltic pumping of a Phan-Thien-Tanner Fluid through asymmetric channel. *Korea-Australia Rheology Journal*, 32(4), 271-285.
  62. Faraz, N., Lu, Z., Hou, L., Khan, Y., & Siddiqi, A. F. (2018, July). Exact solutions of magnetohydrodynamic flow of PTT fluid. In *Journal of Physics: Conference Series* (Vol. 1053, No. 1, p. 012064). IOP Publishing.
  63. Siddiqui, A. M., Azim, Q. A., & Imran, M. (2020). Exact solutions for n-layer concentric flow of PTT fluids through a cylindrical pipe. *Canadian Journal of Physics*, 98(2), 134-141.
  64. Ellahi, R., Hussain, F., Ishtiaq, F., & Hussain, A. (2019). Peristaltic transport of Jeffrey fluid in a rectangular duct through a porous medium under the effect of partial slip: An application to upgrade industrial sieves/filters. *Pramana*, 93, 1-9.
  65. Vaidya, H., Rajashekhar, C., Divya, B. B., Manjunatha, G., Prasad, K. V., & Animasaun, I. L. (2020). Influence of transport properties on the peristaltic MHD Jeffrey fluid flow through a porous asymmetric tapered channel. *Results in Physics*, 18, 103295.
  66. Hasona, W. M., El-Shehkipy, A. A., & Ibrahim, M. G. (2018). Combined effects of magnetohydrodynamic and temperature dependent viscosity on peristaltic flow of Jeffrey nanofluid through a porous medium: Applications to oil refinement. *International Journal of Heat and Mass Transfer*, 126, 700-714.
  67. Vaidya, H., Rajashekhar, C., Manjunatha, G., Prasad, K. V., Makinde, O. D., & Vajravelu, K. (2020). Heat and mass transfer analysis of MHD peristaltic flow

- through a complaint porous channel with variable thermal conductivity. *Physica Scripta*, 95(4), 045219.
68. Riaz, A., Zeeshan, A., Bhatti, M. M., & Ellahi, R. (2020). Peristaltic propulsion of Jeffrey nano-liquid and heat transfer through a symmetrical duct with moving walls in a porous medium. *Physica A: Statistical Mechanics and its Applications*, 545, 123788.
  69. Noreen, S., & Tripathi, D. (2019). Heat transfer analysis on electroosmotic flow via peristaltic pumping in non-Darcy porous medium. *Thermal Science and Engineering Progress*, 11, 254-262.
  70. Manjunatha, G., Rajashekhar, C., Vaidya, H., Prasad, K. V., & Vajravelu, K. (2020). Impact of heat and mass transfer on the peristaltic mechanism of Jeffery fluid in a non-uniform porous channel with variable viscosity and thermal conductivity. *Journal of Thermal Analysis and Calorimetry*, 139, 1213-1228.